University of Verona

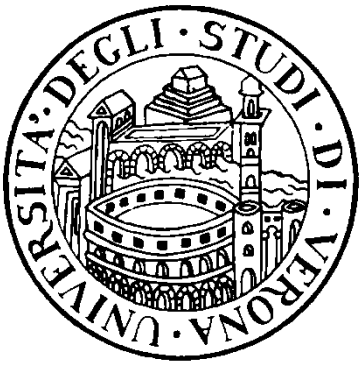

DEPARTMENT OF MEDICINE

GRADUATE SCHOOL FOR LIFE AND HEALTH SCIENCES

DOCTORAL PROGRAM IN BIOMOLECULAR MEDICINE

CURRICULUM IN CLINICAL GENOMICS AND PROTEOMICS

Cycle XXX

Functional Characterization of Erythropoiesis in Fyn$^{-/-}$ mice: a Novel Role of Fyn in Stress Erythropoiesis

Coordinator: PROF.SSA LUCIA DE FRANCESCHI

Tutor: PROF.SSA LUCIA DE FRANCESCHI

Doctoral Student: ELISABETTA BENEDUCE

INDEX

1. ABSTRACT

Erythropoiesis is a dynamic complex multistep process going from committed erythroid progenitors to erythroid precursors and circulating mature red cells. Erythroid maturation is strictly dependent on EPO signaling cascade. EPO physically interacts with its receptor (EPO-R), which expression is downregulated after the basophilic erythroblasts stage.[7] Binding of EPO to EPO-R results in EPO-R conformational change and it requires the activation of Jak2, as primary kinase. STAT5 is a master of erythropoiesis and it resides in cytoplasm. In response to EPO signaling, it binds phospho-tyrosine (Tyr) residues in the nucleus, initiating the transcription of several genes important in terminal erythroid differentiation. Giving the importance of Jak2 kinase as initiator of the EPO signaling cascade, additional kinases, such as Lyn, a Src family kinase, has been described to participate to EPO pathway. Lyn is able to phosphorylate EPO-R, Jak2 itself and STAT5. The activation of EPO/Jak2 signaling pathway is associated with production of reactive oxidative species (ROS), which are also generated by a large amount of iron imported into the cells during heme biosynthesis. During erythropoiesis, ROS might function as second messenger by modulating intracellular signaling pathways. Fyn, a Src kinase, has been previously reported to participate in signaling pathways in response to ROS in various cell types.

Here, we explore the potential contribution of Fyn to normal and stress erythropoiesis by studying 2-4 months-old Fyn knockout mouse strain ($Fyn^{-/-}$) and C57BL/6J as wild-type controls. $Fyn^{-/-}$ mice showed a mild compensated microcytic anemia associated with signs of dyserythropoiesis. Increased ROS levels and Annexin-V^{+} cells were presented in all $Fyn^{-/-}$ erythroblast subpopulations compared to wild-type, suggesting a possible reduction in the efficiency of erythropoietin (EPO) signaling pathway in the absence of Fyn. Indeed, in $Fyn^{-/-}$ erythroblasts we observed a reduction in Tyr-phosphorylation state of EPO-R associated with a compensatory activation of Jak2 without major change in Lyn activity. A reduction in STAT5 activation resulting in down-regulation of *Cish,* a known direct STAT5 target gene, was noted in $Fyn^{-/-}$ erythroblasts. This was paralleled by a reduction in GATA1 and increased HSP70 nuclear translocation compared to wild type, supporting a higher cellular pro-oxidant environment in the absence of Fyn. Using the vitro cell forming colony unit assay, we found a lower CFU-E and BFU-E cells production, which once again was associated with decreased activation of EPO mediated cascade in the absence of Fyn. To explore the possible role of Fyn in stress erythropoiesis, mice were treated with recombinant EPO, phenylhydrazine (PHZ) or doxorubicin (Doxo). $Fyn^{-/-}$ mice showed a low response to EPO compared to wild-type animals and prolonged anemia after either PHZ or Doxo treatment with a delayed hematologic recovery compared to wild-type mice. When we analyzed the expression of a battery of ARE-genes related to oxidative response such as catalase, Gpx, heme-oxygenase 1 and peroxiredoxin-2, we noted up-regulated expression of these genes in sorted $Fyn^{-/-}$ erythroblasts compared to wild-type cells. In agreement, we observed increased activation of the redox-sensitive transcriptional factor Nrf2 targeting ARE-genes, whose regulation has been previously linked to Fyn. In fact, Nrf2 is switched-off by Fyn, ubiquitylated and delivered to the autophagosome by the p62 cargo protein. In $Fyn^{-/-}$ sorted erythroblasts, we observed (i) accumulation of p62 in large clusters; and (ii) reduction of Nrf2-p62 complex compared to wild-type cells. To address the question whether the perturbation of Nrf2-p62 system results in impairment of autophagy in the absence of Fyn, we used LysoTracker to explore late phases of autophagy. Lysosomal progression was defective in $Fyn^{-/-}$ reticulocytes and it was associated with accumulation of p62 during *in vitro* reticulocyte maturation. These data indicate that the absence of Fyn blocks the Nrf2 post-induction response to oxidation, resulting in impaired autophagy. To validate our working hypothesis, we treated $Fyn^{-/-}$ mice with Rapamycin, an inducer of autophagy. In $Fyn^{-/-}$ mice, Rapamycin treatment resulted in decrease dyserythropoiesis, ROS levels and Annexin V^{+} cells, associated with reduction in accumulation of p62 in $Fyn^{-/-}$ erythroblasts. Collectively, our data

enabled us to document a novel role for Fyn in erythropoiesis, contributing to EPO-R activation and harmonizing the Nrf2-p62 adaptive cellular response against oxidation.
Future studies will be designed to further characterize the signaling pathways intersects by Fyn in normal and diseased erythropoiesis.

2. ABBREVIATIONS

ALA: δ aminolevulinic acid

ALAS: δ aminolevulinic acid synthase

AMPK: AMP activated protein kinase

ARE: antioxidant responsive element

Atg 3: autophagy related protein 3

Atg 4: autophagy related protein 4

Atg 5: autophagy related protein 5

Atg 7: autophagy related protein 7

Atg 10: autophagy related protein 10

Atg 12: autophagy related protein 12

Atg 14: autophagy related protein 14

Atg 16: autophagy related protein 16

Atg 101: autophagy related protein 101

BFU-E: burst forming unit-erythroid

BMMC: bone marrow derived mast cell

BMPR: bone morphogenetic protein receptor

β-thal: β-thalassemia

CFU-E: colony forming unit erythroid

CML: chronic myelogenous leukemia

CPgenIII: coproporphynogen III

DOXO: doxorubicin

EKLF: erythroid Kruppel like factor

EPO: erythropoietin

EPO-R: erythropoietin receptor

ERFE: erythroferrone

ERK: extracellular signal regulated kinase

FECH: ferrochelatase

FIP200: FAK family interacting protein of 200 KDa

FOXO 3a: forkhead box 0 3a

Fpn: ferroportin

GAPDH: glyceraldehyde 3-phosphate dehydrogenase

G6PD: glucose-6-phosphate dehydrogenase

Hamp: hepcidin

HBB: hemoglobin B

HBA: hemoglobin A

HistH3: histone H3

HO-1: heme oxygenase 1

Hp: haptoglobin

HSC: hematopoietic stem cell

HSP70: heat shock protein 70

hVps34: class III phosphoinositide 3 kinase

IL-6: interleukin 6

IRE: iron responsive element

IRP: iron responsive protein

Keap1: Kelch like ECH associated protein 1

KIR: Keap1 interacting region

LC3: microtubule associated protein 1A/1B light chain

LDH: lactate dehydrogenase

LIR: LC3 interacting region

mTOR: mammalian target of rapamycin

NAC: N-acetyl cysteine

NQO1: NADPH dehydrogenase quinone 1

Nrf2: nuclear factor (erythroid derived 2) like 2

P: phospho

Pop I: pro-erythroblasts

Pop II: basophilic erythroblasts

Pop III: polychromatic erythroblasts

Pop IV: orthochromatic erythroblasts

PHZ: phenylhydrazine

PPIX: protoporphyrin IX

Prx 1: peroxiredoxin 1

Prx 2: peroxiredoxin 2

PV: polycythemia vera

Rapa: rapamycin

RBC: red blood cell

ROS: reactive oxygen species

SFK: src family kinase

SH1: src homology 1

SH2: src homology 2

SH3: src homology 3

SOD-1: superoxide dismutase 1

TB: total bilirubin

Tyr: tyrosine

TMPRSS6: transmembrane protease serine 6

TPO: thrombopoietin

ULK 1: UNC 51 like kinases 1

3. INTRODUCTION

3.1 Erythropoiesis

Erythrocytes transport and exchange O_2/CO_2, participating to key processes in cellular homeostasis and tissue function(s). In the peripheral circulation, red cells survive 120 days, based on their ability to go through the narrow capillaries on microcirculation system. Aged erythrocytes (i.e.: red cell membrane oxidation, lipid peroxidation) are efficiently removed by macrophages mainly localized in spleen. Thus, erythropoiesis plays a crucial role to ensure the constant renewal of erythroid population.[1]

During development, a first wave of erythropoiesis, described as *primitive* erythropoiesis, begins in the yolk sac, characterized by large and nucleated cells. Subsequently, *definitive* erythropoiesis, in the developing fetal liver, produces small-enucleated cells, which will then occur in the bone marrow of adult.[1]

Erythropoiesis is a dynamic complex multistep process going from committed erythroid progenitors to erythroid precursors and circulating mature red cells (Fig. 1).[2]

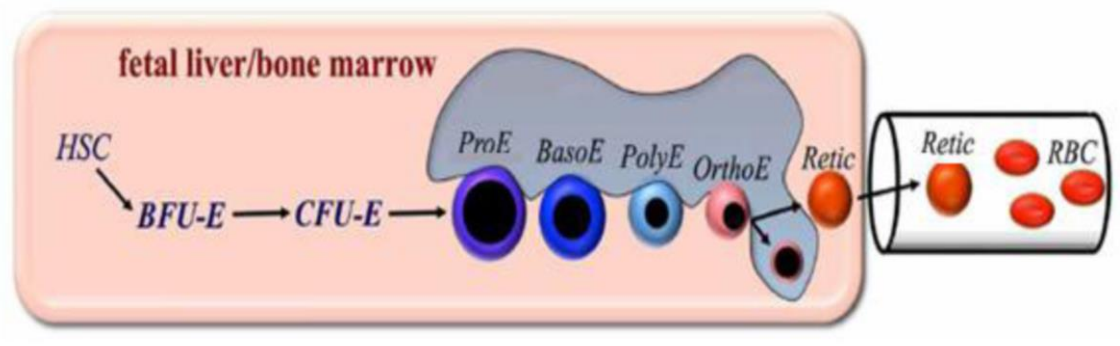

Fig. 1: **The process of erythropoiesis**

(modified from Palis J. Primitive and definitive erythropoiesis in mammals. Front. Physiol. 2014; 5:3)

Erythropoiesis is divided into 3 phases: early erythropoiesis, late erythropoiesis, corresponding to terminal erythroid differentiation, and reticulocyte maturation. Early erythropoiesis refers to the process by which multi-potential hematopoietic stem cells (HSC) proliferate and differentiate into committed erythroid progenitors.[2] The first

erythroid-specific progenitor is the burst forming unit-erythroid (BFU-E), through processes influenced by several multipotent cytokines, such as IL-3 or SCF. The BFU-Es expand and develop into erythropoietin (EPO)-responsive colony forming unit-erythroid (CFU-E), which further expand and differentiate into pro-erythroblasts.[3] Terminal erythroid differentiation begins with morphologically recognizable pro-erythroblasts, which subsequently undergo sequential mitoses to become basophilic, polychromatic, and orthochromatic erythroblasts that enucleate to become reticulocytes. During terminal erythroid differentiation, several changes occur, including decrease in cell size, hemoglobinization, increased chromatin condensation, and enucleation. In addition, terminal differentiation is also accompanied by dramatic changes in the expression, as well as assembly, of membrane proteins.[3-5]

Erythroid maturation is strictly dependent on EPO signaling cascade.[5-6] EPO physically interacts with its receptor (EPO-R), which expression is downregulated after the basophilic erythroblasts stage.[7] Binding of EPO to EPO-R results in EPO-R conformational change and it requires the activation of Jak2, as primary kinase. Jak2 phosphorylates EPO-R, resulting in activation of multiple signaling pathways such as (I) the STAT5-Bcl_{XL} system, involved in maturation and survival of erythroid precursors; and (II) the PI3-Kinase/Akt pathway,[8-10] promoting both anti-apoptotic and proliferation signals.[4]

STAT5 is a master of erythropoiesis and it resides in cytoplasm. In response to EPO signaling, it binds phospho-tyrosine (Tyr) residues (Y343) on EPO-R cytoplasmic tail. STAT5 is then Tyr-phosphorylated and it translocates into the nucleus, initiating the transcription of several genes important in terminal erythroid differentiation.[11-14] This includes genes involved in suppression of cytokine signaling (Cish and Socs3) or in epigenetic regulation (Suv420h2).[15-16]

Recent studies have shown that mice genetically lacking STAT5 develop anemia, due to ineffective erythropoiesis, associated with a blunted response to erythropoietic stress. A reduction in Bcl-$_{XL}$ expression has been documented in $STAT5^{-/-}$ mice, leading to decrease survival of early stage erythroblasts, further supporting the important role of STAT5 in normal and stress erythropoiesis.[11-14]

Abnormalities in Jak2/STAT5 signaling pathway have been described in pathologic erythropoiesis such as β-thalassemia (β-thal) or Polycytemia Vera (PV).[17]

β-thal is an inherited red cell disorder characterized by reduced or absent production of β-globin chains. Ineffective erythropoiesis is one of the hallmarks of β-thal, characterized by (i) block in cell differentiation and expansion of erythroid precursors; (ii) severe oxidation mainly due to accumulation of free alpha chains; (iii) apoptosis of polychromatophilic erythroblasts. Extramedullary erythropoiesis and iron overload are additional elements related to the ineffective erythropoiesis, contributing to clinical severity of β-thal.[18-20] Increased activation of Jak2/STAT5 axis has been shown in β-thal. Evidences in a mouse model for β-thal suggest Jak2/STAT5 axis as possible therapeutic target in β-thal. Ongoing phase II trial with ruxolitinib (NCT02049450), a Jak2 inhibitor, in regularly transfused β-thal patients has shown promising results in reducing extramedullary erythropoiesis and splenomegaly.[21]

Giving the importance of Jak2 kinase as initiator of the EPO signaling cascade, additional kinases, such as Lyn, a Src family kinase, has been described to participate to EPO pathway. Lyn is able to phosphorylate EPO-R, Jak2 itself and STAT5 (see also section 1.2.1).[4,22]

The activation of EPO/Jak2 signaling pathway is associated with production of reactive oxidative species (ROS), which are also generated by a large amount of iron imported into the cells during heme biosynthesis.[23] In erythropoiesis, ROS may function as second messenger through the transient oxidation of cysteine residues on signaling targets, further contributing to increase the complexity of signal transduction in response to EPO. To ensure cell survival, proliferation and differentiation, the control of oxidative stress is crucial during erythropoiesis. This is supported by abnormalities of erythropoiesis reported in mice genetically lacking antioxidant or cytoprotective systems, such as Peroxiredoxin 2 (Prx2) or Superoxide Dismutase 1 (SOD1).[24-25] In β-thal mice, our group has recently shown the importance of the interplay between Prx2 and the redox-sensitive transcription factor, Nrf2 (Nuclear factor (erythroid-derived 2)-like 2) in supporting β-thal pathologic erythropoiesis.[24]

In response to oxidation, Nrf2 binds the Antioxidant Response Element (ARE) region of genes encoding for anti-oxidant or cytoprotective systems, such as heme oxygenase (HO-1), NADPH dehydrogenase quinone 1 (NQO1) or Prxs.[26]

Studies in β-thal erythropoiesis have highlighted the importance of another redox-related transcriptional factor: FOXO3a.[27-28] FOXO3a belongs to the Forkhead Box O

(FoxO) family of transcription factors and responds to oxidative stress by the upregulation of ROS scavenging enzymes such as Superoxide Dismutase 2 (SOD2) or catalase.[28] Mice genetically lacking FOXO3a are extremely sensitive to exogenous oxidative stress, such as that induced by phenylhydrazine (PHZ).[28]

Collectively, these studies indicate the importance of the modulation of intracellular signal transduction during erythropoiesis as well as the adaptive mechanisms activated in response to oxidation. Although progresses have been made in characterization of signaling pathways and cell protective machinery during erythroid maturation, much still remain to be investigated in normal and pathological erythropoiesis.

3.1.2 Erythropoiesis and iron homeostasis

Iron is an essential element in cellular homeostasis and it is involved in redox controlled reactions, required in enzymatic cascade as well as in signal transduction pathways.[29] Since the large part of iron is required in hemoglobin synthesis, erythropoiesis deeply affects iron metabolism.[30] Studies in both acquired and inherited disorders characterized by either iron-deficiency or iron-overload have highlighted new mechanisms involved in iron homeostasis.[29-30]

3.1.3 Hepcidin systemic iron homeostasis

Hepcidin (Hamp) is the master regulator of iron homeostasis. Hamp is mainly synthesized by hepatocytes.[31] Hamp inhibits the transfer of dietary iron from duodenal enterocytes to plasma, the release of recycled iron from macrophages, predominantly in the spleen and the release of stored iron from hepatocytes.[32] This cascade is related to the functional crosstalk between Hamp and its receptor ferroportin (Fpn), resulting in decreased iron release from cells to plasma and extracellular fluid.[31-32]

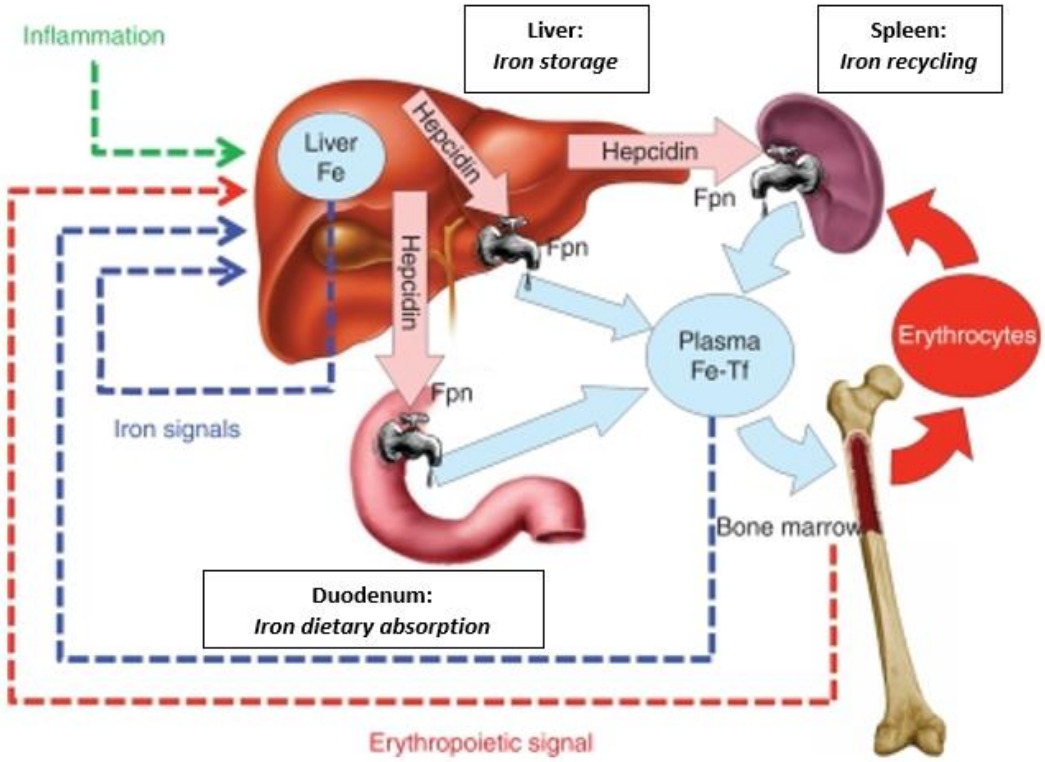

Fig. 2: Iron homeostasis

(modified from Ganz T. Systemic iron homeostasis. Physiol Rev. 2013; 93:1721-41)

Hamp expression is affected by: (I) iron levels or inflammation as stimulatory factors; (II) erythropoietin-stimulated expansion of erythroid precursors as inhibitory factor (Fig. 2).[31]

Transferrin-bound iron concentrations contributes to regulation of Hamp expression. This regulatory pathway involves the bone morphogenetic protein receptor (BMPR) complex that signals predominantly through the SMAD4 pathway towards Hamp.[31-32] BMP6 binding to BMPR, limits further intestinal iron absorption and release of iron from macrophage stores. Hemojuvelin (also known as HFE2), is another iron-specific ligand playing a role in Hamp expression. Hemojuvelin interacts with both BMPs and the BMPR, and it is negatively regulated through specific proteolytic cleavage by transmembrane protease serine 6 (TMPRSS6; also known as matriptase 2).[31-32] Finally, interleukin-6 (IL-6) is also involved in Hamp expression in response to inflammatory storm.[31-32] IL-6 activates the Jak2/STAT3 pathway inducing Hamp expression. Our group has recently shown that the absence of Prx2 results in perturbation of IL6 independent STAT3 activation towards Hamp expression, highlighting the novel role of Prx2 in iron homeostasis.[33]

Progresses in the knowledge of the functional link between iron homeostasis and pathologic erythropoiesis has allowed the identification of Erythroferrone (ERFE).[34] ERFE suppresses Hamp expression through a still unknown mechanism, possibly involving the BMP/SMAD signaling pathway.[35-36]

3.1.4 Erythropoiesis and heme

Heme biosynthesis is another crucial event in erythroid hemoglobinization. In all cells, heme synthesis occurs through 8 enzymatic reactions, divided between mitochondria and cytosol compartments. During erythropoiesis, heme synthesis increases with cell differentiation and it is tightly coordinated with iron acquisition and globin gene synthesis.[37-40]

In heme biosynthesis, the first step is the condensation of succinyl-CoA and glycine to form δ-aminolevulinic acid (ALA) in mitochondrial matrix. This reaction is catalyzed by ALA synthase (ALAS), which is considered a rate-limiting event. There are two isoforms of ALAS, ALAS1 and ALAS2, which are encoded by separated genes. *Alas1* gene is located on chromosome 3 and it is ubiquitously expressed. It plays an important housekeeping function in providing heme in non-erythroid tissues.[37-40] Otherwise, *Alas2* gene is located on the X-chromosome and it is expressed exclusively in erythroid cells. *Alas2* expression strongly increases during the late stages of erythroid differentiation and it is essential for terminal maturation of red cells.[41-42] The expression of *Alas2* is regulated by erythroid-specific transcription factors, such as GATA-1.[43] At post-transcriptional level, *Alas2* expression is sensitive to iron intracellular levels. *Alas2* transcript contains a 5' iron responsive element (IRE) that interacts with iron responsive proteins (IRPs), linking the regulation of heme biosynthesis to the availability of iron in erythroid cells.

ALA is then exported to the cytosol, where it is converted to coproporphyrinogen III (CPgenIII). Then, CPgenIII is imported back to mitochondria and it is converted to protoporphyrin IX (PPIX). Finally, ferrous iron (Fe^{2+}) is incorporated into PPIX to form heme in mitochondrial matrix, a reaction catalyzed by ferrochelatase (FECH) (Fig. 3).[44] Recently, two heme exporters have been described: (I) FLVCR1a, localized in cellular plasma membrane; (II) FLVCR1b, localized in mitochondria plasma membrane. The coordinated expression of FLVCR1a and FLVCR1b contributes to control the size of the

cytosolic heme pool required to sustain metabolic activity during the expansion and hemoglobinization of erythroid cells (Fig. 3).[38-40,45,46]

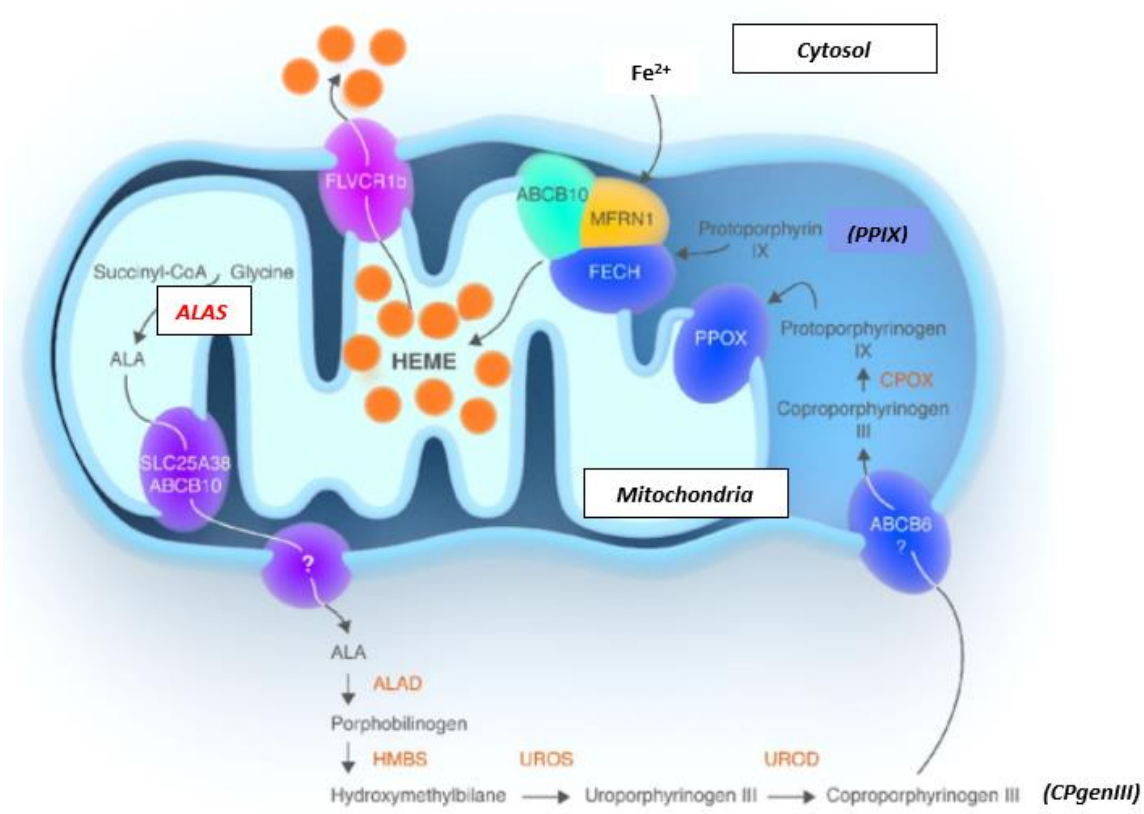

Fig. 3: **Heme biosynthesis**

(modified from Tolosano E, et al. Heme and erythropoiesis: more than a structural role. Haematologica. 2014; 99:973-983)

3.2 Src family kinases (SFKs)

Src family kinases (SFKs) are a group of cytoplasmatic Tyrosine (Tyr)-kinases, which are involved in signal transduction pathways important in cell homeostasis.[47] SFKs comprises 9 members of kinases (Src, Fgr, Hck, Lyn, Yes, Lck, Fyn, Frk and Blk) some of which are expressed in a variety of cell types, whereas other are primarily expressed by hematopoietic cells, such as Lyn, Fyn or Src.[48] SFKs exhibit a conserved domain organization that allows them to establish physical association with receptors and different proteins located upstream/downstream in signal cascades.[48]

All family members are characterized by an N-terminal unique region (50-70 residues) of high variability always encompassing a myristoylation and sometimes a palmitoylation site, flowed by the ~ 50 amino acid Src homology 3 (SH3) domain, which

directs specific association with proline rich motifs related to the PXXP consensus.[49-54] This is followed by ~ 100 amino acid Src homology 2 (SH2) domain which provides the interaction with phosphor-Tyr motifs and confers recognition and regulatory proprieties. The last domain is the kinase (~ 300 residues), or catalytic domain, or Src homology 1 (SH1), responsible for the enzymatic activity (Fig. 4).[49-54]

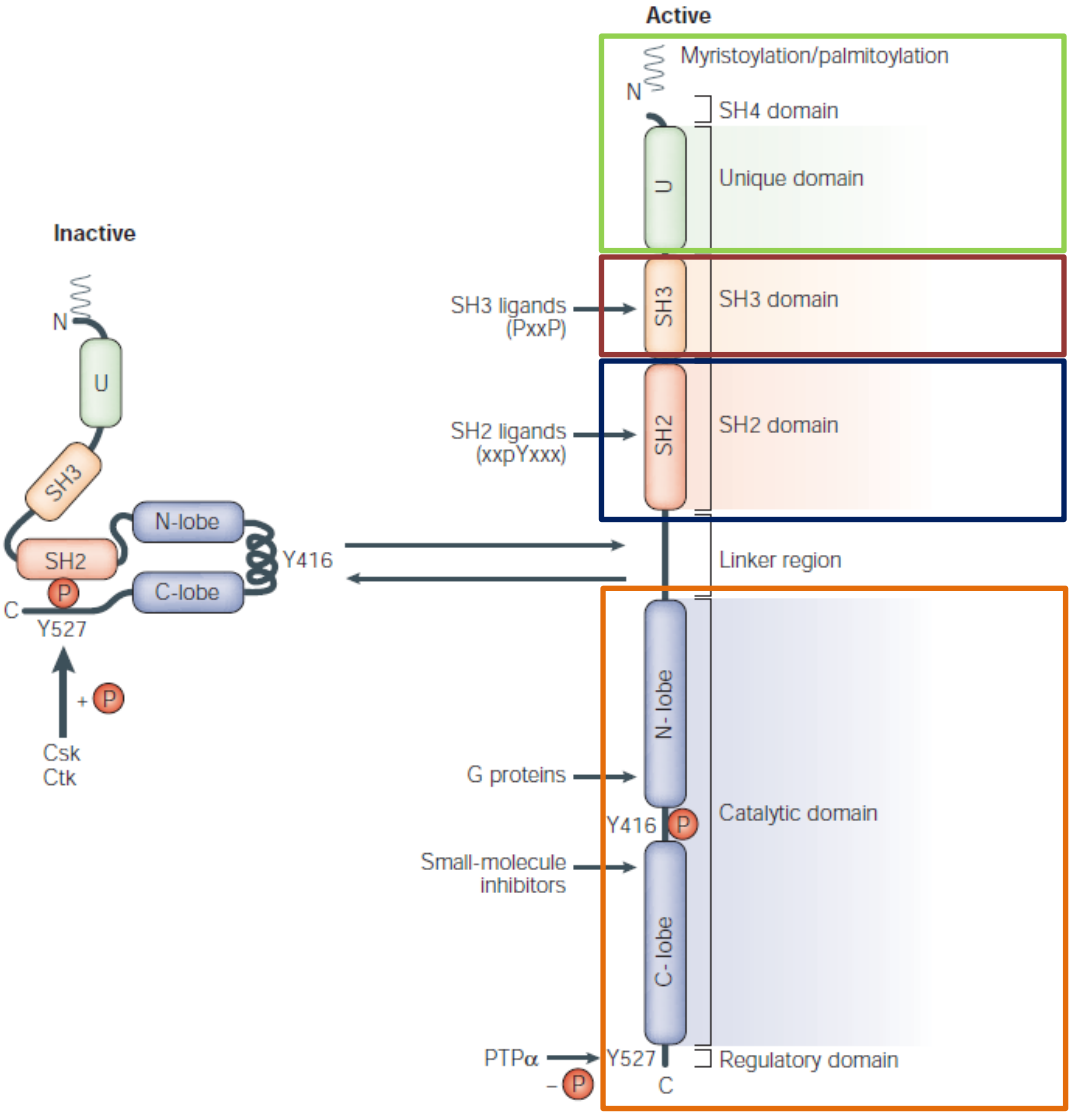

Fig. 4: Domain organization of the SFKs

(modified by Salter MW, et al. Src kinases: a hub for NMDA receptor regulation. Nat Rev Neurosci, 2004; 5:317-328)

SFKs have two Tyr-motifs that regulate their activity in opposing ways. There is the activation loop (A-loop) residue, between the N-lobe and the C-lobe of the kinase domain, that is Tyr-phosphorylated in the fully active configuration, while the C-terminal Tyr-motif is phosphorylated in the fully inactive structure.[55-57] This latter can interact with its own SH2 domain, making phospho-Tyr tail relatively inaccessible to phosphatase catalysis, inactivating SFK.[58] It is likely that the combined interactions of the SH3 and the SH2 domains stabilize the overall inactive SFK's configuration through the synergic effects of the two domains. Tyr-phosphorylation of the A-loop site has been detected in the most highly active forms of SFKs and seems to be important for the maximal kinase activity possibly deleting the auto-inhibitory SH3/SH2 intra-molecular interactions.[59] This phosphorylation is likely to be mediated by a trans-autophosphorylation, indicating that SFK members can crosstalk each other through the phosphorylation of the A-loop site.[60] Thus, SFKs might be present as: 1) *fully closed inactive form* due to the intra-molecular SH3/SH2 interactions, a phosphorylated C-tail and an unphosphorylated A-loop; 2) *partially active form* in which the SH3 and/or SH2 interactions are disrupted, but the A-loop is not phosphorylated; 3) *fully active form* with the A-loop phosphorylated with or without SH3/SH2 association displacement.[61] The autophosphorylation site of SFKs, plays a pivotal role when SFK is un-phosphorylated, forming a short α-helix that prevents substrate binding and sequesters the A-loop Tyr. This makes the A-loop unavailable for phosphorylation, stabilizing the inactive kinase conformation. Otherwise, when the A-loop is phosphorylated, the Tyr forms a salt bridge with a conserved arginine that helps stabilizing the enzymatic active SFK configuration.[62]

3.2.1 SFKs and erythropoiesis

Among SFKs, Lyn has been recently involved in EPO signaling cascade.[63,64] Lyn targets specific Tyr-residue on the cytoplasmic tail of Epo-R, contributing to the signaling events involved in erythroid maturation and differentiation.[63,64] Mouse models either lacking Lyn ($Lyn^{-/-}$) or displaying hyperactive Lyn ($Lyn^{up/up}$), show abnormalities in baseline erythropoiesis and in stress erythropoiesis .[63,64]

Table 1. Effects of the absence or hyperactivation of Lyn on immune-hematopoietic system		
Mouse strain	**Hematological phenotype**	**References**
$Lyn^{-/-}$ mice	- Age-dependent anemia; - Extramedullary erythropoiesis with splenomegaly; - Dyserythropoiesis; - Increase reticulocyte count; - Reduced bone marrow progenitor expansion capacity and impaired precursors maturation/differentiation upon EPO stimulation; - Autoimmune disease related to lymphoid abnormalities; - Perturbations of myelopoiesis with age-related increase of myeloid progenitors.	[64] [65] [66] [67]
$Lyn^{up/up}$ mice	- Abnormal red blood morphology (acanthocytes and spherocyte-like cells); - Chronic mild hemolytic anemia; - Increased progenitor expansion capacity and enhanced precursors maturation and differentiation; - Extramedullary erythropoiesis; - Age-related bone marrow exhaustion.	[68][69] [70]

Studies in these mouse models have allowed the identification of signaling pathways intercrossed by Lyn such as, GAB2/Akt/FOXO3 acting as pro-survival system or ERK1/2 (extracellular-signal-regulated kinase 1/2) as pro-apoptotic signal.[64-67]

$Lyn^{-/-}$ mice show reduced STAT5 activity, which results in decreased expression of Bcl_{XL}, a molecule with anti-apoptotic function in erythropoiesis. [64-67]

In addition, $Lyn^{up/up}$ erythroblasts display increased proteolytically degradation of EPO-R, suggesting an accelerated EPO-R turnover. This is associated with elevated Jak2 activation partially independent from EPO stimulation. Increased EKLF and STAT5 phosphorylation has been noted in $Lyn^{up/up}$ erythroblasts, indicating possible downstream compensatory mechanism to constant activation of Lyn during erythropoiesis in this mouse strain.[68-70] Finally, perturbation of Lyn function also affects

two master systems in erythropoiesis, GATA-1 and EKLF (Erythroid Kruppel-like factor).[64-67]

3.3 Fyn is an emerging SFK

Fyn is another member of SFKs. Fyn is primarily localized to the cytoplasmic leaflet of the plasma membrane, where it phosphorylates Tyr-residues on key targets involved in a variety of different signaling pathways.[71] This is functional to either regulate target proteins activity and/or generate a docking site on target proteins, allowing the recruitment of other signaling molecules.[72] Fyn is important in cell growth and survival, cell adhesion, integrin-mediated signaling, cytoskeletal remodeling, cell motility, immune response and axon guidance.[71]

The large part of available studies on mice genetically lacking Fyn are limited to neurobiology and brain system. [72-74]

3.3.1 Fyn and hematopoiesis

In different blood cells and during hematopoiesis, recent studies have highlighted the role of Fyn as positive mediator of STAT5 function. In mast cell, Fyn is required for FcεRI-mediated STAT5 activation with possible additional role in stabilization of un-phosphorylated STAT5.[75-78] Studies on $Fyn^{-/-}$ bone marrow-derived mast cells (BMMCs) reveal abnormalities of STAT5 activation, leading to impairment of mast cells degranulation.[75] Involvement of Fyn in STAT5 activation has been also documented in chronic myelogenous leukemia (CML).[79] In CML, Fyn has been proposed to contribute to the cyclophosphamide cell resistance, suggesting Fyn as a possible new therapeutic target in CML.[79]

Fyn also participates to thrombopoietin (TPO)-induced cascade during *in vitro* megakaryopoiesis. Thus, Fyn may play a pivotal role as an additional kinase to the canonical TPO/Jak2 pathway in megakaryopoiesis.[80-82]

3.3.2 Fyn is a redox sensor

In different cell types, growing evidence indicate Fyn as primary redox sensor in oxidation-induced signaling pathway.[83-84] Fyn might act as regulatory nexus between oxidation and signal transduction such as in its interaction with Nrf2. In fact, Fyn has been involved in post-induction regulation of the redox-sensitive transcription factor Nrf2.[85-86] In presence of a severe cellular oxidative stress, Nrf2 translocates into the nucleus activating the expression of acute phase defensive genes.[85-86] Then, Nrf2 is switched-off by Fyn, which phosphorylates Tyr-568 on Nrf2, resulting in its nuclear export and ubiquitylation. [85-86] Mutagenesis experiments have shown that mutation of Tyr-213 on Fyn affects both nuclear localization and inactivation of Nrf2, increasing cell susceptibility to death.[85-86] It has been reported that the prolonged activation of Nrf2 results in accumulation of polyubiquitylated proteins with an imbalance between protein synthesis and protein degradation.[87-88] In various cell types, the persistence of Nrf2 signaling has been shown to be linked to impaired autophagy, a main cellular defensive process against the accumulation of damaged proteins.[89]

3.4 Autophagy and erythropoiesis

3.4.1 Autophagy

Autophagy is an efficient catabolic process responsible for the clearance of damaged organelles and proteins, contributing to cell homeostasis.[90-93] Autophagy is generally activated by starvation or low levels of oxidation, whereas a more intense or prolonged oxidative stress overcomes autophagy flux and culminates in cell apoptosis. [94,95] Autophagy starts with the engulfment of cellular materials by a double-layered structure, called the phagophore, that elongates, then closing to form the autophagosome. Finally, mature autophagosomes fuse with lysosomes, creating the autolysosome, where lysosomal hydrolytic enzymes degrade the cellular content (Fig. 5).[96]

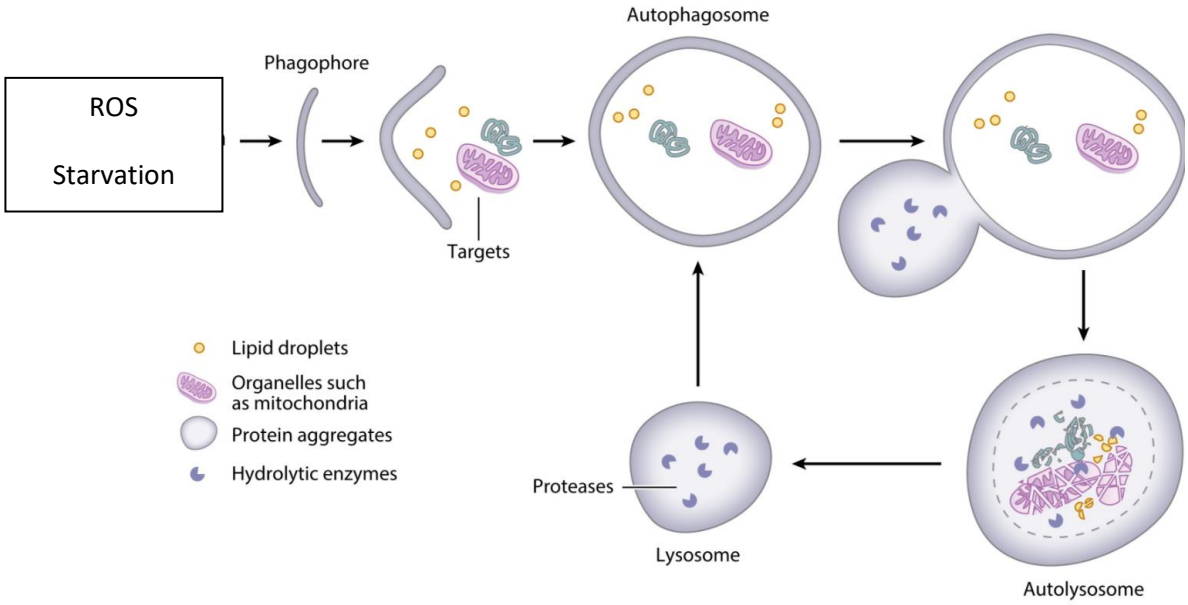

Fig. 5: The process of autophagy
(modified by Dikic I. Proteasomal and autophagic degradation systems. Annu. Rev. Biochem. 2017; 86:193-224)

The core machinery of autophagy consists of autophagy-related proteins (Atg), redox-sensitive proteins that might be either directly modulated by ROS (e.g.: Atg4 or Atg7) or transcriptionally regulated by oxidative stress (e.g.: p62).[97-101] The functional connection between ROS and autophagy is also supported by the improvement of autophagy promoted by exogenous anti-oxidants, such as N-Acetyl-cysteine (NAC).[97-99] Ulk1 phosphorylation is considered one of the main determinants and initiator of autophagy.[91,96] The second key complex is the Beclin1/PI3K3, whose activity is dependent on ULK1 phosphorylation. Beclin1/PI3K3 drives the phagophore formation, followed by the recruitment of ubiquitin-like Atg5-Atg12-Atg16L complex that is required for autophagosome formation.[102] This latter, together with Atg4 and Atg7, can activate the microtubule-associated protein 1A/1B light chain 3 (LC3) via lipidation with phosphatidylethanolamine (PE) to generate LC3-II. LC3-II anchors to inner and outer membranes of autophagosomal structures and it is required for phagophore expansion and fusion.[91,96,102] In addition, LC3-II recruits proteins carrying the LC3-interacting region (LIR) to the autophagosome (Fig.6).[91,103] The cargo elements are then directed by autophagy binding adaptor molecules, such as p62, to the terminal phase of autophagy.[91,104] p62 is a multifunctional protein consisting of different

domains and delivers polyubiquitinated cargoes to autophagy pathway through LIR domains and/or to proteasomal degradation via the N-terminal.[96,104]

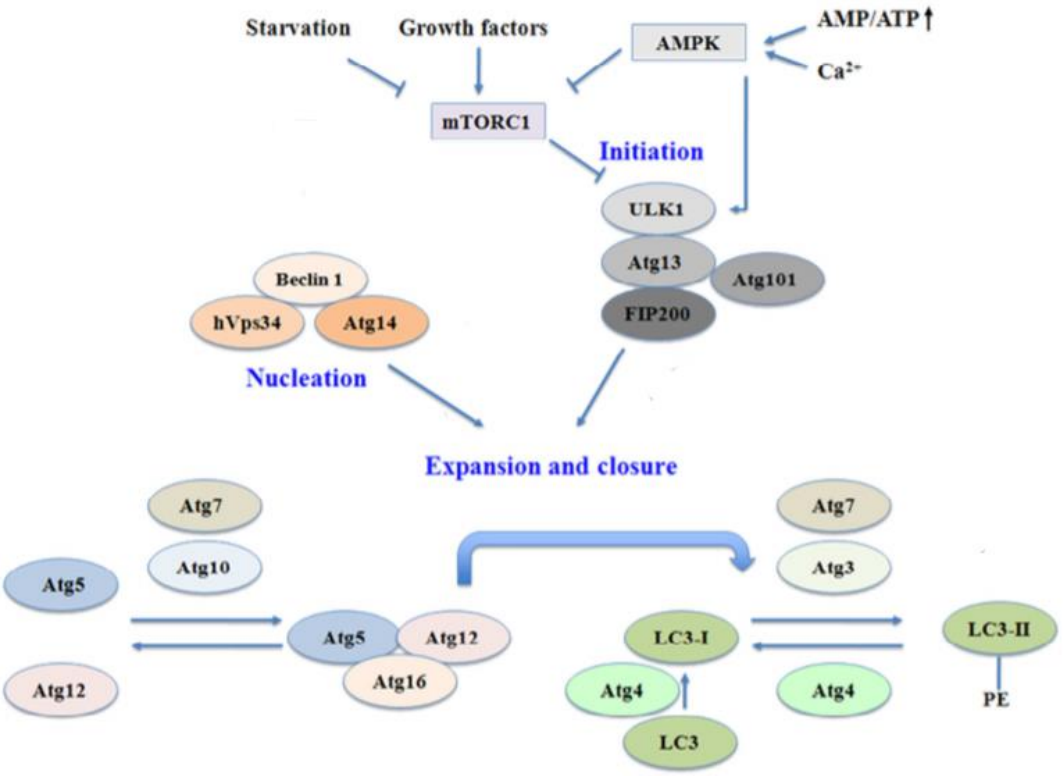

Fig. 6: Schematic representation of autophagy cascade

(modified by Codogno P. Mechanisms and regulation of autophagy in mammalian cells. Atlas of Genetics and Cytogenetics in Oncology and Hematology,2011)

mTORC1= mammalian target of Rapamycin complex 1; **AMPK**= AMP-activated protein kinase; **ULK1=** UNC-51-like kinases 1 **Atg13=** autophagy-related protein 13; **Atg101=** autophagy-related protein 101; **FIP200=** FAK family-interacting protein of 200 kDa; **hVps34=** Class III phosphoinositide 3-kinase; **Atg14=** autophagy-related protein 14; **Atg5=** autophagy-related protein 5; **Atg10=** autophagy-related protein 10; **Atg7=** autophagy-related protein 7; **Atg16=** autophagy-related protein 16; **Atg4=** autophagy-related protein 4; **LC3=** Microtubule-associated protein 1A/1B-light chain 3 (**I,** cytosolic form; **II,** membrane bound form); **Atg3=** autophagy-related protein 3; **Atg12=** autophagy-related protein 12.

3.4.2 Autophagy and erythropoiesis

In erythropoiesis, autophagy plays a pivotal role in removal of organelles, such as ribosomes or mitochondria (mitophagy), as well as of damaged cytosolic proteins, allowing the generation of mature red cells.[104,105] During erythropoiesis, ROS generation, nutrients deprivation and activation of AMP-activated protein kinase

(AMPK) inhibits the mammalian target of rapamycin complex 1 (mTORC1), which is a key repressor of autophagy.[96,105] Studies on mouse models lacking members of the autophagy cascade have allowed the progress in the knowledge on autophagy during erythropoiesis. The table below summarizes the main results on autophagy and erythropoiesis based on the revision of the literature.

Table 2. Mouse models genetically lacking proteins related to autophagy and erythropoiesis

Mouse strain	Protein function	Main findings	Ref.
Ulk1$^{-/-}$ mice	Regulation of mitochondrial and ribosomal clearence	- Reticulocytosis; - Increased mean cell volume (MCV), mean corpuscular hemoglobin level(MCH) and relative distribution width (RDW); - Delayed removal of mitochondria and ribosomes, resulting in delayed red cell maturation; - Splenomegaly;	[105] [106] [107] [108]
Atg5$^{-/-}$ mice	Regulation of autophagosome formation	- Decrease in hematopoietic stem cells proliferation; - Impaired cell cycle progression and increased apoptosis; - Neonatal lethality due to neuronal dysfunction; - Iron deficiency anemia;	[109] [110]
Atg7$^{-/-}$ mice	Regulation of mitochondrial removal	- Reduction in hematopoietic stem cells and progenitors of multiple lineage; - Impaired formation of autophagosomes; - Erythroid maturation defect; - Anemia and reticulocytosis; - -Impaired clearance of mitochondria	[111] [112] [113] [114]

Nix$^{-/-}$ mice	Modulation of mitochondrial clearance and autophagosome formation	- Presence of abnormal mitochondrial residues; - Hemolytic anemia and erythroid hyperplasia; - Increased caspase activation and phosphatidylserine exposure leading to cell death and erythroid maturation defect; - -Reticulocytosis; - Abnormal reticulocytes maturation;	[115] [116] [117]

3.4.3 Autophagy and Nrf2

On steady state, Nrf2 is stabilized in the cytoplasm by Kelch-like ECH-associated protein 1 (Keap1).[118,119] Under oxidation, Nrf2 is activated, dissociated from Keap1 and it translocates into the nucleus. When Nrf2 function is completed, Nrf2 migrates into the cytoplasm to be ubiquitylated. In the meantime, p62 interacts with Keap1 through the Keap1-interacting region (KIR), re-directing Keap-1 towards autophagic degradation (Fig. 8).[96,120]

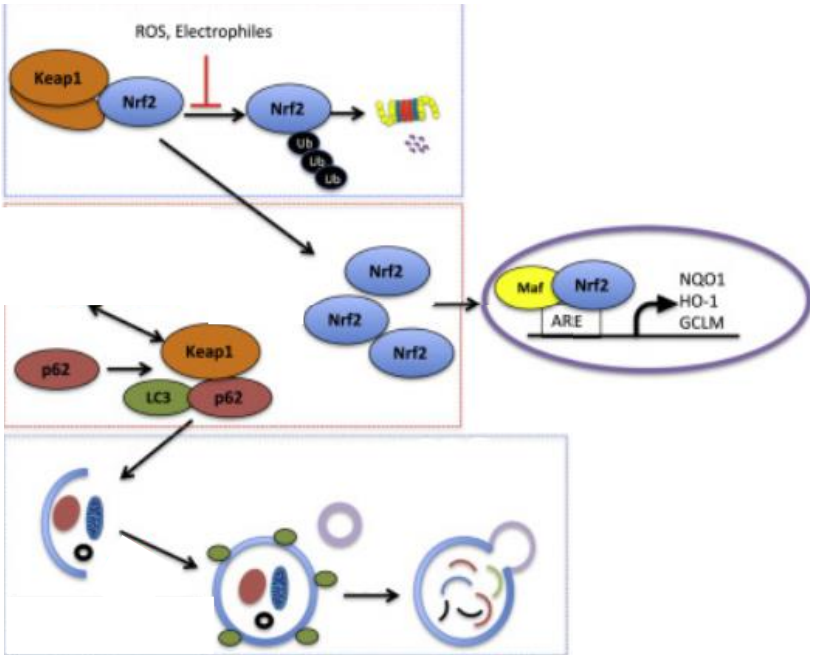

Fig. 8: **The p62-KEAP1-Nrf2 axis in stress response**
(modified by Zhang DD, et al. p62 links autophagy and Nrf2 signaling. FRBM, 2015;88:199-204)

Thus, an interplay has been established between Nrf2 degradation and autophagy. p62 is involved in protein quality control mechanism. It binds to the Nrf2 shuttle protein Keap1, participating to Keap1 turnover. Thus, accumulation of p62 might be used as hallmark of impaired autophagy.[121] Our group has recently reported a new molecular link between defective autophagy in terminal erythroid differentiation in patients with chorea-acanthocytosis.[121] Once again, the accumulation of p62 was a marker of repressed autophagy in this model of diseased red cell.

4. REFERENCES

1. **Palis J, Robertson S, et al.** Development of erythroid and myeloid progenitors in the yolk sac and embryo proper of the mouse. Development. 1999; **126**:5073-5084.
2. **Orkin SH, et al.** Hematopoiesis: an evolving paradigm for stem cell biology. Cell. 2008; **132**:631-634.
3. **Krantz SB**. Erythropoietin. Blood. 1991; **77**:419-434.
4. **Ingley E, Tilbrook PA, et al.** New insights into the regulation of erythroid cells. IUBMB Life. 2004; **56**:177-184.
5. **Constantinescu SN, Ghaffari S, et al.** The erythropoietin receptor: structure, activation and intracellular signal trasduction. Trends Endocrin Met. 1999; **10**:18-23.
6. **Fang J, et al.** EPO modulation of cell-cycle regulatory genes, and cell division, in primary bone marrow erythroblasts. Blood. 2007; **110**:2361-2370.
7. **Rivella S, et al.** What can we learn from ineffective erythropoiesis in thalassemia? Blood Rev. 2017; **17**:30131-5.
8. **Karthinkeyan G, Lewis LK, et al.** The mitochondrial protein frataxin prevents nuclear damage. Hum Mol Genet. 2002; **11**:1351-1362.
9. **Marinkovic D, et al.** Foxo3 is required for the regulation of oxidative stress in erythropoiesis. Journal of Clinical Investigation. 2007; **117**:2133-2144.
10. **De Franceschi L, et al.** Oxidative stress modulates heme synthesis and induces peroxiredoxin-2 as a novel cytoprotective response in beta thalassemic erythropoiesis. Haematologica. 2011; **96**:1595-1604.
11. **Socolovsky M, et al.** Stat5 signaling specifies basal versus stress erythropoietic responses through distinct binary and graded dynamic modalities. PLOS Biol. 2012; **10**:e1001383.
12. **Lodish HF, et al.** Ineffective erythropoiesis in Stat5a(-/-)5b(-/-) mice due to decreased survival of early erythroblasts. Blood. 2001; **98**:3261-73.
13. **Socolovsky M, et al.** Suppression of Fas-FasL coexpression by erythropoietin mediates erythroblast expansion during the erythropoietic stress response in vivo. Blood. 2006; **108**:123-33.

14. **Perkins AC, et al.** Direct targets of pSTAT5 signalling in erythropoiesis. PLoS One. 2017; **12**:e0180922.
15. **McCarthy DJ, et al.** Differential regulation of SOCS genes in normal and transformed erythroid cells. Oncogene. 2003; **22**:3221-30.
16. **Yoshimura A, et al.** CIS, a cytokine inducible SH2 protein, is a target of the JAK-STAT5 pathway and modulates STAT5 activation. Blood. 1997; **89**:3148-54.
17. **Rivella S, et al.** Modulators of erythropoiesis: emerging therapies for hemoglobinopathies and disorders of red cell production. Hematol Oncol Clin North Am. 2014; **28**:375-86.
18. **Rivella S.** Ineffective erythropoiesis and thalassemias. Curr Opin Hematol. 2009; **16**:187-94.
19. **Rivella S.** The role of ineffective erythropoiesis in non-transfusion-dependent thalassemia. Blood Rev. 2012; **26**:S12-S15.
20. **Ginzburg Y, Rivella S**. beta-thalassemia: a model for elucidating the dynamic regulation of ineffective erythropoiesis and iron metabolism. Blood. 2011; **118**:4321-4330.
21. **Makis A, et al.** 2017 Clinical trials update in new treatments of β-thalassemia. Am J Hematol. 2016; **91**:1135-1145.
22. **Thomas SM, Brugge JS**. Cellular functions regulated by Src family kinase. Annu Rev Cell Dev Biol. 1997; **13**:513-609.
23. **Marty C, et al.** A role for reactive oxygen species in JAK2 V617F myeloproliferative neoplasm progression. Leukemia. 2013; **27**:2187-95.
24. **Mattè A, et al.** The Interplay Between Peroxiredoxin-2 and Nuclear Factor-Erythroid 2 Is Important in Limiting Oxidative Mediated Dysfunction in β-Thalassemic Erythropoiesis. Antioxid Redox Signal. 2015; **23**:1284-97.
25. **Fujii J, et al.** Elevated oxidative stress in erythrocytes due to a SOD1 deficiency causes anaemia and triggers autoantibody production. Biochem J. 2007; **402**:219-27.
26. **Kovac S, et al.** Nrf2 regulates ROS production by mitochondria and NADPH oxidase. Biochim Biophys Acta. 2015; **1850**:794-801.
27. **Franco SS, et al.** Resveratrol accelerates erythroid maturation by activation of FoxO3 and ameliorates anemia in beta-thalassemic mice. Haematologica. 2014; **99**:267-275.

28. **Ghaffari S, et al.** Foxo3 is required for the regulation of oxidative stress in erythropoiesis. J Clin Invest. 2007; **117**:2133-44.

29. **Moura IC, et al.** Erythropoiesis and transferrin receptors. Curr Opin Hematol. 2015; **22**:193-8.

30. **Li H, Ginzburg YZ.** Crosstalk between iron metabolism and erythropoiesis. Adv Hematol. 2010; **2010**:605435.

31. **Ganz T.** Systemic iron homeostasis**.** Physiol Rev. 2013; **93**:1721-41.

32. **Ganz T, Nemeth E.** Iron homeostasis in host defence and inflammation. Nat Rev Immunol. 2015; **15**:500-10.

33. **Mattè A, et al.** Peroxiredoxin-2: A Novel Regulator of Iron Homeostasis in Ineffective Erythropoiesis. Antioxid Redox Signal. 2017; **28**:1-14.

34. **Ganz T, et al.** Identification of erythroferrone as an erythroid regulator of iron metabolism. Nat Genet. 2014; **46**:678-84.

35. **Camaschella C, et al.** The mutual control of iron and erythropoiesis. Int J Lab Hematol. 2016; **38**:20-6.

36. **Nai A, et al.** Limiting hepatic Bmp-Smad signaling by matriptase-2 is required for erythropoietin-mediated hepcidin suppression in mice. Blood. 2016; **127**:2327-36

37. **Chiabrando D, Tolosano E, et al.** Heme and erythropoiesis: more than a structural role. Haematologica. 2014; **99**:973-83.

38. **Fiorito V, Tolosano E, et al.** Crucial role of FLVCR1a in the maintenance of intestinal heme homeostasis. Antioxid Redox Signal. 2015; **23**:1410-23.

39. **Tolosano E.** Increasing serum transferrin to reduce tissue iron overload due to ineffective erythropoiesis. Haematologica. 2015; **100**:565-6.

40. **Mercurio S, Tolosano E, et al.** The heme exporter Flvcr1 regulates expansion and differentiation of committed erythroid progenitors by controlling intracellular heme accumulation. Haematologica. 2015; **100**:720-9.

41. **Harigae H, et al.** Differential roles of GATA-1 and GATA-2 in growth and differentiation of mast cells. Genes Cells. 1998; **3**:39-50.

42. **Harigae H, et al.** Deficient heme and globin synthesis in embryonic stem cells lacking the erythroid-specific delta-aminolevulinate synthase gene. Blood. 1998; **91**:798-805.

43. **Kaneko K, et al.** Identification of a novel erythroid-specific enhancer for the ALAS2 gene and its loss-of-function mutation which is associated with congenital sideroblastic anemia. Haematologica. 2014; **99**:252-61.

44. **Ajioka RS, et al.** Biosynthesis of heme in mammals. Biochim Biophys Acta. 2006; **1763**:723-36.

45. **Chiabrando D, Tolosano E, et al.** The mitochondrial heme exporter FLVCR1b mediates erythroid differentiation. J Clin Invest. 2012; **122**:4569-79.

46. **Fleming MD, et al.** Mitochondrial heme: an exit strategy at last. J Clin Invest. 2012; **122**:4328-30.

47. **Cohen DM**. SRC family kinases in cell volume regulation. Am J Physiol. 2005; **288**:C483-493.

48. **Espada J.** An Update on Src Family of Nonreceptor Tyrosine Kinases Biology. Int Rev Cell Mol Biol. 2017; **331**:83-122.

49. **Brown MT, Cooper JA**. Regulation, substrates and functions of Src. Biochim Biophys Acta. 1996; **1287**:121-149.

50. **Ingley E**. Src family kinases: Regulation of their activities, levels and identification of the new pathways. Biochimica et Biophysica Acta. 2008; **1784**:56-65

51. **Boggon TJ, Eck MJ**. Structure and regulation of Src family kinases. Oncogene. 2004; **23**:7918-7927.

52. **Koegl M, Zlatkine P, et al.** Palmitoylation of multiple Src-family kinases at a homologous N-terminal motif. Biochem J. 1994; **303**:749-753.

53. **Resh MD**. Fatty acylation of proteins: new insights into membrane targeting of myristoylated and palmitoylated proteins. Biochimica et Biophysica Acta. 1999; **1451**: 1-16.

54. **Koch C, Anderson D, et al**. SH2 and SH3 domains: elements that control interactions of cytoplasmic signaling proteins. Science. 1991; **252**:668-674.

55. **Sicheri F, Moarefi I, et al.** The crystal structure of the Src family tyrosine kinase Hck. Nature. 1997; **385**:602-609.
56. **Williams JC, Weijland A, et al.** The 2.35 A crystal structure of the inactivated form of chicken Src: a dynamic molecule with multiple regulatory interactions. J. Mol. Biol. 1997; **274**:757-775.
57. **Xu W, Harrison SC, Eck MJ.** Three dimensional structure of the tyrosine kinase c-Src. Nature. 1997; **385**:595-602.
58. **Wang D, Esselman WJ, et al.** Substrate conformational restriction and CD45-catalysed dephosphorylation of tail tyrosine-phosphorylated Src protein. J. Biol. Chem. 2002;**277**: 40428-40433.
59. **Sun G, Sharma AK, et al**. Autophosphorylation of Src and Yes blocks their inactivation by Csk phosphorylation. Oncogene. 1998; **17**:1587-1595.
60. **Sun G, Ramdas L, et al.** Effect of autophosphorylation on the catalytic and regulatory properties of protein tyrosine kinase Src. Arch. Biochem. Biophys. 2002; **397**:11-17.
61. **Chong YP, Ia KK, et al.** Endogenous and synthetic inhibitors of the Src-family protein tyrosine kinases. Biochim. Biophys. Acta. 2005; **1754**:210-220.
62. **Smart JE, Oppermann H, et al.** Characterization of sites for tyrosine phosphorylation in the transforming protein of Rous sarcoma virus (pp60v-src) and its normal cellular homologue (pp60c-src). Proc. Natl. Acad. Sci. U. S. A. 1981; **78**:6013-6017.
63. **Chin H, et al.** Lyn physically associates with the erythropoietin receptor and may play a role in activation of the Stat5 pathway. Blood. 1998; **91**:3734-45.
64. **Ingley E, et al.** Lyn kinase plays important roles in erythroid expansion, maturation and erythropoietin receptor signalling by regulating inhibitory signalling pathways that control survival. Biochem J. 2014; **459**:455-66.
65. **Karur VG, et al.** Lyn kinase promotes erythroblast expansion and late-stage development. Blood. 2006; **108**:1524-32.
66. **Ingley E, et al.** Lyn deficiency reduces GATA-1, EKLF and STAT5, and induces extramedullary stress erythropoiesis. Oncogene. 2005; **24**:336-43.
67. **Harder KW, et al.** Perturbed myelo/erythropoiesis in Lyn-deficient mice is similar to that in mice lacking the inhibitory phosphatases SHP-1 and SHIP-1. Blood. 2004; **104**:3901-10.

68. **Ingley E, et al.** Gain-of-function Lyn induces anemia: appropriate Lyn activity is essential for normalerythropoiesis and Epo receptor signaling. Blood. 2013; **122**:262-71.
69. **Tilbrook PA, et al.** Maturation of erythroid cells and erythroleukemia development are affected by the kinase activity of Lyn. Cancer Res. 2001; **61**:2453-8.
70. **Harder KW, et al.** Gain-and loss-of-function Lyn mutant mice define a critical inhibitory role for Lyn in the myeloid lineage. Immunity. 2001; **15:**603-15.
71. **Resh MD.** Fyn, a Src family tyrosine kinase. Int J Biochem Cell Biol. 1998; **30**:1159-1162.
72. **Liu YN, et al.** Fyn kinase-regulated NMDA receptor- and AMPA receptor-dependent pain sensitization in spinal dorsal horn of mice. Eur J Pain. 2014; **18**:1120-1128.
73. **Babus LW, et al.** Decreased dendritic spine density and abnormal spine morphology in Fyn knockout mice. Brain Res. 2011; **1415**:96-102.
74. **Grant SG, et al.** Impaired long-term potentiation, spatial learning, and hippocampal development in Fyn mutant mice. Science. 1992; **258**:1903-1910.
75. **Ryan JJ, et al.** Novel mechanism for Fc{epsilon}RI-mediated signal transducer and activator of transcription 5 (STAT5) tyrosine phosphorylation and the selective influence of STAT5B over mast cell cytokine production. J Biol Chem. 2012; **287**:2045-54.
76. **Olivera A, et al.** A current understanding of Fc epsilon RI-dependent mast cell activation. Curr Allergy Asthma Rep. 2008; **8**:14-20.
77. **Olivera A, et al.** Src family kinases and lipid mediators in control of allergic inflammation. Immunol Rev. 2007; **217**:255-68.
78. **Ryan JJ, et al.** The Fyn-STAT5 Pathway: A New Frontier in IgE- and IgG-Mediated Mast Cell Signaling. Front Immunol. 2012; **3**:117.
79. **Wei Y, et al.** Investigating critical genes and gene interaction networks that mediate cyclophosphamide sensitivity in chronic myelogenous leukemia. Mol Med Rep. 2017; **16**:523-532.
80. **Huang Z, et al.** PSTPIP2 dysregulation contributes to aberrant terminal differentiation in GATA-1-deficient megakaryocytes by activating LYN. Cell Death Dis. 2014; **5**:e988.

81. **Lannutti BJ, et al.** Identification and activation of Src family kinases in primary megakaryocytes. Exp Hematol. 2003; **31**:1268-74.
82. **Lannutti BJ, et al.** Lyn tyrosine kinase regulates thrombopoietin-induced proliferation of hematopoietic cell lines and primary megakaryocytic progenitors. Blood. 2004; **103**:3736-43.
83. **Kim JE, et al.** Fyn is a redox sensor involved in solar ultraviolet light-induced signal transduction in skin carcinogenesis. Oncogene. 2016; **35**:4091-101.
84. **Sanguinetti AR, et al.** Fyn is required for oxidative- and hyperosmotic-stress-induced tyrosine phosphorylation of caveolin-1. Biochem J. 2003; **376**:159-68.
85. **Kaspar WJ, et al.** Tyrosine phosphorylation controls nuclear export of Fyn allowing Nrf2 activation of cytoprotective gene expression. The FASEB Journal. 2011; **25**:1076-1087.
86. **Hayes JD, et al.** The Nrf2 regulatory network provides an interface between redox and intermediary metabolism. Trends Biochem Sci. 2014; **39**:199-218.
87. **Huang Y, et al.** The complexity of the Nrf2 pathway: beyond the antioxidant response. J Nutr Biochem. 2015; **26**:1401-13.
88. **Niture SK, et al.** Nrf2 signaling and cell survival. Toxicol Appl Pharmacol. 2010; **244:**37-42.
89. **Zhangv DD, et al.** p62 links autophagy and Nrf2 signaling. Free Radic Biol Med. 2015; **88**:199-204.
90. **Warnes G.** Flow cytometric assays for the study of autophagy. Methods. 2015; **82**:21-8.
91. **Colombo MI, et al.** Autophagy: A necessary event during erythropoiesis. Blood Rev. 2017; **31**:300-305.
92. **Klionsky DJ, et al.** The regulation of autophagy - unanswered questions. J Cell Sci. 2011; **124**:161-70.
93. **Saftig P, et al.** Autophagy: a lysosomal degradation pathway with a central role in health and disease. Biochim Biophys Acta. 2009; **1793**:664-73.
94. **Marino G, et al.** Self-consumption: the interplay of autophagy and apoptosis. Nat Rev Mol Cell Biol. 2014; **15**:81-94.
95. **Scott RC, et al.** Role and regulation of starvation-induced autophagy in the Drosophila fat body. Dev Cell. 2004; **7**:167-78.

96. **Dikic I.** Proteasomal and Autophagic Degradation Systems. Annu Rev Biochem. 2017; **86**:193-224.
97. **Karantza V, et al.** The interplay between autophagy and ROS in tumorigenesis. Front Oncol 2012;**2**:171.
98. **Elazar Z, et al.** Regulation of autophagy by ROS: physiology and pathology. Trends Biochem Sci 2011;**36**:30-8.
99. **Ciriolo MR, et al.** Under the ROS...thiol network is the principal suspect for autophagy commitment. Autophagy 2010;**6**:999-1005.
100. **Elazar Z, et al.** Reactive oxygen species are essential for autophagy and specifically regulate the activity of Atg4. EMBO J. 2007;**26**:1749-60.
101. **Johansen T, et al.** p62/SQSTM1 is a target gene for transcription factor NRF2 and creates a positive feedback loop by inducing antioxidant response element-driven gene transcription. J Biol Chem. 2010; **285**:22576-91.
102. **Tooze SA, et al.** Autophagosome formation--the role of ULK1 and Beclin1-PI3KC3 complexes in setting the stage. Semin Cancer Biol. 2013; **23**:301-9.
103. **Codogno P, et al.** Mechanisms and regulation of autophagy in mammalian cells. Atlas of Genetics and Cytogenetics in Oncology and Haematology. 2011.
104. **Liu HF, et al.** p62 links the autophagy pathway and the ubiqutin-proteasome system upon ubiquitinated protein degradation. Cell Mol Biol Lett. 2016; **21**:29.
105. **An X, et al.** Autophagy as a regulatory component of erythropoiesis. Int J Mol Sci. 2015; **16**:4083-94.
106. **Shimizu S, et al.** Ulk1-mediated Atg5-independent macroautophagy mediates elimination of mitochondria from embryonic reticulocytes. Nat Commun. 2014; **5**:4004.
107. **Tooze SA, et al.** siRNA screening of the kinome identifies ULK1 as a multidomain modulator of autophagy. J Biol Chem. 2007; **282**:25464-74.
108. **Thompson CB, et al.** Ulk1 plays a critical role in the autophagic clearance of mitochondria and ribosomes during reticulocyte maturation. Blood. 2008; **112**:1493-502.

109. **Kuma A, et al.** Autophagy-monitoring and autophagy-deficient mice. Autophagy. 2017; **13**:1619-1628.

110. **Shimizu S, et al.** Discovery of Atg5/Atg7-independent alternative macroautophagy. Nature. 2009; **461**:654-8.

111. **Mortensen M, et al.** The autophagy protein Atg7 is essential for hematopoietic stem cell maintenance. J Exp Med. 2011; **208**:455-67.

112. **Ney PA, et al.** Mitochondrial clearance is regulated by Atg7-dependent and -independent mechanisms during reticulocyte maturation. Blood. 2009; **114**:157-64.

113. **Komatsu M, et al.** Impairment of starvation-induced and constitutive autophagy in Atg7-deficient mice. J Cell Biol. 2005; **169**:425-34.

114. **Mortensen M, et al.** Loss of autophagy in erythroid cells leads to defective removal of mitochondria and severe anemia in vivo. Proc Natl Acad Sci U S A. 2010; **107**:832-7.

115. **Ney PA, et al.** NIX induces mitochondrial autophagy in reticulocytes. Autophagy. 2008; **4**:354-6.

116. **Wang J, et al.** Essential role for Nix in autophagic maturation of erythroid cells. Nature. 2008; **454**:232-5.

117. **Mortensen M, et al.** Mitochondrial clearance by autophagy in developing erythrocytes: clearly important , but just how much so? Cell Cycle. 2010; **9**:1901-6.

118. **Jaiswal Ak, et al.** Nrf2:INrf2 (Keap1) signaling in oxidative stress. Free Radic Biol Med. 2009; **47**:1304-9.

119. **Yamamoto M, et al.** Stress-sensing mechanisms and the physiological roles of the Keap1-Nrf2 system during cellular stress. J Biol Chem. 2017; **292**:16817-16824.

120. **Stenmark H, et al.** p62, an autophagy hero or culprit? Nat Cell Biol. 2010; **12**:207-9.

121. **Lupo F, et al.** A new molecular link between defective autophagy and erythroid abnormalities in chorea-acanthocytosis. Blood. 2016; **128**:2976-2987.

5. AIM of the study

Role of Fyn in normal and stress erythropoiesis

6. MATERIALS AND METHODS

6.1 Drugs and chemicals

NaCl, Na_3VO_4, TRIS, Tween 20, EDTA, choline, $MgCl_2$, MOPS, Na_2HPO_4, KH_2PO_4, NaF, bicine, β-mercaptoethanol, benzamidine, glycine, glycerol, potassium cyanide, bromphenol blue, sodium dodecil sulphate (SDS), hydrocortisone, albumin from bovine serum (BSA), May-Grunwald-Giemsa's Azur-Eosin-Methylene Blue solution, were obtained by Sigma-Aldrich (Missouri, USA); dithiotreithol (DTT) was from Fluka (Buchs, Switzerland); protease inhibitor cocktail tablets were from Roche (Basel, Switzerland); 40% Acrylamide/Bis Solution, 37.5:1 was from BIO-RAD (California, USA); Luminata Forte Western Hrp solution was from Merck Millipore (Billerica, Massachusetts, USA); Prestained Protein Ladder, Triton X-100 and Temed were purchased from GE Healthcare Life Biosciences (Little Chalfont, UK); Annexin V Binding Buffer was from eBioscience (San Diego, USA); Dulbecco's Phosphate Buffered Saline (DPBS) was from Lonza (Belgium); Iscove's Modified Dulbecco's Medium (IMDM), alpha-MEM, L-glutamine and Fetal Cow Serum (FCS) were from TermoFisher (Massachusetts, USA); Penicillin-Streptamicin and Amphotericin were from Euroclone (Milan, Italy); MethoCult™ M3234 was from StemCell Techologies (Milan, Italy).

6.2 Mice strains

We studied the following mouse strains: C57BL/6J as normal control (wild-type; WT) and $Fyn^{-/-}$ mice. Since in preliminary experiments we observed a more severe hematological phenotype in $Fyn^{-/-}$ female mice, we used female mice aging from 2 to 4 months old. Mouse blood was collected by retro-orbital venipuncture in anesthetized mice using heparinized capillares according to the general guidelines of local animal facility, University of Verona. Whenever indicated, anemia was induced by intraperitoneal injection of PHZ (40 mg/Kg body weight)[1]or Doxorubicin (0.25 mg/Kg body weight).[2] Blood was collected at day 2, 4, 8 and 14 from PHZ injection and at day 3, 6 and 9 after Doxorubicin injection. Spleen and bone marrow were collected at day 2,4,8 and 14 from PHZ injection and at day 9 after Doxorubicin injection. EPO (10 U/mice).[3] was intraperitoneally injected for 5 days. Blood was collected at day 6, 8 and 11 after EPO administration. Rapamycin (10 mg/Kg)[4] was intraperitoneally injected in

a single dose and spleen and bone marrow were collected after 1 week from Rapamycin administration.

6.3 Hematological parameters

Hematological parameters were evaluated on Siemens ADVIA 120 Hematology System. Hematocrit and hemoglobin were manually determined.[5,6]

6.4 Flow cytometric analysis of mouse erythroid precursors and cell sorting of murine bone marrow erythroblasts

Cells from WT and $Fyn^{-/-}$ mice bone marrows and spleens were collected in BEPS (BEPS: PBS 1X, BSA 1%, EDTA 2 mM, NaCl 25 mM). The erythroid precursors were analyzed as previously described[7] using CD44-Ter119 strategy. Briefly, cells were centrifuged at 1,500 rpm for 5 min at 4°C and resuspended in the proper volume of BEPS. Cells were incubated first with CD16/32, to block Fc receptors, CD45-APC-Cy7, CD44-FITC, CD71-PE and Ter119-APC (eBioscience, San Diego, USA) antibodies for 30 min at 4°C in the dark. Cells were washed and centrifuged at 1,500 rpm for 5 min at 4°C, resuspended in BEPS and 7AAD, for cell viability, was added immediately before the analysis. All the analysis were performed with the flow cytometer FACSCantoII™ (Becton Dickinson, San Jose, CA, USA). Data were stored and processed using FACSDiva software (Becton Dickinson Immunocytometry System, San Jose, CA, USA). The biparametric scatter plots were analyzed with FlowJo software version vX.0.7 (Tree Star, Ashland, OR, USA) (Fig. 9).

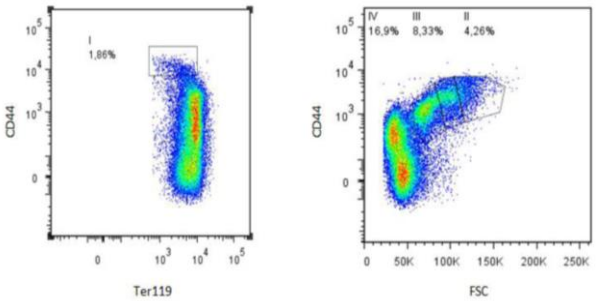

Fig. 9: Example of cytofluorimetric scatter for erythroid precursors from WT mice. **Left panel:** analysis of $CD44^{+}$ $Ter119^{low}$ Pop I corresponding to pro-erythroblasts. **Right panel**: analysis of $CD44^{+}$-$Ter119^{+}$ Pop II, III, IV, corresponding to basophilic, polychromatic and orthochromatic erythroblasts respectively.

Population III and IV corresponding to polychromatic and orthochromatic erythroblasts and total erythroblasts ($CD44^{+}Ter119^{+}FSC^{high}$) were sorted from bone marrow of both mouse strains as previously reported.[7] Sorted cells were used for (i) morphological analysis of erythroid precursors on cytospin preparations stained with May Grunwald-Giemsa; (ii) immunoblot analysis and (iii) RT-PCR analysis.[5,6] For immunoblot analysis the following specific antibodies were used: anti P-Ser473-Akt, anti Akt, anti P-Ser2448-mTOR, anti mTOR (Cell Signaling, Massachusetts, USA), anti P-Ser40-Nrf2, anti catalase, anti Nrf2, anti Prx1, anti Prx2, anti p62, anti Rab5 (Abcam, Cambridge, UK), anti Keap1 (Proteintech, Manchester, UK), anti GATA-1, anti HSP70, anti G6PD, anti NQO1 and GAPDH (Santa Cruz Biotechnology, Texas, USA) and HistH3 (Cell Signaling, Massachusetts, USA) as loading control. Whenever indicated we carried out immunoprecipitation (IP) experiments as previously reported.[5] Briefly, $1.5*10^{6}$ sorted $CD44^{+}Ter119^{+}FSC^{high}$ cells from WT and $Fyn^{-/-}$ were resuspended in Complete Bicine Solution (CBS: Bicine 25 mM, Triton X-100 1.5%, Na_3VO_4 1 mM, NaF 1 mM, EDTA 1 mM, in the presence of protease inhibitors) and underwent 3 cycles of freeze/thaw. The supernatant was collected and incubated with washed IP beads (Thermo Scientific, MA, USA) and phosphoTyr antibodies (PY99; Santa Cruz Biotechnology, Texas, USA and 4G10; Millipore, Massachussets, USA). The day after beads were spinned down, washed with CBS without inhibitors and solubilized with SB2X+β for 1h at RT. Before loading gels, beads were heated at 60°C for 4 min. Filters were incubated overnight with anti EPO-R (Sigma-Aldrich, Missouri, USA), anti STAT5, anti Lyn (Santa Cruz Biotechnology, Texas, USA), anti Jak2 (Cell Signaling Technology, Danvers, USA) and anti IgG rabbit (GE Healthcare Life Sciences, Little Chalfont, UK) as loading control.
Secondary anti-rabbit and anti-mouse antibodies were purchased from GE Healthcare Life Biosciences (Little Chalfont, UK). Images were acquired using Image Quant Las Mini 4000 Digital Imaging System (GE Healthcare Life Sciences, Little Chalfont, UK).

6.5 Annexin V analysis of mouse erythroid precursors

Analysis of apoptotic erythroblasts from WT and $Fyn^{-/-}$ mice was carried out on the CD44-Ter119 gated cells using the Annexin-V PE Apoptosis detection kit (eBioscience, San Diego, CA, USA) following the manufacturer instructions[8]. Flow cytometric analysis was carried out with the FACSCantoII™ flow cytometer (Becton Dickinson, San Jose,

CA, USA). Data were stored and processed using FACSDiva software (Becton Dickinson Immunocytometry System, San Jose, CA, USA). The biparametric scatter plots were analyzed with FlowJo software version vX.0.7 (Tree Star, Ashland, OR, USA).

6.6 Analysis of ROS levels on different populations of erythroid precursors

The ROS levels of erythroid precursors from WT and $Fyn^{-/-}$ mice were determined using the General Oxidative Stress Indicator CM-H_2DCFDA (LifeTechnologies, Carlsbad, CA, USA) on erythroid precursors as previously described[9] with minor changes. Briefly, CD44-PE, Ter119-APC, CD45-APC-Cy7 (eBioscience, San Diego, USA) stained cells, from mouse bone marrow, were incubated with CM-H_2DCFDA (10 µM in PBS, BSA 1% at 37°C for 20 min). Cells were then washed once with PBS BSA 1%, stained in ice with 7-AAD and analyzed with the FACSCantoII™ flow cytometer (Becton Dickinson, San Jose, CA, USA). Data were stored and processed using FACSDiva software (Becton Dickinson Immunocytometry System, San Jose, CA, USA). The biparametric scatter plots were analyzed with FlowJo software version vX.0.7 (Tree Star, Ashland, OR, USA).

6.7 Murine BFU-E and CFU-E assay

Incomplete MethoCult™ (M3234) media was thawed at room temperature (15 - 25°C) or overnight at 4°C. $0.2*10^6$ cells from BM of WT and $Fyn^{-/-}$ mice were collected in Complete α-MEM (α-MEM, 1% Penicillin-Streptomicin, 1% Hydrocortisone, 1% nucleotides, Gentamicin 0,025 mg/L, Amphotericin 0,5 ug/mL) and then added to MethoCult™ media. Growth factors (SCF 50 ng/mL, IL-3 10 ng/mL and EPO 3U/mL) were added fresh every time to complete α-MEM. Media were vortexed to ensure all components were thoroughly mixed (let the tube stand for at least 5 minutes to allow the bubbles to rise to the top). MethoCult™ mixture containing cells was dispensed into sterile culture dishes. Empty wells were filled with sterile water. The plates were incubated at 37°C and 5% CO_2. After 5 and 10 days, WT and $Fyn^{-/-}$ CFU-Es and BFU-Es, were picked up, counted and solubilize in CBS with inhibitors. We carried out IP experiments on WT and $Fyn^{-/-}$ CFU-Es. Briefly, $2*10^6$ CFU-Es from WT and $Fyn^{-/-}$ were resuspended in CBS with inhibitors and underwent 3 cycles of freeze/thaw. The supernatant was collected and incubated with washed IP beads and phosphor-Tyr antibodies (PY99; Santa Cruz Biotechnology, Texas, USA and 4G10; Millipore, Billerica,

Massachusetts, USA). The day after beads were spinned down, washed with CBS without inhibitors and solubilized with SB2X+β for 1h at RT. Before loading gels, beads were heated at 60°C for 4 min. Filters were incubated overnight with anti EPO-R (Sigma-Aldrich, Missouri, USA), anti STAT5, anti Lyn (Santa Cruz Biotechnology, Texas, USA), anti Jak2 (Cell Signaling Technology, Danvers, USA) and anti IgG rabbit (GE Healthcare Life Sciences, Little Chalfont, UK) as loading control.

6.8 In vitro maturation of reticulocytes from WT and Fyn$^{-/-}$ mice after PHZ treatment

WT and Fyn$^{-/-}$ mice were intraperitoneally injected with PHZ (40 mg/kg) at day 0, 1 and 3. One week after the first injection of PHZ, blood from WT and Fyn$^{-/-}$ mice was collected.[10] Washed and packed RBCs from heparinized whole blood were used for (i) cytosol preparation, as previously described[11-13], (ii) LysoTrack and MitoTrack staining and (iii) in vitro maturation of reticulocytes. For in vitro maturation, blood was diluted 1:500 in 1.5 ml of maturation medium (60% IMDM, 2mM L-glutamine, 100U Penicillin-Streptomicin, 30% FCS, 1% BSA and 1X Amphotericin) and cultured in a 24-well tissue culture plate in a cell culture incubator at 37°C with 5% of CO_2 for 3 days.

6.9 MitoTracker and LysoTracker analysis on RBCs and cultured reticulocytes after PHZ treatment

RBCs and cultured reticulocytes from PHZ treated WT and Fyn$^{-/-}$ mice underwent lysosome and mitochondria staining using the Lysotracker Green DND-26 (ThermoFisher Scintific) and the MitoTracker Deep Red (ThermoFisher Scientific), following the manufacturer's instructions.[14] Cells were analyzed with the FACSCantoII™ flow cytometer (Becton Dickinson, San Jose, CA, USA). Data were stored and processed using FACSDiva software (Becton Dickinson Immunocytometry System, San Jose, CA, USA). The biparametric scatter plots were analyzed with FlowJo software version vX.0.7 (Tree Star, Ashland, OR, USA).

7. RESULTS

7.1 Fyn$^{-/-}$ mice display a mild mycrocitic anemia

We first analyzed the hematological parameters of wild-type (WT) and Fyn$^{-/-}$ mice (Table 3). Fyn$^{-/-}$ mice showed a very mild hypochromic anemia as defined by reduction in hemoglobin (Hb) levels and lower mean corpuscular volume (MCV) (Table 3). This was associated with slight but significant increase in reticulocyte count in Fyn$^{-/-}$ mice compared to WT.

TABLE 3. HEMATOLOGICAL DATA OF WT AND Fyn$^{-/-}$ MICE

	WT mice (*n*=10)	**Fyn$^{-/-}$ mice (*n*=10)**
Hct (%)	48.2 ± 1.3	46.1 ± 0.8*
Hb (g/dl)	15.9 ± 0.6	14.3 ± 0.5*
MCV (fl)	50.3 ± 0.4	46.5 ± 1.3*
MCH (g/dl)	15.3 ± 0.3	14.8 ± 1.1
CHCM (g/dL)	26.4±0.5	29.6 ± 1.4*
RDW (%)	11.6 ± 0.3	13.2 ± 0.4*
Retics (10^3 cells/uL)	451± 40.7	559 ± 45*

Hct: hematocrit; **Hb:** hemoglobin; **MCV:** mean corpuscular volume; **MCH:** mean corpuscular haemoglobin; **CHCM:** mean cellular hemoglobin concentration; **RDW:** red blood cell distribution width; **Retics:** reticulocytes; *p <0.05 compared to WT mice.

Increased total bilirubin (TB) and plasma lactate dehydrogenase (LDH) levels were observed in Fyn$^{-/-}$ mice compared to healthy controls (Fig. 1a). Up-regulation of haptoglobin (Hp) gene expression was found in liver from Fyn$^{-/-}$ mice (Fig. 1b, left panel); whereas, plasma Hp levels showed a trend to increase without reaching statistical significance compared to WT (Fig. 1b, right panel). No iron-overload was detected in either liver or spleen from Fyn$^{-/-}$ mice (Fig. 1c). Up-regulation of EPO mRNA

expression was found in Fyn$^{-/-}$ mice (Fig. 1d). Collectively, these data suggest the presence of a very mild hemolytic compensated microcytic anemia in mice genetically lacking Fyn.

Fig. 1

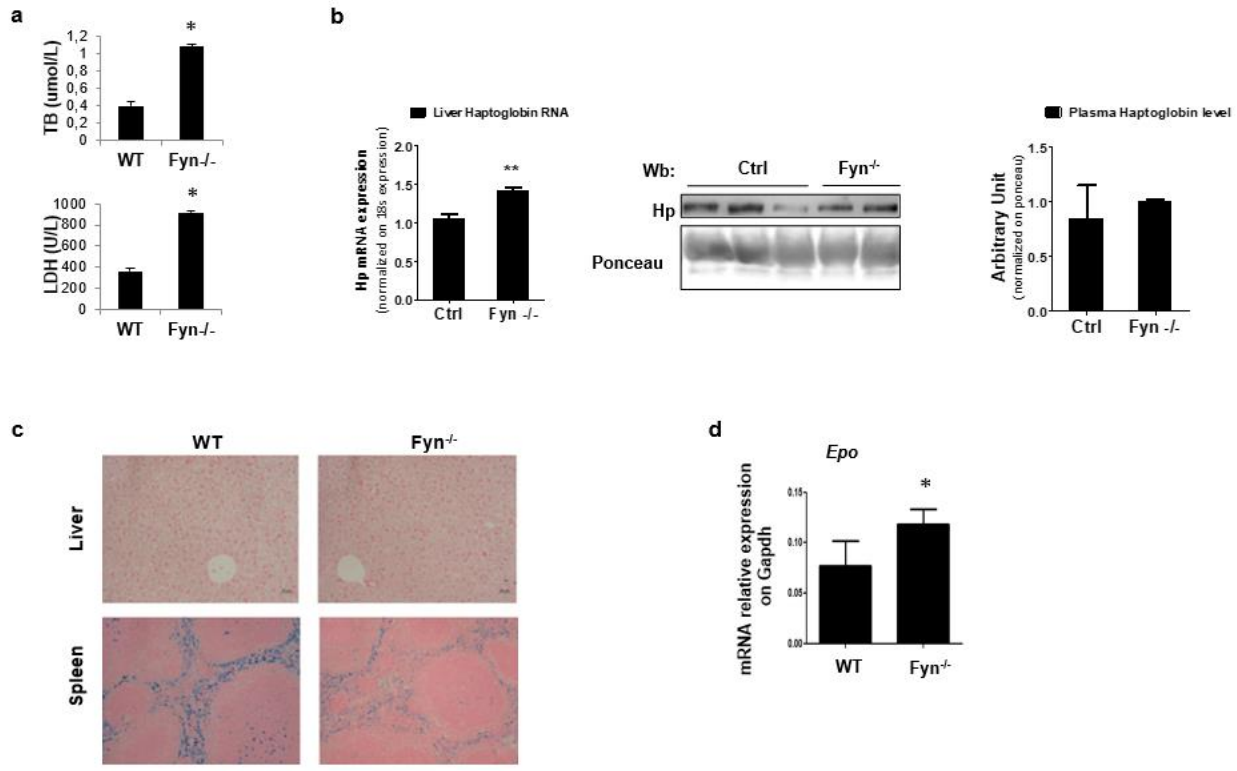

Fig. 1: (a): TB and plasma LDH levels. Data are presented as means±SD (*n*=6); *p< 0.05 compared to WT mice [in collaboration with Prof E.Tolosano, Universityof Torin, Italy]. **(b):** RT-PCR expression of Hp on liver from WT and Fyn$^{-/-}$ mice. Experiments were performed in triplicate. Error bars represent the standard deviations (means±SD); *p< 0.05 compared to WT mice. [in collaboration with Prof. A. Iolascon and Dr. L. De Falco, University Federico II, Naples]; Immunoblot analysis of Hp in WT and Fyn$^{-/-}$ mice. Ponceau Red was used as loading control (densitometric analysis are reported in supplementary data); Plasma levels of Hp in WT and Fyn$^{-/-}$ mice [in collaboration with Prof E.Tolosano, University of Torin, Italy]. **(c):** Iron staining (Pearl's Prussian blue) in liver and spleen from WT and Fyn$^{-/-}$ mice. One representative image from the other six with similar results is presented. **(d):** RT-PCR expression of EPO on kidney from WT and Fyn$^{-/-}$ mice. Experiments were performed in triplicate. Error bars represent the standard deviations (means±SD); *p< 0.05 compared to WT mice [in collaboration with Prof. A. Iolascon and Dr. L. De Falco, University Federico II, Naples]. TB, total bilirubin; LDH, lactate dehydrogenase; RT-PCR, real time polymerase chain reaction; Hp, haptoglobin; EPO, erythropoietin.

7.2 The absence of Fyn is associated with dyserythropoiesis, increased oxidative stress and low GATA-1 nuclear translocation

We carried out morphological analysis of sorted erythroblasts from WT and Fyn$^{-/-}$ mice. As shown in Fig. 2a, signs of dyserythropoiesis mainly involving Pop II and Pop III were detected in Fyn$^{-/-}$ mice compared to WT. This was associated with increased erythroid precursors (CD71^{+}Ter119^{+}cells; Fig. 2b) without evidences of extramedullary erythropoiesis. We then measured the generation of ROS in sorted erythroblasts from both mouse strains. We found higher ROS levels in Fyn$^{-/-}$ erythroblasts compared to WT (Fig. 2c, upper panel). Increased amount of Annexin-V positive erythroblasts was found in Fyn$^{-/-}$ mice (Fig. 2c; lower panel).

Fig. 2

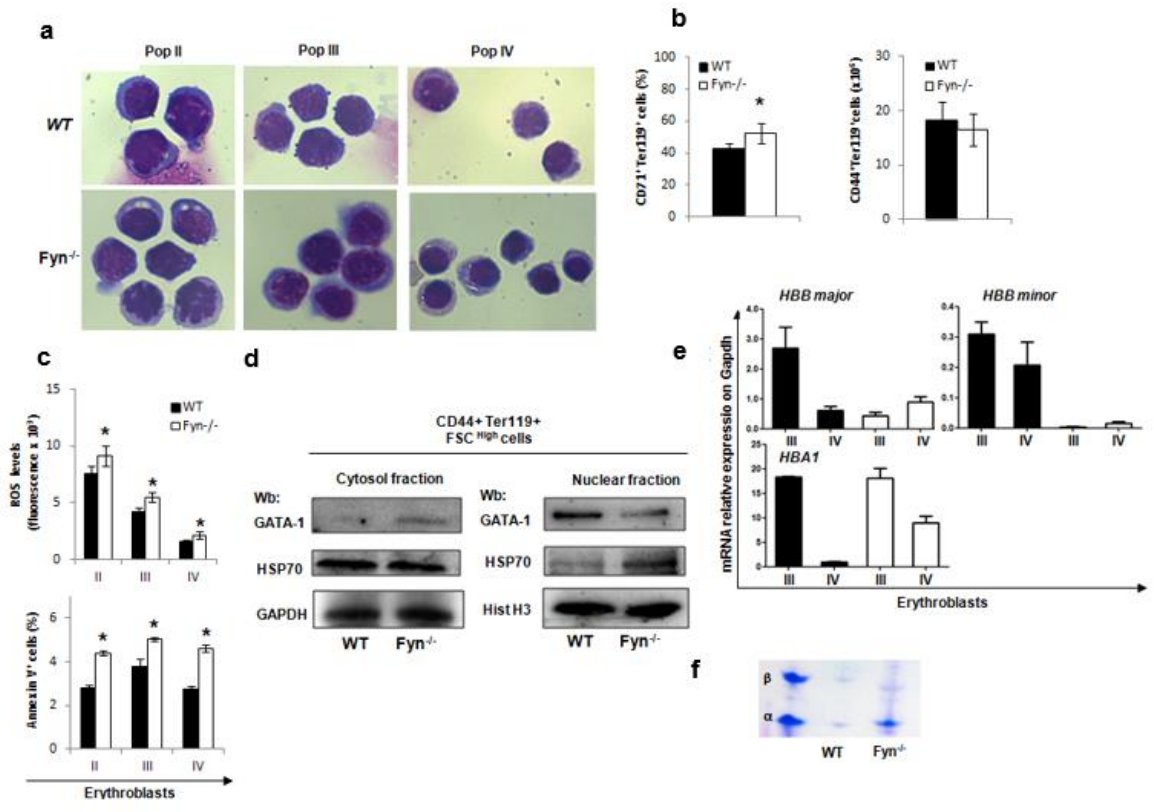

Fig. 2: **(a):** Morphological analysis of cytospins from sorted WT and Fyn$^{-/-}$ erythroblasts stained with May-Grunwald-Giemsa. Representative micropictures from other six with similar results. **(b):** Analysis of total erythroblasts in WT and Fyn$^{-/-}$ mice (Ter119-CD71 based gating). Data are presented as means±SD (n= 8); *p< 0.05 compared to WT mice. **(c) Upper panel:** ROS levels of erythroblast in populations II - IV from WT and Fyn$^{-/-}$ mice (Pop II, basophilic

erythroblasts; Pop III, polychromatic erythroblasts; Pop IV, orthochromatic erythroblasts). Data are presented as means±SD (*n*=8); *p< 0.05 compared to WT mice. **Lower panel:** Annexin-V^{+} erythroblasts in populations II-IV from WT and Fyn$^{-/-}$ mice (Pop II, basophilic; Pop III, polychromatic; Pop IV, orthochromatic erythroblasts). Data are presented as means±SD (*n*=8); *p< 0.05 compared to WT mice. **(d):** Immunoblot analysis with specific antibody against GATA-1 and HSP70 on cytosolic and nuclear fraction of sorted CD44^{+}Ter119^{+}FSC^{high} cells. GAPDH and HistH3 were used as loading controls. One representative gel from three with similar results is presented. Densitometric analysis are reported in supplementary data. **(e):** RT-PCR expression of HBB major, HBB minor and HBA1 on sorted Pop III and Pop IV from WT and Fyn$^{-/-}$ bone marrow (Pop III, polychromatic erythroblasts; Pop IV, orthochromatic erythroblasts). Experiments were performed in triplicate. Error bars represent the standard deviations (means±SD [in collaboration with Prof. A. Iolascon and Dr. L. De Falco, University Federico II, Naples]. **(f):** TAU Gel Electrophoresis of α/β-globins from WT and Fyn$^{-/-}$ circulating red cells. ROS, reactive oxygen species; TAU, Triton-Acetic-Urea; RT-PCR, real time polymerase chain reaction.

β-thalassemia (β-thal; see also introduction section 3.1) is a human model of stress erythropoiesis and it is characterized by increased ROS levels and hyperactivation of Jak2-STAT5 signaling pathway. In β-thal erythropoiesis oxidation affects nuclear translocation of GATA-1, a key transcriptional factor involved in erythroid maturation events. Thus, we evaluated GATA-1 in Fyn$^{-/-}$ erythropoiesis. In sorted Fyn$^{-/-}$ erythroblasts, we observed reduced GATA-1 nuclear translocation compared to WT (Fig. 2d). This was associated with increased HSP70 nuclear translocation, similarly to that described in β-thal erythroblasts. Indeed, a significant decrease in β-globin chain synthesis, was evident in Fyn$^{-/-}$ mouse erythroblasts (Fig. 2e). An accumulation of the α-globin chains (α-globin aggregates) was detected in circulating Fyn$^{-/-}$ red cells (Fig. 2f). These data suggest a possible reduced efficiency of EPO signaling cascade in the absence of Fyn.

7.3 The absence of Fyn is associated with reduced efficiency of EPO-signaling pathway

We then explored Jak2-STAT5 Tyr-phosphorylation state, which is strictly dependent on the efficiency of EPO signaling cascade. In sorted Fyn$^{-/-}$ erythroblasts, we observed reduced activation of EPO-R (decreased Tyr-phosphorylation state of EPO-R), compared to WT erythroblasts (Fig. 3a). This was associated with increased Jak2 compensatory activation, without major difference in Lyn functional state (Fig 3a). In sorted Fyn$^{-/-}$ erythroblasts, STAT5 activation was significantly decreased, as supported by down-regulation of *Cish*, an exclusively STAT5 regulated gene (Fig. 3b).

Using the vitro erythroid cell forming colony unit assay, we found a lower CFU-E and BFU-E cells production from Fyn$^{-/-}$ bone marrow cells in presence of standard EPO stimulation (3 U/ml) (Fig. 3c). This was again associated with decreased activation of EPO mediated signaling cascade in Fyn$^{-/-}$ CFU-E with compensatory hyperactivation of Jak2 (Fig. 3d). Since the absence of Fyn results in low efficiency of EPO signaling cascade, the hyperactivation of Jak2 may be related to increase ROS levels characterizing Fyn erythroblasts.

To better understand the role Fyn in EPO-signaling cascade, we treated both mouse strains with recombinant EPO (10 U/day for 5 days; red arrows in Fig. 4a).[3] Increase of Hct and reticulocytes (as CD71^{+}Ter119^{+} circulating cells) was blunted in Fyn$^{-/-}$ mice compared to WT animals (Fig. 4a). Collectively, these data indicate a reduction in the efficiency of EPO signaling pathway in the absence of Fyn.

Fig. 3

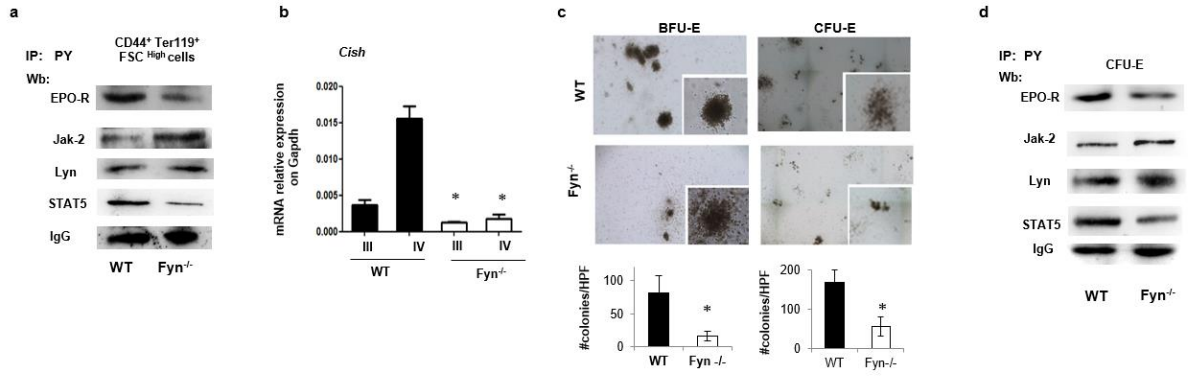

Fig. 3: **(a):** Anti phosphor-Tyr immunoprecipitation analysis of Jak2-STAT5 signaling pathway on sorted CD44^{+}Ter19^{+}FSC^{high} cells from WT and Fyn$^{-/-}$ mice. IgG were used as loading control. One representative gel from three with similar results is presented. Densitometric analysis are reported in supplementary data. **(b):** RT-PCR expression of Cish on sorted Pop III and Pop IV from WT and Fyn$^{-/-}$ bone marrow (Pop III, polychromatic erythroblasts; Pop IV, orthochromatic erythroblasts). Experiments were performed in triplicate. Error bars represent the standard deviations (means±SD); *p< 0.05 compared to WT mice. [in collaboration with Prof. A. Iolascon and Dr. L. De Falco, University Federico II, Naples]. **(c):** In vitro colony-forming unit assay of BFU-Es and CFU-Es from WT and Fyn$^{-/-}$ mice. Data are presented as means±SD (n=5); *p< 0.05 compared to WT mice. **(d):** anti phosphor-Tyr immunoprecipitation analysis of Jak2-STAT5 signaling pathway on CFU-Es from WT and Fyn$^{-/-}$ mice. IgG were used as loading control. One representative gel from three with similar results is presented. Densitometric

analysis are reported in supplementary data. RT-PCR, real time polymerase chain reaction; CFU-E, erythroid colony-forming unit; BFU-E, erythroid burst-forming unit.

7.4 Fyn$^{-/-}$ mice display a high sensitivity to PHZ or Doxorubicin induced stress erythropoiesis

We then treated both mouse strains with either PHZ (40 mg/Kg; red arrows in Fig. 4b) or Doxorubicin (0.25 mg/Kg; red arrow in Fig. 5a). In mice, PHZ is known to induce severe oxidation and acute hemolytic anemia, while Doxorubicin temporary represses erythropoiesis with ROS generation.[1,2]

As shown in Fig. 4b, PHZ induced a similar marked drop in Hct levels in both mouse strains at day 2 after PHZ injection. In Fyn$^{-/-}$ mice, we observed a delayed increase in Hct levels at day 4 and 8 compared to WT. The increase in reticulocyte count in PHZ treated Fyn$^{-/-}$ mice was blunted compared to WT mice, showing a peak at day 8 after PHZ injection (Fig. 4b). As shown in Fig. 4c, we found increased levels of total erythroblasts in bone marrow and spleen from both mouse strains following PHZ injection. In Fyn$^{-/-}$ spleen, the increase in erythroid precursors was blunted at day 4, with a compensatory increase at day 14 after PHZ administration (Fig. 4c, upper panel). In bone marrow, we observed a mild increase in total erythroblasts in both mouse strains at day 2 and 4 after PHZ injection (Fig. 4c, lower panel). Noteworthy, in Fyn$^{-/-}$ mice we found a marked increase in bone marrow total erythroblasts at day 8 after PHZ, suggesting a possible compensatory mechanism in Fyn$^{-/-}$ mice do to the lack of splenic response following PHZ treatment (Fig. 4c, lower panel). At day 4 and 8 after PHZ injection, the amount of Annexin-V^{+} cells was higher in Fyn$^{-/-}$ polychromatic and orthochromatic erythroblasts in both bone marrow and spleen compared to WT animals (data not shown).

Fig. 4

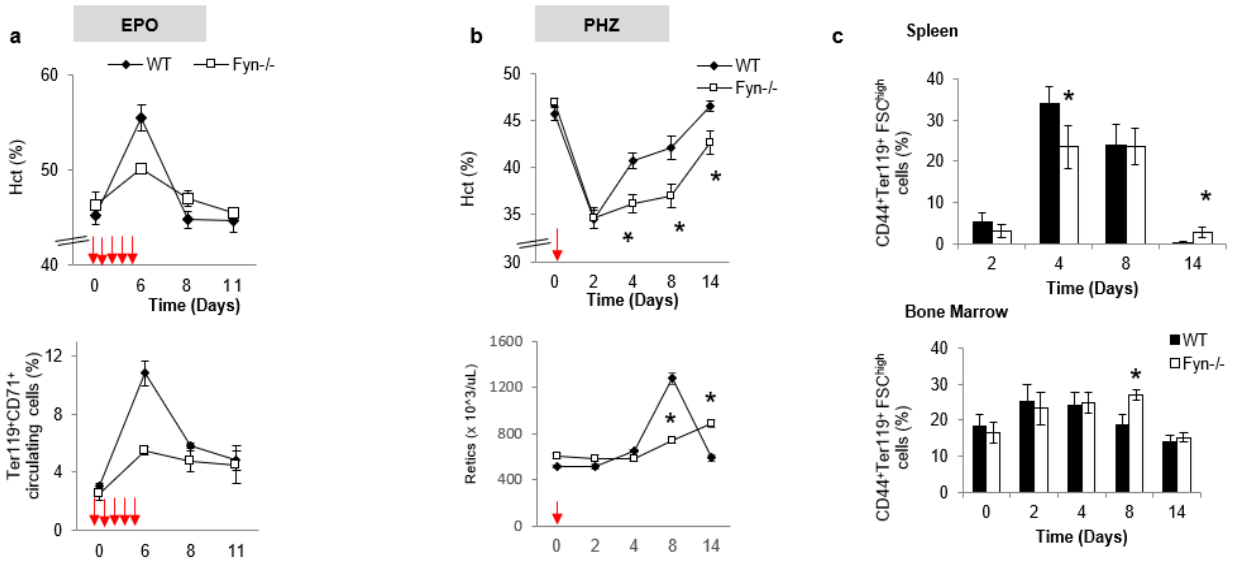

Fig. 4: **(a):** Hematocrit (Hct) and reticulocyte count in WT and Fyn$^{-/-}$ mice after EPO injection (10 U/mice; red arrows). Data are presented as means±SD (*n*= 5). **(b):** Hematocrit (Hct) and reticulocyte count in WT and Fyn$^{-/-}$ mice after PHZ injection (40 mg/kg, red arrow). Data are presented as means±SD (*n*= 5); **p*< 0.05 compared to WT mice **(c):** Total erythroblasts in WT and Fyn$^{-/-}$ bone marrow and spleen after PHZ injection. Data are presented as means±SD (*n*= 5); **p*< 0.05 compared to WT mice. EPO, erythropoietin; PHZ, phenylhydrazine; Hct, hematocrit.

In Fyn$^{-/-}$ mice, Doxorubicin induced a more severe and prolonged anemia compared to WT. We also found a delay in reticulocytes response compared to Doxorubicin treated WT animals (Fig. 5a). Total erythroblasts were determined at day 9 after Doxorubicin administration in both spleen and bone marrow.[2] In Fyn$^{-/-}$ mice, we observed a significant reduction in both bone marrow and spleen erythroblasts, compared to vehicle treated controls (Fig. 5b). Increased amount of Annexin V^{+} polychromatic and orthochromatic erythroblasts was observed at day 9 after Doxorubicin administration in Fyn$^{-/-}$ mice compared doxorubicin treated WT animals (data not shown).

These data suggest an increased sensitivity of Fyn$^{-/-}$ mice to stress erythropoiesis, further supporting the importance of Fyn in EPO signaling cascade.

Fig. 5

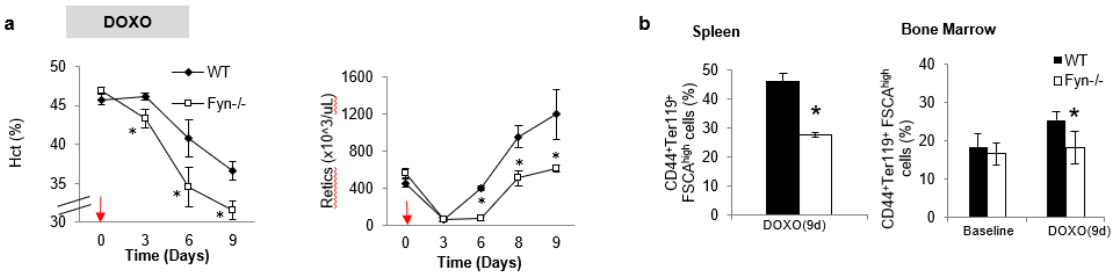

Fig. 5: **(a):** Hematocrit (Hct) and reticulocyte count in WT and Fyn$^{-/-}$ mice after Doxorubicin injection (0.25 mg/kg; red arrow). Data are presented as means±SD (*n*= 5); **p*< 0.05 compared to WT mice. **(b):** Analysis of total erythroblasts in bone marrow and spleen from WT and Fyn$^{-/-}$ mice after Doxorubicin injection. Data are presented as means±SD (*n*= 5). **p*< 0.05 compared to WT mice. DOXO, doxorubicin; Hct, hematocrit.

7.5 Fyn$^{-/-}$ mice display increased Akt

Previous studies have shown that EPO-Jak2 pathway can activate Akt, which is also directly modulated by ROS (Fig. 6a).[15] Thus, we evaluated Akt function in sorted erythroblasts from both mouse strains. As shown in Fig. 6b, Fyn$^{-/-}$ mouse erythroblasts displayed increased active Akt (Ser 473) compared to WT cells (Fig. 6b). Activation of Akt might affect multiple targets involved in response to oxidation. Akt might (I) functionally interact with the redox sensitive transcriptional factor Nrf2, resulting in Nrf2 activation; or (II) activate mTOR, which phosphorylation represses autophagy.[15,16]

Fig. 6

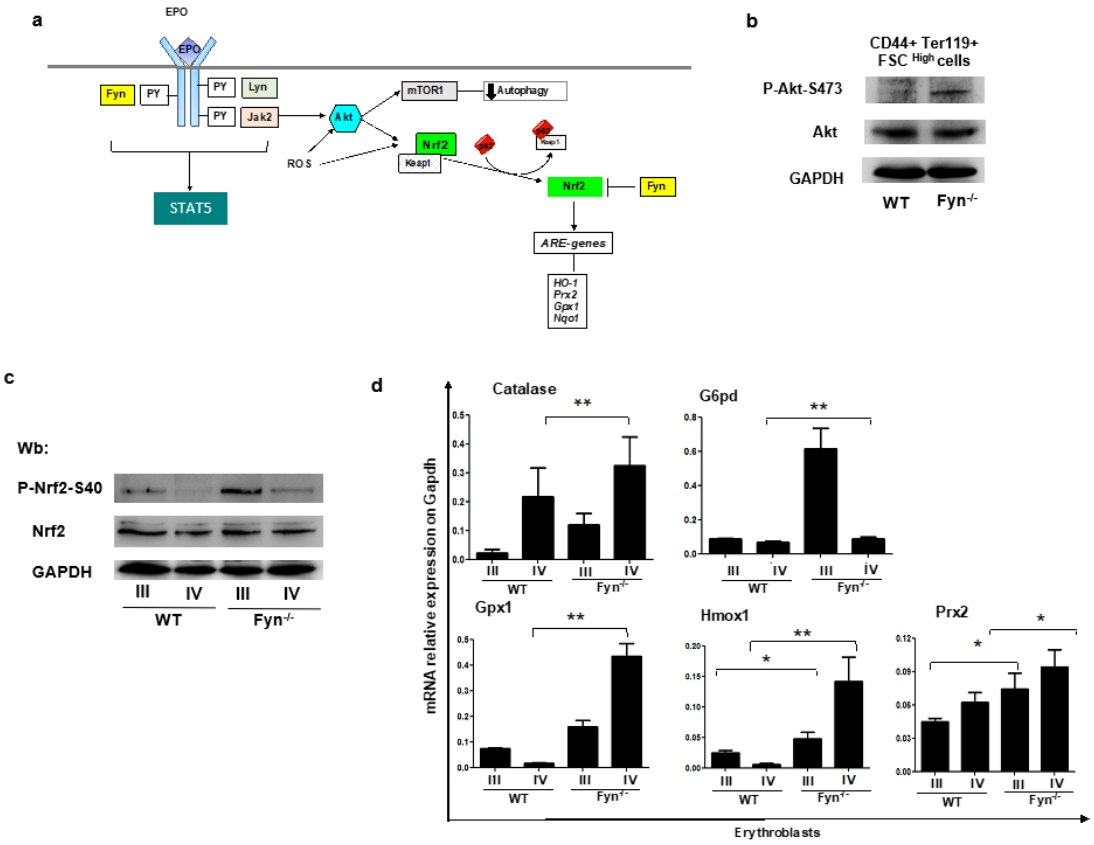

Fig. 6: **(a):** Schematic representation of EPO signaling pathway intercrossed with autophagy and Nrf2 redox-sensitive systems. **(b):** Immunoblot analysis with specific antibodies against p-Ser473-Akt and Akt from WT and Fyn$^{-/-}$ sorted CD44^{+}Ter119^{+}FSC^{high} erythroblasts. GAPDH was used as loading control. One representative gel from three with similar results is presented. Densitometric analysis are reported in supplementary data. **(c):** Immunoblot analysis with specific antibodies against p-Ser40-Nrf2 and Nrf2 from WT and Fyn$^{-/-}$ sorted Pop III and Pop IV (Pop III, polychromatic erythroblasts; Pop IV, orthochromatic erythroblasts). GAPDH was used as loading control. One representative gel from three with similar results is presented. Densitometric analysis are reported in supplementary data. **(d):** RT-PCR expression of Catalase, G6pd, Gpx1, Hmox1 and Prx2 on sorted Pop III and Pop IV from WT and Fyn$^{-/-}$ bone marrow (Pop III, polychromatic erythroblasts; Pop IV, orthochromatic erythroblasts). Experiments were performed in triplicate. Error bars represent the standard deviations (means±SD); *p< 0.05 compared to WT mice. [in collaboration with Prof. A. Iolascon and Dr. L. De Falco, University Federico II, Naples].

In Fyn$^{-/-}$ erythroblasts, we found increased activation of Nrf2 (Ser40) compared to WT cells, most likely related to the absence of Fyn as key post-induction regulator of Nrf2 (Fig. 6c). This was supported by up-regulation of ARE-genes for anti-oxidant and cytoprotective systems such as Catalase, G6PD, GPX1, HO-1 and Prx2 (Fig. 6d).

Immunoblot analysis with specific antibodies showed increased expression of the encoded proteins, validating the molecular data (Fig. 7).

Fig. 7

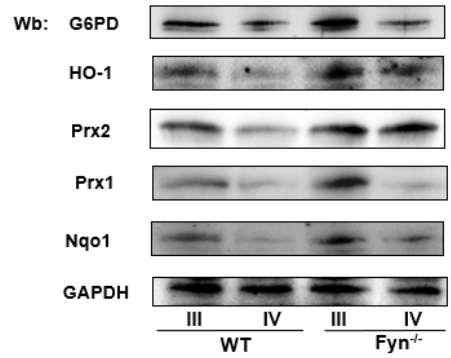

Fig. 7: Immunoblot analysis with specific antibodies against G6PD, HO-1, Prx2, Prx1 and NQO1 from WT and $Fyn^{-/-}$ sorted Pop III and Pop IV. GAPDH was used as loading control. One representative gel from three with similar results is presented. Densitometric analysis are reported in supplementary data.

7.6 In $Fyn^{-/-}$ mice, activation of mTOR impairs autophagy, leading to abnormalities on the *in vitro* reticulocyte maturation

Previous studies have shown that autophagy plays a key role in erythropoiesis, contributing to the correct maturation and differentiation of erythroid precursors (ref). Although modulation of mTOR during erythropoiesis is only partially known, mTOR is a key protein in autophagy and its activation by Akt represses autophagy.[16] In $Fyn^{-/-}$ mouse erythroblasts, we found increased active mTOR (Ser2448) associated with accumulation of p62 and Rab5, both proteins involved in late phase of autophagy (Fig. 8a). Moreover, in $Fyn^{-/-}$ erythroblasts, we found accumulation of Keap1, the physiologic inhibitor of Nrf2 (Fig. 8a).[17] These data suggest an impairment of autophagy processes during erythropoiesis in the absence of Fyn.

Since autophagy has been shown to be important during reticulocyte maturation[18], we analyzed *in vitro* reticulocyte maturation from PHZ treated mice.[10] We found reduced $Fyn^{-/-}$ reticulocyte maturation compared to WT (Fig. 8b, left panel). This was associated with decreased lysosomal clearance, as shown by LysoTrack analysis, without major difference in mitochondrial clearance, as shown by MitoTrack analysis (Fig. 8b, right

panel). An accumulation of p62, was again detected in maturing reticulocytes in the absence of Fyn, further supporting the impairment of autophagy in Fyn$^{-/-}$ mice (Fig. 8c).

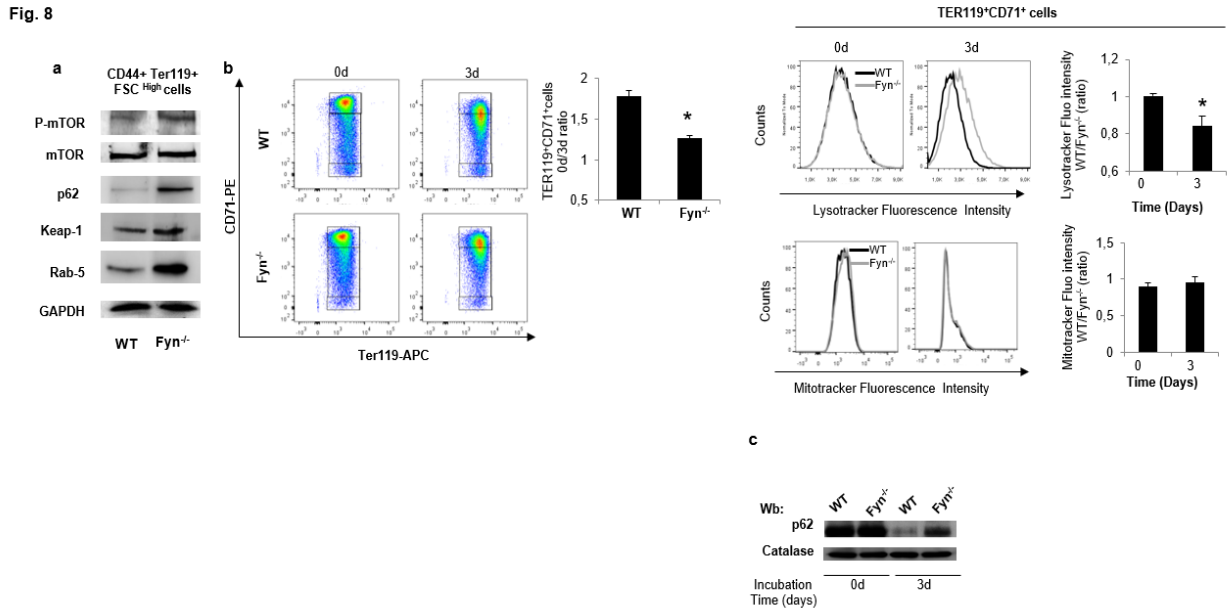

Fig. 8: **(a):** Immunoblot analysis with specific antibodies against p-Ser2448-mTOR, mTOR, p62, Keap1 and Rab5 from WT and Fyn$^{-/-}$ sorted CD44^{+}Ter119^{+}FSC^{high} erythroblasts. GAPDH was used as loading control. One representative gel from three with similar results is presented. Densitometric analysis are reported in supplementary data. **(b) (Left)** Flow cytometric scatter of RBCs at day 0 and after 3 days of in vitro maturation from PHZ treated WT and Fyn$^{-/-}$ mice. One representative of 3 independent experiments with similar results. Data are shown as means±SD (n=3); *p< 0.05 compared to WT mice. **(Right)** Flow cytometry of RBCs at day 0 and after 3 days of in vitro maturation from PHZ treated WT and Fyn$^{-/-}$ mice intravitally stained with LysoTracker and MitoTracker. One representative of 3 independent experiments with similar results. Data are shown as means±SD (n=3); *p< 0.05 compared to WT mice. **(c):** Immunoblot analysis with specific antibodies against p62 in RBCs at day 0 and after 3 days of in vitro maturation from PHZ treated WT and Fyn$^{-/-}$ mice. Catalase was used as loading control. One representative gel from three with similar results is presented. Densitometric analysis are reported in supplementary data.

7.7 The mTOR inhibitor Rapamycin unlocks autophagy and ameliorates erythropoiesis in Fyn$^{-/-}$ mice

We then treated both mouse strains with Rapamycin (10 mg/Kg), a known mTOR inhibitor, which has been shown to promote autophagy and beneficially impact stress erythropoiesis in other mouse models.[4]

Rapamycin administration reduced total bone marrow Fyn$^{-/-}$mouse erythroblasts, while no significant effects were observed in control animals as previously reported

(Fig. 9a).[4] A significant reduction in generation of ROS and in the amount of Annexin-V^{+} cells was found only in erythroid precursors from Fyn$^{-/-}$ mice (Fig. 9b, 9c). In agreement with the activation of autophagy we observed decreased levels of p62 in Rapamycin treated Fyn$^{-/-}$ erythroblasts compared to vehicle treated animals (Fig. 9d). No major change was observed in hematologic parameters as previously reported.[4] These data suggest that the inhibition of mTOR unlocks autophagy and ameliorates erythropoiesis in Fyn$^{-/-}$ mice.

Fig. 9

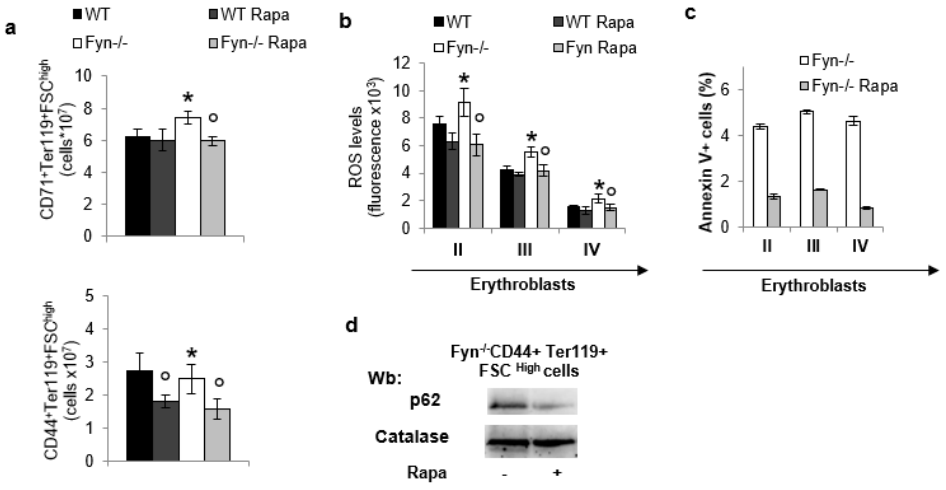

Fig. 9: (a): Analysis of total erythroblasts in WT and Fyn$^{-/-}$ bone marrow (Ter119-CD44 based gating) treated with either vehicle or Rapamycin. Data are presented as means±SD (n= 5); *p< 0.05 compared to WT mice; °p < 0.05 compared to vehicle treated mice **(b):** ROS levels of erythroblast in populations II - IV from WT and Fyn$^{-/-}$ mice treated with either vehicle or Rapamycin (Pop II, basophilic erythroblasts; Pop III, polychromatic erythroblasts; Pop IV, orthochromatic erythroblasts). Data are presented as means±SD (n=5); *p< 0.05 compared to WT mice; °p < 0.05 compared to vehicle treated mice. **(c):** Annexin-V^{+} erythroblasts in populations II-IV from WT and Fyn$^{-/-}$ mice treated with either vehicle or Rapamycin. (Pop II, basophilic; Pop III, polychromatic; Pop IV, orthochromatic erythroblasts). Data are presented as means±SD (n=5); *p< 0.05 compared to WT mice; °p < 0.05 compared to vehicle treated mice. **(d):** Immunoblot analysis with a specific antibody against p62 from Fyn$^{-/-}$ sorted CD44^{+}Ter119^{+}FSC^{high} erythroblasts treated with either vehicle or Rapamycin. Catalase was used as loading control. One representative gel from three with similar results is presented. Densitometric analysis are reported in supplementary data.

8. DISCUSSION

Here, we found a novel role of Fyn in EPO-mediated signaling pathway in normal and stress erythropoiesis. Fyn affects EPO-R and STAT5 Tyr-phosphorylation state, without change in Lyn activity but overactivation in Jak2 (Fig. 3). This suggests Fyn as a new downstream regulator of STAT5 phosphorylation similarly to that described in Lyn$^{-/-}$ mice.[3] We carried out a protein alignment using ClustalW2 for Fyn and Lyn (Fig. 10). The superposed alignment gives a 62% identity and 78% sequence similarities using Blastp algorithm (Fig. 10).

Alignment Score: 54.30

Fig. 10: ClustalW2 alignment between Fyn and Lyn kinases

Previous studies have shown that Lyn targets STAT5, modulating its Tyr-phosphorylation state.[3] The high similarity between Fyn and Lyn allow us to propose Fyn as possible new modulator of STAT5 in erythroid cells.

The reduction in STAT5 activation observed in Fyn$^{-/-}$ mouse erythroblasts supports this interplay and it is in agreement with previous reports in other cell types (i.e. such mast cells and CML cells)[19,20]. In Fyn$^{-/-}$ mice, the reduction in STAT5 activation may be responsible for the microcytic anemia as previously reported in mice genetically lacking STAT5.[21]

In Fyn$^{-/-}$ mice, the reduced efficiency of EPO signaling pathway was also indicated by increased ROS levels and cell apoptosis of the different erythroblast subpopulations (Fig. 2). The synergic effect of reduced EPO signaling and increased oxidation results in decreased GATA-1 nuclear translocation similarly to that observed in β-thal erythropoiesis.[22] Indeed, the unbalance in β-globin chain synthesis with accumulation of free α-globin chains further support the functional impact of Fyn on erythroid maturation (Fig. 2).

We then explored Jak2/STAT5 pathway in early and late erythropoiesis in Fyn$^{-/-}$ mice. The reduction in STAT5 activity observed in both erythroblasts and erythroid progenitors (CFU-Es) indicate the critical role of Fyn in modulating the temporary dynamics of EPO-induced erythroid maturation (Fig. 3). In Fyn$^{-/-}$ mice, failure in response to recombinant EPO supports the proposed role for Fyn in EPO signaling cascade (Fig 4a).

To understand the role of Fyn in stress erythropoiesis, we exposed Fyn$^{-/-}$ mice to either PHZ or Doxorubicin. Fyn$^{-/-}$ mice display high sensitivity to both PHZ and Doxorubicin with a blunt response of erythropoiesis to these stressful conditions (Fig. 4b, 5). In Fyn$^{-/-}$ mice, increased oxidation results in Jak2 overoxidation leading to increased activity of Akt that is an important signal to ensure erythroid survival and maturation (Fig 6b).[23,24] Akt intersects several pathways such as Nrf2, a redox sensitive transcriptional factor, and mTOR, the gatekeeper of autophagy.[15,16] Fyn$^{-/-}$ mice display activation of Nrf2, resulting in up-regulation of ARE genes and the related encoded proteins for antioxidant systems (Fig. 6, 7). However, the up-regulation of these cytoprotectors is unable to counteract oxidation of Fyn$^{-/-}$ erythroblasts. In cell homeostasis, the prolonged oxidation might overcome autophagy, resulting in cell apoptosis.[25] This seems to be the case of Fyn$^{-/-}$ erythroblasts where we found increased cell apoptosis (Fig. 2c). It is of note that Fyn$^{-/-}$ mouse erythroblasts display mTOR activation resulting in impairment of autophagy as supported by accumulation of p62. Since p62 is an

autophagy adaptor important in protein quality control system, the accumulation of p62 is generally used as a marker of blockage of the autophagic flux.[25,26] Thus, we propose that the absence of Fyn might result in impairment of late phase of autophagy during erythroid maturation (Fig. 8a). In agreement, we found a reduction in *in vitro* reticulocyte maturation with delayed lysosomal clearance and again accumulation of p62 in $Fyn^{-/-}$ mouse reticulocytes (Fig. 6b, c). Our group has recently reported an impairment of autophagy with accumulation of p62 in both erythroblasts and red cells from patient with chorea acanthocytosis. This, further support the crucial role of autophagy in erythropoiesis.[27] Since no change in mitochondrial clearance was found in $Fyn^{-/-}$ *in vitro* maturating reticulocytes, we might reasonably exclude alteration of mitophagy in $Fyn^{-/-}$ mice. This is also supported by similar Nix protein content observed in *in vitro* maturating reticulocytes from both mouse strains (data not shown).[25,27]

We carried out the revision of the literature on pharmacologic activators of autophagy and erythropoiesis. (Table 4).

Table 4. Studies on the effects of Rapamycin on erythropoiesis and diseased red cells

	Main results	Ref.
Rapamycin (10 mg/kg) in C57B6/2J mice for 3 days	-**Relative low impact on erythroid growth and proliferation:** reduction in the reticulocyte count, without changes in reticulocyte volume or Hb content per cell; -**No significant effect on bone marrow adult erythropoiesis:** slight reduction of early erythroid precursors without major differences; -**No significant alterations on mTORC1 downstream signaling pathway in reticulocytes:** weak reduction in S6 kinase (S6K) activity, a widely used marker for mTOR activation; -**Co-administration of PHZ (50 mg/kg) and Rapamycin delays the response to stress erythropoiesis:** • Increased mortality of mice after 6 days following PHZ; • Delayed release of stress reticulocytes and decrease in spleen size compared to PHZ-treated mice; • Reduced early erythroid precursors proliferation in the spleen, suggesting a critical role of mTORC1 signaling during stress erythropoiesis; • No major changes in EPO levels.	**[4]**
MLN0128, a selective mTOR inhibitor	-**Profound effects on erythroid growth and proliferation:** • decrease in reticulocytes number, volume and hemoglobin content;	**[4]**

(2 mg/kg) in C57B6/2J mice for 3 days	• Decreased proliferation of early erythroid precursors with increased late stage erythroblasts; • Complete block of mTOR downstream signaling pathway; -**Co-administration of PHZ (50 mg/kg) is lethal after 3 days of treatment:** critical role of mTORC 1/2 signaling in response to acute hemolytic anemia.	
INK128, dual mTORC1/2 inhibitor (1 mg/kg) in humanized sickle cell mice for 3 weeks	-**In SCD mice**: Increased erythrocytes count, Hct and Hb content; Reduced reticulocytosis; Markedly decreased spleen size without changes in total body weight.	**[28]**
Sirolimus, selective mTORC1 inhibitor (5 mg/kg) in humanized sickle cell mice for 3 weeks	-**In both transplanted and non-transplanted SCD mice**, • Increased Hct and Hb, after 1 week of treatment; • Decreased splenomegaly; • Increased RBC lifespan; • Improved erythroid maturation; • Decreased iron deposition in kidney and liver; • Decreased stroke volume (reduced sickling/ vaso-occlusive crisis).	**[28]**
Rapamycin, an mTOR inhibitor (4 mg/kg) in FOXO3$^{-/-}$mice for 5 days/week for 2 weeks	- **In FOXO3$^{-/-}$mice and β-thal mice**: • Increased Hb levels (Foxo3$^{-/-}$ mice and β-thal mice); • No major effect on total erythroblast count, but ameliorated terminal erythroid differentiation (β-thal mice); • Blocked cell cycle progression in immature erythroblasts (β-thal mice); • Amelioration of the β-globin gene expression (β-thal mice); • Significant reduction in EPO levels;	**[29]**

EPO: erythropoietin; mTOR: mammalian target of Rapamycin; PHZ: phenylhydrazine; Hct: hematocrit; Hb: hemoglobin; β-thal: β-thalassemia; SCD: sickle cell disease; RBC: red blood cell

These results suggest that autophagy plays a key role in erythroid maturation and that modulation of the autophagic process might beneficially impact diseased erythropoiesis.[4,28,29] In our model, Rapamycin administration reduces total erythroblasts and ameliorates cellular homeostasis by reduction of oxidation (Fig. 9a, b). The activation of autophagy reduces cell apoptosis as indicated by the decrease amount of Annexin V^{+} cells (Fig. 9c). The restoration of the balance between apoptosis and autophagy results in decreased cellular levels of p62 (Fig. 9d). Our data indicate

that the absence of Fyn might affect autophagic lysosomal clearance system, which is particularly crucial during reticulocyte maturation.

In conclusion, we unveil the role of Fyn as a new kinase in EPO signaling cascade, increasing the complexity of EPO pathway, which already requires Jak2 as primary kinase and Lyn as additional kinase.[30] In $Fyn^{-/-}$ mice, the overactivation of Jak2 increases Akt function, resulting in persistent activation of Nrf2 and impairment of autophagy by mTOR activation. This results in cellular dysfunction which becomes evident when $Fyn^{-/-}$ mice were exposed to stressful conditions, such as PHZ or Doxorubicin.

Future studies will be designed to further characterize the signaling pathways intersects by Fyn in normal and diseased erythropoiesis. The co-administration of Rapamycin with PHZ, will help us in dissecting the contribution of activated autophagy in response to stress erythropoiesis. In $Fyn^{-/-}$ mice, other more selective inhibitors of either mTORC1 or mTORC1/2 might be tested to better understand whether the beneficial effect of Rapamycin is strictly dependent on its inhibitory effect on mTORC1 or involves other important factors in autophagy.

Since intense or persistent oxidation might block autophagy[31], we plan to treat $Fyn^{-/-}$ mice with N-Acetyl-Cysteine (NAC) as exogenous antioxidant molecule.[32,33]

9. REFERENCES

1. **De Franceschi, et al.** Oxidative stress and β-thalassemic erythroid cells behind the molecular defect. Oxid Med Cell Longev. 2013; **2013**:985210.
2. **Bartnikas TB, et al.** Transferrin is a major determinant of hepcidin expression in hypotransferrinemic mice. Blood. 201; **117**:630-7.
3. **Ingley E, et al.** Lyn deficiency reduces GATA-1, EKLF and STAT5, and induces extramedullary stress erythropoiesis. Oncogene. 2005; **24**:336-43.
4. **Friedman JM, et al.** A critical role for mTORC1 in erythropoiesis and anemia. Elife. 2014; **3**:e01913.
5. **De Franceschi L, et al.** In vivo reduction of erythrocyte oxidant stress in a murine model of beta-thalassemia. Haematologica. 2004; **89**:1287-1298.
6. **De Franceschi L, et al.** Combination therapy of erythropoietin, hydroxyurea, and clotrimazole in a beta thalassemic mouse: a model for human therapy. Blood. 1996; **87**:1188-1195.
7. **Liu J, et al.** Quantitative analysis of murine terminal erythroid differentiation in vivo: novel method to study normal and disordered erythropoiesis. Blood. 2013; **121**:43-49.
8. **Franco SS, et al.** Resveratrol accelerates erythroid maturation by activation of FoxO3 and ameliorates anemia in beta-thalassemic mice. Haematologica. 2014; **99**:267-275.
9. **Mattè A, et al.** The Interplay Between Peroxiredoxin-2 and Nuclear Factor-Erythroid 2 Is Important in Limiting Oxidative Mediated Dysfunction in β-Thalassemic Erythropoiesis. Antioxid Redox Signal. 2015; **23**:1284-97.
10. **Pahl HL, et al.** A novel role for nuclear factor-erythroid 2 in erythroid maturation by modulation of mitochondrialautophagy.Haematologica. 2016; **101**:1054-64.
11. **Mattè A, et al.** Peroxiredoxin-2 expression is increased in beta-thalassemic mouse red cells but is displaced from the membrane as a marker of oxidative stress. FRBM. 2010; **49**:457-466.

12. **Mattè A, et al.** The novel role of peroxiredoxin-2 in red cell membrane protein homeostasis and senescence. Free Radic Biol Med. 2014; **76:**80-8.
13. **Mattè A, et al.** Membrane association of peroxiredoxin-2 in red cells is mediated by the N-terminal cytoplasmic domain of band 3. Free Radic Biol Med. 2013; **55**:27-35.
14. **Lupo F, et al.** A new molecular link between defective autophagy and erythroid abnormalities in chorea-acanthocytosis. Blood. 2016; **128**:2976-2987.
15. **Kakkar P, et al.** Essential role of PH domain and leucine-rich repeat protein phosphatase 2 in Nrf2 suppressionvia modulation of Akt/GSK3β/ Fyn kinase axis during oxidative hepatocellular toxicity. Cell Death Dis. 2014; **5**:e1153.
16. **Shi M, et al.** ROS signaling under metabolic stress: cross-talk between AMPK and AKT pathway. Mol Cancer. 2017; **16**:79.
17. **Galli F, et al.** Nrf2-p62 autophagy pathway and its response to oxidative stress in hepatocellular carcinoma. Transl Res. 2017; pii: S1931-5244(17)30318-3.
18. **Lane JD, et al.** The ins and outs of human reticulocyte maturation: autophagy and the endosome/exosome pathway. Autophagy. 2012; **8**:1150-1.
19. **Ryan JJ, et al.** The Fyn-STAT5 Pathway: A New Frontier in IgE- and IgG-Mediated Mast Cell Signaling. Front Immunol. 2012; **3**:117.
20. **Wei Y, et al.** Investigating critical genes and gene interaction networks that mediate cyclophosphamide sensitivity in chronic myelogenous leukemia. Mol Med Rep. 2017; **16**:523-532.
21. **Zhu BM, et al.** Hematopoietic-specific Stat5-null mice display microcytic hypochromic anemia associated with reduced transferrin receptor gene expression. Blood. 2008; **112**:2071-80.
22. **Courtois G, et al.** HSP70 sequestration by free α-globin promotes ineffective erythropoiesis in β-thalassaemia. Nature. 2014; **514**:242-6.
23. **Marinkovic D, et al.** Foxo3 is required for the regulation of oxidative stress in erythropoiesis. Journal of Clinical Investigation. 2007; **117**:2133-2144.
24. **De Franceschi L, et al.** Oxidative stress modulates heme synthesis and induces peroxiredoxin-2 as a novel cytoprotective response in beta thalassemic erythropoiesis. Haematologica. 2011; **96**:1595-1604.

25. **Colombo MI, et al.** Autophagy: A necessary event during erythropoiesis. Blood Rev. 2017; **31**:300-305.
26. **Yamamoto M, et al.** The selective autophagy substrate p62 activates the stress responsive transcription factor Nrf2 through inactivation of Keap1. Nat Cell Biol. 2010; **12:**213-23.
27. **Zhang J, et al.** Autophagy as a regulatory component of erythropoiesis. Int J Mol Sci. 2015; **16**:4083-94.
28. **Wang J, et al.** mTOR Inhibition improves anaemia and reduces organ damage in a murine model of sickle cell disease. Br J Haematol. 2016; **174**:461-9.
29. **Gaffari S, et al.** FOXO3-mTOR metabolic cooperation in the regulation of erythroid cell maturation and homeostasis. Am J Hematol. 2014; **89**:954-63.
30. **Ingley E, Tilbrook PA, et al.** New insights into the regulation of erythroid cells. IUBMB Life. 2004; **56**:177-184.
31. **Karantza V, et al.** The interplay between autophagy and ROS in tumorigenesis. Front Oncol 2012; **2**:171.
32. **Elazar Z, et al.** Regulation of autophagy by ROS: physiology and pathology. Trends Biochem Sci 2011; **36**:30-8.
33. **Ciriolo MR, et al.** Under the ROS...thiol network is the principal suspect for autophagy commitment. Autophagy 2010; **6**:999-1005.

10. PAPERS AND ABSTRACTS

Free Radical Biology and Medicine 112 (2017) 376–386

Contents lists available at ScienceDirect

Free Radical Biology and Medicine

journal homepage: www.elsevier.com/locate/freeradbiomed

Original article

Peroxiredoxin-2 plays a pivotal role as multimodal cytoprotector in the early phase of pulmonary hypertension

Enrica Federti[a], Alessandro Matté[a], Alessandra Ghigo[b], Immacolata Andolfo[c], Cimino James[b], Angela Siciliano[a], Christophe Leboeuf[d], Anne Janin[d,e,f], Francesco Manna[c], Soo Young Choi[g], Achille Iolascon[c], Elisabetta Beneduce[a], Davide Melisi[a], Dae Won Kim[g], Sonia Levi[h,i], Lucia De Franceschi[a,*]

[a] Dept. of Medicine, University of Verona-AOUI Verona, Verona, Italy
[b] Molecular Biotechnology Center and Department of Molecular Biotechnology and Health Science, University of Torino, Torino, Italy
[c] CEINGE and Dept. of Biochemistry, University of Naples, Naples, Italy
[d] Inserm, U1165, Paris F-75010, France
[e] Université Paris 7- Denis Diderot, Paris, France
[f] AP-HP, Hôpital Saint-Louis, F-75010 Paris, France
[g] Institute of Bioscience and Biotechnology, Hallym University, Gangwon-do, Republic of Korea
[h] Division of Neuroscience, San Raffaele Scientific Institute, Milano, Italy
[i] Vita-Salute San Raffaele University, Milano, Italy

ARTICLE INFO

Keywords:
Peroxiredoxin-2
Chronic hypoxia
Autophagy
ER stress

ABSTRACT

Pulmonary-artery-hypertension (PAH) is a life-threatening and highly invalidating chronic disorder. Chronic oxidation contributes to lung damage and disease progression. Peroxiredoxin-2 (Prx2) is a typical 2-cysteine (Cys) peroxiredoxin but its role on lung homeostasis is yet to be fully defined. Here, we showed that $Prx2^{-/-}$ mice displayed chronic lung inflammatory disease associated with (i) abnormal pulmonary vascular dysfunction; and (ii) increased markers of extracellular-matrix remodeling. Hypoxia was used to induce PAH. We focused on the early phase PAH to dissect the role of Prx2 in generation of PAH. Hypoxic $Prx2^{-/-}$mice showed (i) amplified inflammatory response combined with cytokine storm; (ii) vascular activation and dysfunction; (iii) increased PDGF-B lung levels, as marker of extracellular-matrix deposition and remodeling; and (iv) ER stress with activation of UPR system and autophagy. Rescue experiments with *in vivo* the administration of fused-recombinant-PEP-Prx2 show a reduction in pulmonary inflammatory vasculopathy and in ER stress with down-regulation of autophagy. Thus, we propose Prx2 plays a pivotal role in the early stage of PAH as multimodal cytoprotector, targeting oxidation, inflammatory vasculopathy and ER stress with inhibition of autophagy. Collectively, our data indicate that Prx2 is able to interrupt the hypoxia induced vicious cycle involving oxidation-inflammation-autophagy in the pathogenesis of PAH.

1. Introduction

Pulmonary artery hypertension (PAH) is a life threatening highly invalidating chronic disorder [1–3]. Although in the last decade progresses have been made in the identifications of factors involved in its pathogenesis, much still remains to be investigated in the mechanism involved in the early stage of PAH [3–5]. Regardless of the initial event, the combination of chronic inflammation and chronic

Abbreviations: PAH, pulmonary artery hypertension; PBS, phosphate buffer; qRT-PCR, quantitative real time; ARDS, acute respiratory distress syndrome; ARE, anti-oxidant responsive element; Atg4, autophagy related 4; ATF6, activating transcription factor 6; Chop, C/EBP [CCAAT/enhancer-binding protein]-homologous protein; BAL, bronchoalveolar lavage; ET-1, endothelin 1; ER, endoplasmic reticulum; GAPDH, glyceraldehyde 3-phosphate dehydrogenase; HO-1, heme oxygenase 1; HSP, heat shock protein; HY stress, hypoxia stress; IRE1, inositol-requiring 1; IL-1b, interleukin 1b; IL-6, interleukin 6; IL-10, interleukin 10; LPS, lipopolysaccharides; NAC, N-acetyl-cysteine; NF-kB, nuclear factor kappa-light-chain-enhancer of activated B cells; Nrf2, nuclear factor-erythroid 2; PAH, pulmonary artery hypertension; PDGF-B, Platelet-derived growth factor subunit B; PEP Prx2, Prx2 fused to cell penetrating carrier PEP1 peptide; Prx2, peroxiredoxin-2; SMCs, smooth muscle cells; SOD-1, superoxide dismutase 1; Trdx, Thioredoxin reductase; PERK, PKR-like endoplasmic reticulum kinase; UPR, unfolded protein response; sXbp1, spliced X-box binding protein 1; GADD34, growth arrest and DNA damage-inducible protein; VCAM-1, vascular cell adhesion molecule 1; MDA, malondialdehyde; RV, right ventricular; RVSP, right ventricular systolic pressure; PAT, pulmonary acceleration time; ET, ejection time; ICAM-1, intercellular adhesion molecule 1; ANP, atrial natriuretic peptide; Ulk 1, Serine/threonine-protein kinase Ulk1; LC3 I/II, microtubule-associated protein 1A/1B-light chain 3

* Correspondence to: Dept of Medicine, University of Verona- AOUI Verona, Policlinico GB Rossi- P.le L Scuro, 10, 37134 Verona, Italy.
E-mail address: lucia.defranceschi@univr.it (L. De Franceschi).

http://dx.doi.org/10.1016/j.freeradbiomed.2017.08.004
Received 9 May 2017; Received in revised form 2 August 2017; Accepted 4 August 2017
Available online 09 August 2017

hypoxia promote a high pro-oxidant environment, mediating disease progression [1,2,4,6,7].

In this scenario, efficient catabolic pathways to either buildup misfolded/unfolded proteins or to clear intracellular damaged proteins are required [8–11]. Studies in different models of PAH have shown that cellular response to face the accumulation of damaged proteins is mainly through endoplasmic reticulum (ER) stress followed by the activation of autophagy to clear damaged proteins and to reduce ER stress [10,12,13]. Indeed, classic chaperones such as heat shock protein 90 and 70 (HSP) are upregulated in PAH, indicating the requirement of chaperone systems to deal with the accumulation of damaged proteins [14].

Prx2 is a typical 2-cysteine (Cys) peroxiredoxin ubiquitously expressed. Prx2 has been largely investigated in erythroid cells, where it is able to scavenge low concentration of H_2O_2 without inactivation due to over-oxidation [15]. Recently, in different cell models, Prx2 has been also linked to chaperone activity, priming cells to better tolerate oxidation [16,17]. Studies in mouse genetically lacking Prx2 ($Prx2^{-/-}$) have highlighted its protective role against LPS induced lethal shock and acute distress syndrome (ARDS), suggesting a possible contribution of Prx2 in inflammatory response [17–23]. In addition, *in vitro* and *in vivo* model of ischemic/reperfusion stress highlighted the key role of Prx2 as anti-oxidant system [24,25].

Here, we studied the role of Prx2 in development of pulmonary hypertension in mice genetically lacking Prx2 ($Prx2^{-/-}$), using hypoxic stress to explore the early stage of early phase of pulmonary hypertension. Our data collectively indicate that Prx2 plays a pivotal role in the early phase of hypoxia induced pulmonary hypertension as anti-oxidant system and chaperone. The administration of Prx2 fused to cell-penetrating carrier PEP (cell penetrating peptide; PEP Prx2; [19]) (i) reduces local and systemic inflammation; (ii) prevents vascular activation and PDGF-B up-regulation; (iii) alleviates ER stress and (i) down-regulates autophagy activation in response to hypoxia. Thus, PEP Prx2 might represent an interesting new multimodal therapeutic option in the early stage PAH.

2. Materials and methods

2.1. Drugs and chemicals

Details are reported in Supplemental materials and methods.

2.2. Mouse strains and design of the study

C57B6/2J mice as wildtype controls (WT) and $Prx2^{-/-}$ mice aged between 4 and 6 months both male and female were used in the present study [19,26]. The Institutional Animal Experimental Committee, University of Verona (CIRSAL) and by the Italian Ministry of Health approved the experimental protocols. Where indicated WT and $Prx2^{-/-}$ mice were treated with 1) N-Acetyl-Cysteine (NAC) at the dosage of 100 mg/kg/d (in NaCl 0.9%, NaOH 36 mM, pH 9.4; ip) or vehicle only for 3 weeks [19,20]; 2) PEP Prx2 (in PBS) or vehicle at the dosage of 3 mg/kg/d ip or vehicle for 4 weeks before and during hypoxia [19]. Whenever indicated, mice were exposed to hypoxia (8% oxygen for 10 h, 3 days, 7 days) (Hy) as previously described [27–29]. To collect organs, animals were first anesthetized with isoflurane, bronchoalveolar lavage (BAL) was collected and then mice were euthanized. Organs were immediately removed and divided into two and either immediately frozen in liquid nitrogen or fixed in 10% formalin and embedded in paraffin for histology.

2.2.1. Bronchoalveolar lavage (BAL) measurements

BAL fluids were collected and cellular contents were recovered by centrifugation and counted by microcytometry as previously reported [27]. Percentage of neutrophils was determined on cytospin centrifugation. Remaining BAL samples were centrifuged at 1500 × *g* for 10 min at 4 °C. The supernatant fluids were used for determination of total protein content [27].

2.3. Lung molecular analysis

2.3.1. Lung histology

Multiple (at least five) three-micron whole mount sections were obtained for each paraffin-embedded lung and stained with hematoxylin eosin, Masson's trichome, and May-Grünwald-Giemsa. α-smooth muscle actin immunohistochemistry (IHC) on lungs was carried out as previously reported [27,30]. Lung pathological analysis was carried out by blinded pathologists as previously described [27,30]. Based on previous reports (18, 38), the pathological criteria for lung histopathology were as follows: i) Bronchus: Mucus: 0: no mucus; +: mucus filling less than 50% of the area of the bronchus section; ++: mucus filling more than 50% of the area of the bronchus section. (ii) Inflammatory infiltrate density: 0: less than 5 inflammatory cells per field; +: 5–30 inflammatory cells per field; ++ more than 30 inflammatory cells per field. (iii) Thrombi: 0: no thrombus; + presence of a thrombus in one field, at magnification 250.

2.3.2. Immunoblot analysis

Frozen lung and heart from each studied group were homogenized and lysed with iced lyses buffer (LB containing: 150 mM NaCl, 25 mM bicine, 0.1% SDS, Triton 2%, EDTA 1 mM, protease inhibitor cocktail tablets (Roche), 1 mM Na_3VO_4 final concentration) then centrifuged 10 min at 4 °C at 12,000*g*. Proteins were quantified and analyzed by mono-dimensional SDS polyacrylamide gel electrophoresis. Gels were transferred to nitrocellulose membranes for immuno-blot analysis with specific antibody. Details are reported in Supplemental materials and methods [21,27,31–33]. Whenever indicated Prx2 dimerization was studied in lung from PBS perfused mice containing 100 mM NEM, using an approach similar to that reported by Kumar et al. [34].

2.3.3. RNA isolation, cDNA preparation and quantitative RT-PCR

Total RNA was extracted from tissues using Trizol reagent (Life Technologies, Monza, Italy). Synthesis of cDNA from total RNA (1 μg) was performed using Super Script II First Strand kits (Life Technologies). Quantitative RT-PCR (qRT- PCR) was performed using the SYBR-green method, following standard protocols with an Applied Biosystems ABI PRISM 7900HT Sequence Detection system. Relative gene expression was calculated using the $2^{(-\Delta Ct)}$ method, where ΔCt indicates the differences in the mean Ct between selected genes and the internal control (GAPDH). qRT-PCR primers for each gene were designed with Primer Express 2.0 (Life Technologies) (primer sequences are reported in Table 1S) [27,30].

2.4. MDA assay

MDA was determined as previously reported [35].

2.5. Evaluation of right ventricular hypertrophy and echocardiography measurements

Hearts were fixed with 10% formaldehyde for 24 h. The right ventricular (RV) free wall was separated from the left ventricular with septum (LV + S) under dissection microscope. RV and LV + S were separately weighed and used to calculate the ratios RV/(LV + S)/body weight [36]. Transthoracic echocardiography was performed with a Vevo 2100 echocardiograph (Visual Sonics, Toronto, Canada) equipped with a 22–55 MHz transducer (MicroScan Transducers, MS500D) as previously reported [27,37].

2.6. Statistical analysis

Data were analyzed using either *t*-test or the 2-way analysis of

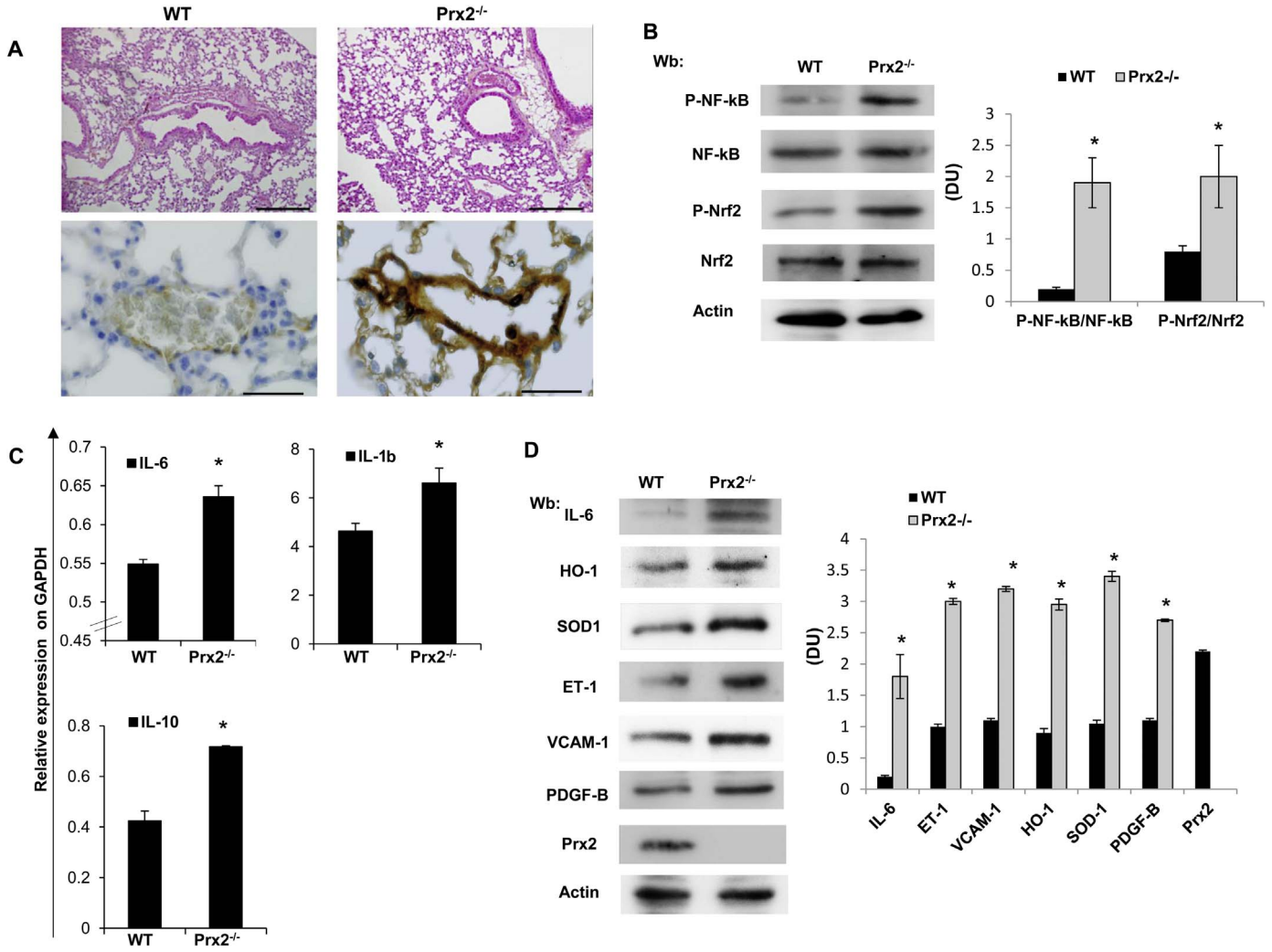

Fig. 1. The absence of Prx2 promotes lung inflammation, increased pulmonary vascular activation and extra-matrix remodeling markers. A. Comparison of Prx2$^{-/-}$ with WT mice shows an increased peribronchial edema in Prx2$^{-/-}$ mice (upper panel Hematoxylin Eosin ×250) and deposits of alpha actin in vascular walls in Prx2$^{-/-}$ mice (lower panel Immunohistochemistry using anti alpha actin antibody × 600). **B**. Immunoblot analysis with specific antibodies against phospho-NF-kB (P-NF-kB), NF-kB, phospho-Nrf2 (P-Nrf2) and Nrf2 of lung from wildtype (WT) and Prx2$^{-/-}$ mice under normoxic condition. One representative gel from six with similar results is presented. **Right panel**. Densitometric analysis (DU: Density Units) of immunoblots is shown as means ± SD (n = 6); *p < 0.05 compared to wildtype. **C**. IL-6, IL-1b, IL-10 mRNA levels in lung tissues (normalized to GADPH) from WT and Prx2$^{-/-}$ mice. * p < 0.05 (WT vs Prx2$^{-/-}$). Each sample (WT; Prx2$^{-/-}$) is a pool from 5 mice. Representative of three independent experiments. **D**. Immunoblot analysis with specific antibodies against IL-6, heme-oxygenase 1 (HO-1), endothelin-1 (ET-1), superoxide dismutase (SOD-1), vascular cell adhesion molecule-1 (VCAM-1), platelet derived growth factor-B (PDGF-B) and peroxiredoxin-2 (Prx2) of lung from wildtype (WT) and Prx2$^{-/-}$ mice under normoxic condition. One representative gel from six with similar results is presented. **Right panel**. Relative quantification of immunoreactivity (DU: Density Units) of IL-6, HO-1, SOD1, ET-1, VCAM1, PDGF-B and Prx2 of lung from wildtype (WT) and Prx2$^{-/-}$ mice under normoxic condition. Data are shown as means ± SD (n = 6); *p < 0.05 compared to wildtype.

variance (ANOVA) for repeated measures between the mice of various genotypes. A difference with a P value less than 0.05 was considered significant.

3. Results

3.1. Mice genetically lacking Prx2 show lung inflammation, increased pulmonary vascular activation and extracellular-matrix remodeling

Lung histopathologic analysis showed increased peribronchial edema without changes in the number of mucus cells in Prx2$^{-/-}$ mice under normoxia compared to wildtype animals (Fig. 1A, upper panel). The systematic study for α-smooth cells expression showed a staining in broken line only on bronchial sections of Prx2$^{-/-}$ mice, suggesting an initial pulmonary vessel muscularization (Fig. 1A, lower panel). Increased bronchoalveolar lavage (BAL) levels of proteins and of total leukocytes were detected in Prx2$^{-/-}$ mice compared to wildtype, indicating an abnormal pulmonary vascular leakage (Fig. 1SA).

In Prx2$^{-/-}$ mice, we observed increased active form of NF-kB and Nrf2, two redox related transcriptional factors, compared to wildtype animal (Fig. 1B).

This was associated with increased lung MDA levels (Fig. 1SB) and up-regulation of the pro-inflammatory cytokines IL-6, IL-1b and IL10 that are known targets of NF-kB (Fig. 1C). We confirmed the increased expression of IL-6 by immunoblot analysis in lung from Prx2$^{-/-}$ mice compared to wildtype animals (Fig. 1D). The activation of Nrf2 in the absence of Prx2 was supported by the up-regulation of Nrf2 related systems such as HO-1, a vascular and lung cytoprotector, and SOD-1, a potent anti-oxidant enzyme supports (Fig. 1D) [38]. We also observed higher levels of (i) endothelin-1 (ET-1), the most potent vasoconstrictive and broncho-constrictive cytokine [30]; (ii) VCAM-1, a marker of vascular endothelial activation [27]; and (iii) PDGF-B, a known factor involved in lung extra-cellular matrix remodeling [39] (Fig. 1D).

These data link the absence of Prx2 with persistent lung inflammation, endothelial vascular activation, and extracellular matrix remodeling.

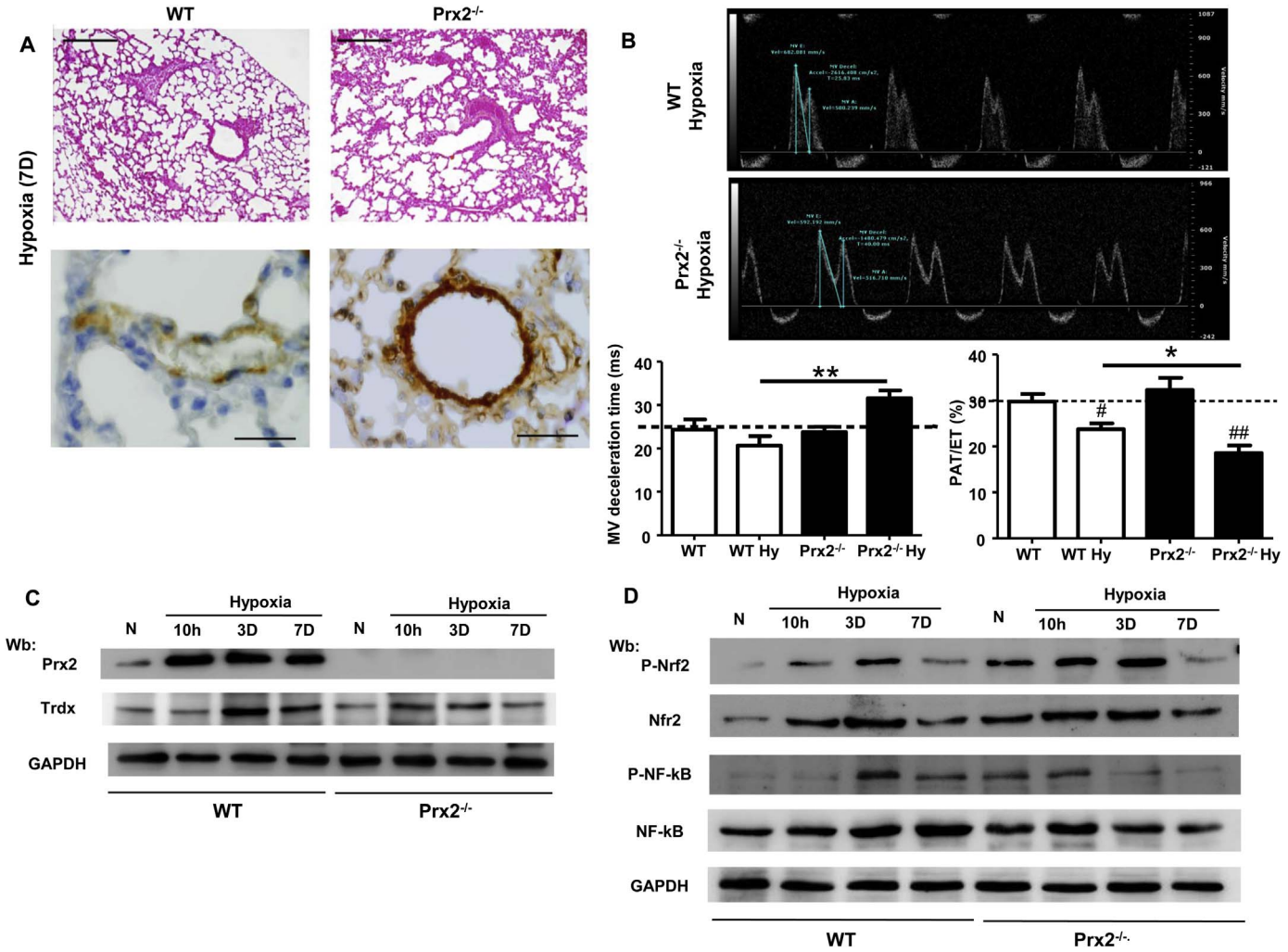

Fig. 2. In Prx2$^{-/-}$ mice, hypoxia induces early stage pulmonary hypertension and is associated with activation of redox-related transcriptional factors. A. Comparison of Prx2$^{-/-}$ with WT mice shows a sparse inflammatory infiltrate and an increased peribronchial edema in Prx2$^{-/-}$ mice (upper panel Hematoxylin Eosin ×250) and deposits of alpha actin in vascular walls in Prx2$^{-/-}$ mice (lower panel Immunohistochemistry using anti alpha actin antibody × 600). **B.** Representative images of mitral inflow pattern recorded by Doppler echo imaging in wildtype (WT) and Prx2$^{-/-}$ mice under hypoxia as in Fig. 1A. **Lower panels**. Average mitral valve deceleration time (left panel) and pulmonary acceleration time (PAT) to ejection time (ET) ratio (right panel). *p < 0.05 and **p < 0.01 WT *vs* Prx2$^{-/-}$ mice; #p < 0.05 and ##p < 0.01 hypoxia *vs* basal by one-way ANOVA followed by Newman-Keuls Multiple Comparison test. The black dashed lines have been added to the graph to favor visual comparison between the white bars *vs* the black bars. **C.** Immunoblot analysis with specific antibodies against peroxiredoxin-2 (Prx2) and thioredoxin-reductase 1 (Trdx) of lung wildtype (WT) and Prx2$^{-/-}$ mice under normoxia (N) exposed to hypoxia) for 10 h (10 h), 3 days (3D), 7 days (7D). One representative gel from six with similar results is presented. Densitometric analysis of immunoblots is shown in Fig. 2SA. **D.** Immunoblot analysis with specific antibodies against phospho-NF-kB (P-NF-kB), NF-kB, phospho-Nrf2 (P-Nrf2) and Nrf2 of lung wildtype (WT) and Prx2$^{-/-}$ mice under normoxia (N) and exposed to hypoxia (Hy) for 10 h (10 h), 3 days (3D), 7 days (7D). One representative gel from six with similar results is presented. Densitometric analysis of immunoblots is shown in Fig. 2SB.

3.2. Prolonged hypoxia promotes the development of early stage pulmonary hypertension in Prx2$^{-/-}$ mice

Based on our previous report, showing the development of early stage PAH in a mouse model for sickle cell disease but not in wildtype mice [36], we exposed both mouse strains to hypoxia (Hy) 8% oxygen for 7 days. As shown in Fig. 2A, hypoxia induced sparse inflammatory cell infiltrate with some peribronchial edema in Prx2$^{-/-}$ mice. On the bronchial epithelium there was no significant change in the number of mucus cells in both mouse strains. On vascular sections, no thrombus was found in any of the mouse groups. The systematic study for α-actin deposition revealed the presence of almost linear staining around bronchial and vascular sections in Prx2$^{-/-}$ mice (Fig. 2A, lower panel). While, α-actin depositions were sparse in hypoxic wildtype mice.

We evaluated the presence of RV hypertrophy in both mouse strains exposed to 7days hypoxia. In Prx2$^{-/-}$ mice, we observed a slight but significant increase in RV/(LV + S) ratio (normoxia: 0.21 ± 0.03 *vs* hypoxia 0.34 ± 0.05; $n = 6$, $P < 0.05$), whereas no changes were observed in wildtype mice in agreement with our previous report [36]. This was associated with a significant increase in mitral valve deceleration time and a reduction in pulmonary acceleration time/ ejection time ratio (Fig. 2B), indicating early diastolic dysfunction and increased right ventricular systolic pressure in Prx2$^{-/-}$ mice. In addition, we found hypoxia induced increased expression of SOD-1 in heart from both mouse strains, but to a higher extent in Prx2$^{-/-}$ mice (Fig. 1SD). Hypoxia induced up-regulation of (i) VCAM-1 and ICAM-1; and (ii) atrial natriuretic peptide (ANP) was also observed in both mouse strains (Fig. 1SD).

Our findings are consistent with the development of early stage of PAH promoted by severe oxidation and amplified inflammatory response in Prx2$^{-/-}$ mice exposed to 7-days hypoxia.

3.3. Prx2 plays an important role as cytoprotective system against hypoxia induced PAH

In order to follow-up the generation of PAH in Prx2$^{-/-}$ mice, we studied both mouse strains at different time intervals between 0 to 7-days hypoxia to identify the optimal window-time to analyze

mechanism(s) involved in development of PAH. BAL protein and leukocyte count were significantly increased in Prx2$^{-/-}$ mice during hypoxia at 10 h, 3 days and 7 days compared to wildtype animals (data not shown).

Hypoxia markedly increased Prx2 expression in lung from wildtype mice at 10 h, 3 days and 7 days of exposure (Fig. 2C; Fig. 2SA). This was associated with time dependent increased expression of thioredoxin-reductase, a Prx2 repairing system (Trdx; Fig. 2C; Fig. 2SA). The modulation of Trdx expression during hypoxia even in the absence of Prx2, may be possible related to the fact that Trdx is part of different NADPH-dependent pathways [19,40].

In Prx2$^{-/-}$ mice exposed to hypoxia, we observed a rapid and sustained activation of Nrf2 in response to hypoxia, while there was a reduction in activation of NF-kB (Fig. 2D, 2SB). Otherwise, wildtype mice showed an early response of Nrf2 at 10 and 3-h hypoxia, partially overlapping the activation of NF-kB observed at 3 and 7 days hypoxia (Figs. 2D, 2SB). These data suggest that Nrf2 might be a precocious back-up mechanism in response to hypoxia, which is early activated in both mouse strains, but to higher extent in mice genetically lacking Prx2.

Since pro-inflammatory cytokines are modulated by oxidation and participates to the development of PAH [3,41,42], we evaluated IL1b and IL6 expression in lung from both mouse strains during hypoxia. In Prx2$^{-/-}$ mice, IL-1b mRNA levels were significantly increased at 3 days of hypoxia compared to wildtype animals, which displayed increased IL-1b expression only at 7-days hypoxia (Fig. 3A). In Prx2$^{-/-}$ mice, lung IL-6 mRNA expression was significantly upregulated at 3 days of hypoxia followed by a decreased at 7 days of hypoxia to levels still higher than those observed in wildtype mice (Fig. 3B). These data support an earlier and amplified inflammatory response in Prx2$^{-/-}$ mice in response to hypoxia compared to wildtype animals.

We then evaluated markers of pulmonary vascular remodeling (ET-1, PDGF-B, ANP) and vascular endothelial activation (VCAM-1 and ICAM-1). As shown in Fig. 3C, ET-1 expression was increased in both mouse strains but to a higher extent in Prx2$^{-/-}$ mice compared to wildtype; while PDGF-B levels increased earlier, reaching higher and constant levels in Prx2$^{-/-}$ mice compared to wildtype during hypoxia. VCAM-1 and ICAM-1 expression was similarly increased in both mouse strains at 7 days hypoxia (Fig. 3D). Whereas, ANP levels were higher in Prx2$^{-/-}$ mice than in wildtype animals exposed to prolonged hypoxia (Fig. 3D).

Collectively, these data indicate that the absence of Prx2 accelerates vascular activation and extra-cellular matrix remodeling, amplifying inflammatory response and oxidation during hypoxia.

3.4. The absence of Prx2 is associated with endoplasmic reticulum (ER) stress and up-regulation of ATF6

Studies in different models of PAH have shown that hypoxia and/or PDGF-B and /or ET-1 induce severe proteins damage, which promotes endoplasmic reticulum stress (ER), triggering unfolded protein response (UPR) system [10,11,13,43]. When the accumulation of damaged proteins exceeds the ER capacity, ER stress leads to activation of autophagy as adaptive mechanism to clear accumulated misfolded/unfolded proteins [11,44]. UPR system is characterized by 3 branches: IRE, PERK and ATF6, this latter has been reported to be mainly involved in PAH [12,45]. As shown in Fig. 4A, ATF6, Chop and sXbp1 were up-regulated in lung from Prx2$^{-/-}$ mice under normoxia compared to wildtype animals. Whereas, GADD34 was downregulated in Prx2$^{-/-}$ mice compared to wildtype animals (Fig. 4A). In response to hypoxia, we observed dynamic changes of the main UPR systems: (i) ATF6; (ii) GADD34 and Chop, related to PERK and Xbp1, a component of IRE branch [10]. As shown in Fig. 4B, increased mRNA levels of both Chop and Xbp1 were observed at 10 h in Prx2$^{-/-}$ mice, while GADD34 was still significantly increased at 3-days hypoxia compared to normoxic Prx2$^{-/-}$ animals. In chronically exposed Prx2$^{-/-}$ mice, ATF6 and sXbp1 mRNA levels were again higher than in normoxia Prx2$^{-/-}$ animals (Fig. 4B). Wildtype animals show an early signs of ER stress with up-regulation of ATF6 and Xbp1 at 10-h hypoxia, with no major change in chronic hypoxia (Fig. 4B). It is of note that in lung from wildtype mice, we found Prx2 organized in multimers, possible reflecting the acquisition of chaperone like function (data not shown) [31,46,47].

These data indicate that the absence of Prx2 triggers ER stress during hypoxia, contributing to the early appearance of PAH in Prx2$^{-/-}$ mice.

3.5. PEP Prx2 treatment rescues prolonged hypoxia induced heart and lung inflammatory vasculopathy and prevents ER stress

To address the question whether Prx2 plays a role in lung chronic inflammatory disease, we firstly evaluated the impact of recombinant fusion protein PEP Prx2 (1.5 mg/kg/day ip; 3 weeks) to both mouse strains under room air condition. In normoxic Prx2$^{-/-}$ mice, PEP Prx2 treatment (i) prevented Nrf2 and NF-kB activation (Fig. 3SA); (ii) reduced HO-1 protein expression (Fig. 3SB); and (iii) decreased the levels of ET-1, VCAM-1 and PDGF-B (Fig. 3SB). No major changes were observed in wildtype animals (Fig. 3SA, 3SB). In order to evaluate whether the effects of PEP Prx2 treatment were specific of Prx2 or related to a general anti-oxidant effect, we treated both mouse strains with NAC (100 mg/kg/day for 3 weeks), a known anti-oxidant agent previously used in other *in vitro* and *in vivo* models of PAH [6,48]. No changes were present in the levels of Nfr2 and NF-kB activation in Prx2$^{-/-}$ mice treated with NAC, suggesting that the effects of PEP Prx2 are peculiar of Prx2 and not only related to its general antioxidant effects (data not shown).

In Prx2$^{-/-}$ mice exposed to 7 days hypoxia, PEP Prx2 treatment significantly reduced the hypoxia mediated diastolic dysfunction and ameliorated RVSP, as suggested by the increased in PAT/ET ratio (Fig. 4C, 4SA). In agreement, in heart from PEP Prx2 treated Prx2$^{-/-}$ mice exposed to 7 days hypoxia, we found a reduction of ANP expression as well as of markers of vascular endothelial activation (Fig. 4D). This was associated with a decrease in levels of SOD-1 and in oxidation of proteins from heart of hypoxic Prx2$^{-/-}$ mice treated with PEP Prx2 (Fig. 4SB). We found similar evidences of the beneficial effects of PEP Prx2 on lung from Prx2$^{-/-}$ mice exposed to prolonged hypoxia. As shown in Fig. 5A, PEP Prx2 promoted a significant reduction in chronic hypoxia induced increase of ANP, VCAM-1, ICAM-1 and PDGF-B levels compared to vehicle treated Prx2$^{-/-}$ animals. In addition, PEP Prx2 decreased the hypoxia induced ATF6 expression, suggesting a possible role of Prx2 as chaperone in agreement with the reduced expression of classic chaperone HSP70 and 90 (Fig. 5B).

To better understand the role of Prx2 in development of PAH, we chose to further study Prx2$^{-/-}$ mice at day 3 of hypoxia. This represents the turning point in the imbalance between oxidation/anti-oxidant activities and the activation of cellular defense mechanisms against cytotoxic effects of accumulation of damage proteins. Indeed, we found a significant increase in the amount of Prx2 dimers in lung from wildtype after 3 days hypoxia compared to normoxic wildtype animals (Fig. 4SC), supporting the role of Prx2 as H_2O_2 sensor generated during hypoxia as previously shown in other models [34,49].

3.6. In Prx2$^{-/-}$ mice, PEP Prx2 prevents the hypoxia induced oxidative stress and reduces inflammatory vascular activation and extracellular matrix remodeling

PEP Prx2 administration prevented the hypoxia induced increased in BAL protein and leukocyte content in both mouse strains (Fig. 4SD). This was associated with a marked reduction in protein oxidation state in both mouse strains exposed to 3 days hypoxia and treated with PEP Prx2, supporting the local anti-oxidant effect of exogenous PEP Prx2 treatment during hypoxia stress (Fig. 5C). In agreement, we found that PEP Prx2 administration prevented the hypoxia induced Nrf2 and NF-kB activation in both mouse strains (Fig. 5D, 5SA). This was paralleled

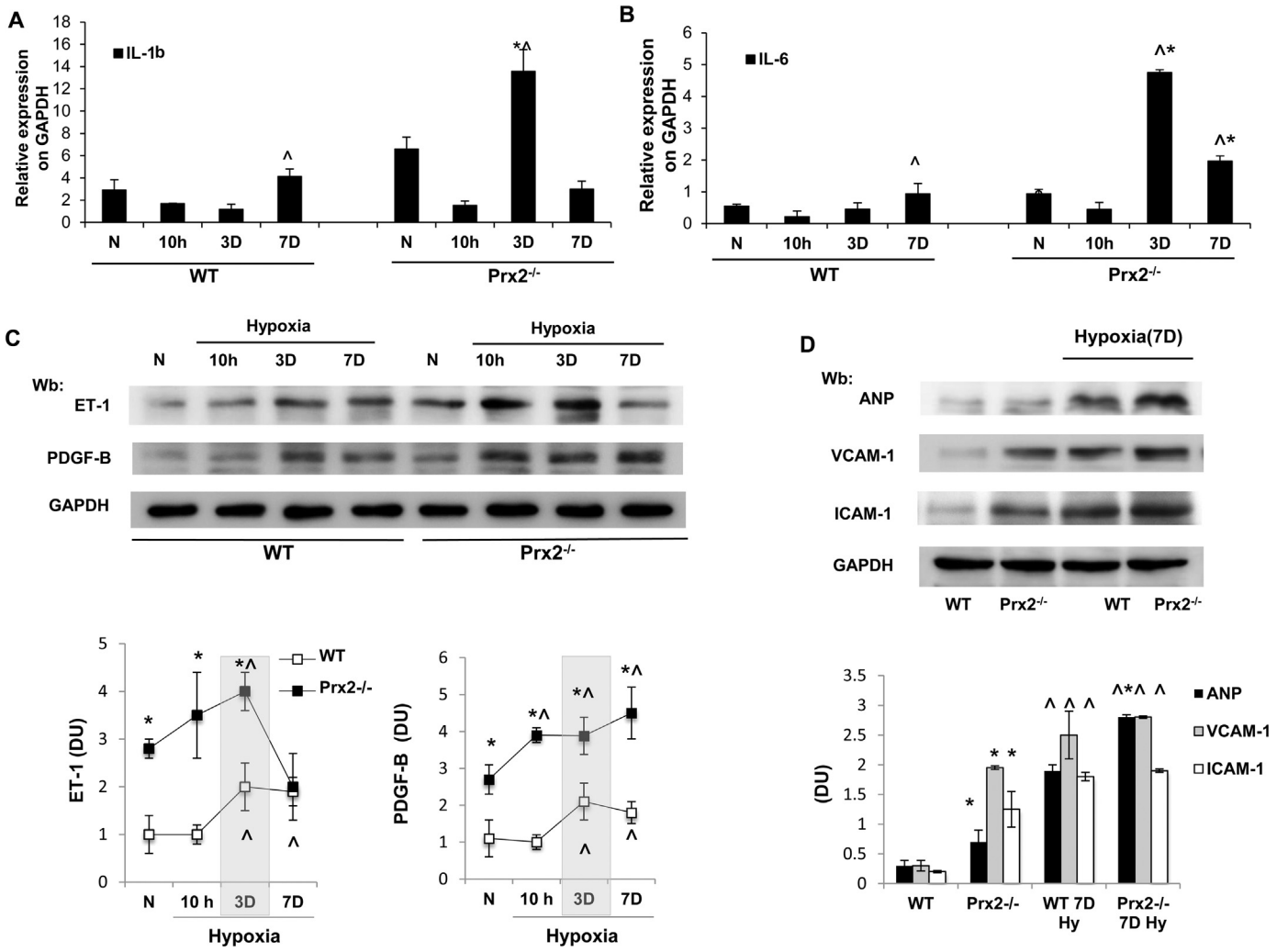

Fig. 3. In Prx2$^{-/-}$ mice, hypoxia is associated with amplified inflammatory response, vascular activation and increased expression of PDGF-B, a marker of extracellular matrix remodeling. A-B. IL-1b (**A**) and IL-6 (**B**) mRNA levels in lung tissues (normalized to GADPH) wildtype (WT) and Prx2$^{-/-}$ mice under normoxia (N) and exposed to hypoxia for 10 h (10 h), 3 days (3D), 7 days (7D). *p < 0.05 compared to wildtype; ^ p value < 0.05 compared to normoxic mice. Each sample is a pool from 5 mice. Representative of three independent experiments. **C. Upper panel**. Immunoblot analysis with specific antibodies against endothelin-1 (ET-1) and platelet derived growth factor-B (PDGF-B) of lung from wildtype (WT) and Prx2$^{-/-}$ mice under normoxia (N) and exposed to hypoxia for 10 h (10 h), 3 days (3D), 7 days (7D). One representative gel from six with similar results is presented. **Lower panel**. Relative quantification of immunoreactivity (DU: Density Units) of ET-1 and PDGF-B in lung from wildtype (WT) and Prx2$^{-/-}$ mice under normoxia (N) and exposed to hypoxia for 10 h (10 h), 3 days (3D), 7 days (7D). Data are shown as means ± SD (n = 6). *p < 0.05 compared to wildtype; ^ p < 0.05 compared to normoxic mice. The grey area highlights the changes in the ET-1 and PDGF-B expression in the mouse strains at 3 days hypoxia. **D. Upper panel**. Immunoblot analysis with specific antibodies against atrial natriuretic peptide (ANP), vascular adhesion molecule -1 (VCAM-1) and intracellular adhesion-molecule- 1 (ICAM-1) of lung from wildtype (WT) and Prx2$^{-/-}$ mice under normoxia (lane 1 and 2) and exposed to 7 days (7D) hypoxia. One representative gel from six with similar results is presented. **Lower panel**. Relative quantification (DU: Density Units) of immunoreactivity of ANP, VCAM-1, ICAM-1 in lung from wildtype (WT) and Prx2$^{-/-}$ mice under normoxia and exposed to 7 days (7D) hypoxia. Data are shown as means ± SD (n = 6); *p < 0.05 compared to wildtype; ^ p < 0.05 compared to normoxic mice.

by the reduction in HO-1, IL-6, ET-1, VCAM-1 and PDGF-B (Fig. 6A).

These data suggest that PEP Prx2 treatment during hypoxia is able to (i) decrease local pulmonary inflammation and oxidation, (ii) reduce systemic inflammatory response; (iii) beneficially affect hypoxia abnormalities in pulmonary vascular leakage; and (iv) prevent hypoxia activation of redox-sensitive transcriptional factors Nrf2 and NF-kB.

3.7. PEP Prx2 alleviates ER stress and down-regulates autophagy in Prx2$^{-/-}$ mice exposed to hypoxia

As shown in Fig. 6B, PEP Prx2 significantly down-regulated G-ADD34 in lung from Prx2$^{-/-}$ mice compared to vehicle treated animals. This was associated with a marked decrease in HSP70 and 90 expression in lung from both mouse strains exposed to 3 days hypoxia and treated with PEP Prx2 (Fig. 6C). This is agreement with previous reports on preventing PAH development by blocking ER stress with exogenous chemical chaperones [12].

Since a link between ER stress and activation of autophagy has been proposed to deal the accumulation of damaged proteins [10,44], we evaluated key elements of autophagy machinery and the effects of PEP Prx2 treatment in both mouse strains at 3 days hypoxia. Based on revision of the literature, we chose to analyze the expression of (i) autophagy related proteins ULk1 that is required for initiation of autophagy; (ii) LC3 I/II, a coordinator of phagosomal membranes and (iii) p62, a key cargo protein and component of inclusion bodies; and (iv) pro-caspase 3/caspase 3, involved in digestion of damaged proteins [9,50–52]. As shown in Fig. 7A, normoxic Prx2$^{-/-}$ mice showed increased LC3-II formation associated with increased expression of Ulk1 and p62 compared to wildtype mice. This was associated with higher expression of pro-caspase 3/caspase 3, indicating an activation of autophagy to clear intracellular oxidative damaged proteins in Prx2$^{-/-}$ mice. In both mouse strains, hypoxia markedly activated autophagy as supported by increased LC3I/II expression, consumption of Ulk1 and reduction of p62, suggesting a clearance of p62 positive inclusion

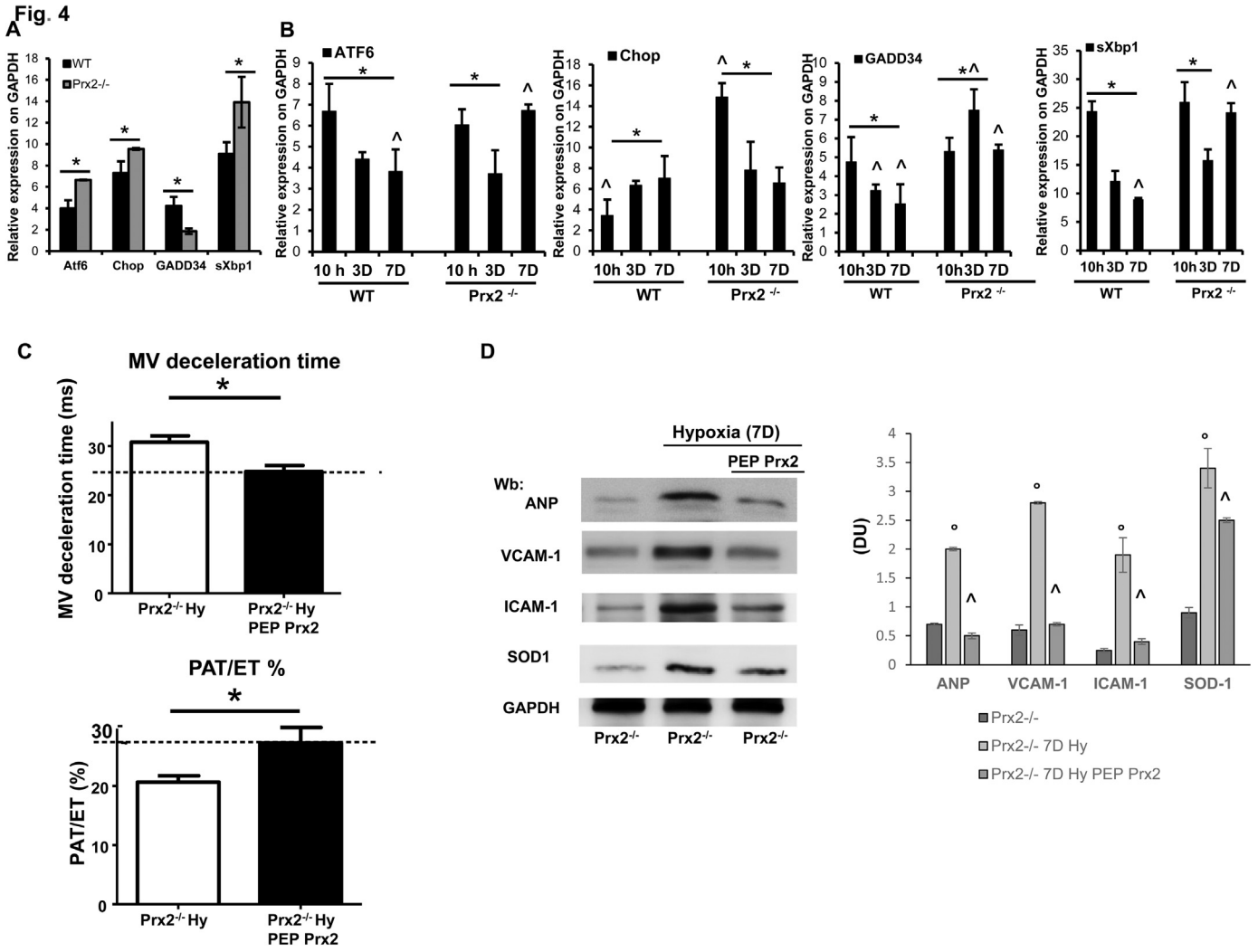

Fig. 4. Hypoxia induces ER stress in Prx2$^{-/-}$ mice and PEP Prx2 administration prevents the hypoxia induced diastolic dysfunction with reduction of inflammatory vasculopathy. A-B. ATF6, CHOP, GADD34, sXBP1 mRNA levels in lung tissues wildtype (WT) and Prx2$^{-/-}$ mice under normoxia (N) *p < 0.05 compared to wildtype. Each sample is a pool from 5 mice. Representative of three independent experiments **(A)**. ATF6, CHOP, GADD34, sXBP1 mRNA levels in lung tissues (normalized to GADPH) wildtype (WT) and Prx2$^{-/-}$ mice exposed to hypoxia for 10 h (10 h), 3 days (3D), 7 days (7D). Each sample is a pool from 5 mice. **(B)** ATF6 *p < 0.05 for WT mice 10 h vs 3D; 10 h vs 7D. ATF6 *p < 0.05 for Prx2$^{-/-}$ mice 10 h vs 3D; ^ p < 0.05 for WT mice 7D vs Prx2$^{-/-}$ mice 7D. CHOP *p < 0.05 for WT mice 10 h vs 3D; 10 h vs 7D. CHOP *p < 0.05 for Prx2$^{-/-}$ mice 10 h vs 3D; 10 h vs 7D; ^ p < 0.05 for WT mice 10 h vs Prx2$^{-/-}$ mice 10 h. GADD34 *p < 0.05 for WT mice 10 h vs 3D; 10 h vs 7D. GADD34 *p < 0.05 for Prx2$^{-/-}$ mice 10 h vs 3D. sXbp1 *p < 0.05 for WT mice 10 h vs 3D; 10 h vs 7D. ^ p < 0.05 for WT mice 7D vs Prx2$^{-/-}$ mice 3D and 7D. sXbp1 *p < 0.05 for Prx2$^{-/-}$ mice 10 h vs 3D. ^ p < 0.05 for WT mice 7D vs Prx2$^{-/-}$ mice 7D. **C.** Average mitral valve deceleration time (left panel) and pulmonary acceleration time (PAT) to ejection time (ET) ratio (right panel); *p < 0.05 vehicle treated Prx2$^{-/-}$ mice *vs* PEP Prx2 treated Prx2$^{-/-}$ mice; by one-way ANOVA followed by Newman-Keuls Multiple Comparison test. The black dashed lines have been added to the graph to favor visual comparison between the white bars *vs* the black bars. Representative images of mitral inflow pattern recorded by Doppler echo imaging in Prx2$^{-/-}$ mice treated with PEP Prx2 are shown in Fig. 4SA. **D.** Immunoblot analysis with specific antibodies against atrial natriuretic peptide (ANP), vascular adhesion molecule -1 (VCAM-1), intracellular adhesion-molecule- 1 (ICAM-1) and superoxide dismutase-1 (SOD-1) of heart from Prx2$^{-/-}$ mice under normoxia (lane 1) and exposed to 7 days (7D) hypoxia treated with either vehicle or PEP Prx2. One representative gel from six with similar results is presented; GAPDH was used as protein loading control. **Right panel**. Relative quantification of immunoreactivity (DU: Density Units) of ANP, VCAM-1, ICAM-1, SOD1 of heart from Prx2$^{-/-}$ mice under normoxia and exposed to 7 days (7D) hypoxia treated with either vehicle or PEP Prx2. Data are presented as means ± SD (n = 6); ^p < 0.05 compared to Prx2$^{-/-}$ normoxic mice; ° p < 005 compared to vehicle treated mice.

bodies containing damaged proteins (Fig. 7A). It is of note that the procaspase/caspase 3 ratio was also increased in both mouse models exposed to hypoxia, but to higher extent in Prx2$^{-/-}$ mice compared to wildtype (Fig. 7A).

As a proof of concept that Prx2 is important in the crossroad between hypoxia induced oxidation and autophagy, we evaluated the effects of PEP Prx2 treatment on autophagy in mice exposed to 3 days hypoxia. As shown in Fig. 7A, PEP Prx2 administration rescued the hypoxia induced activation of autophagy. These data indicate that Prx2 acts as multimodal cytoprotective system and is important to prevent the development of PAH.

4. Discussion

Here, we firstly show the novel role of Prx2 as lung multimodal cytoprotector against hypoxia induced PAH. Our data also indicate that Prx2 is required in management of the physiologic oxidation in lung under room air condition. In fact, normoxic Prx2$^{-/-}$ mice show we lung chronic inflammatory vasculopathy and vascular dysfunction, associated with activation of extracellular matrix remodeling. This is in agreement with previous studies in mouse models genetically lacking other anti-oxidant systems such as SOD-1, which show increased susceptibility to both acute and chronic lung injury [53–55].

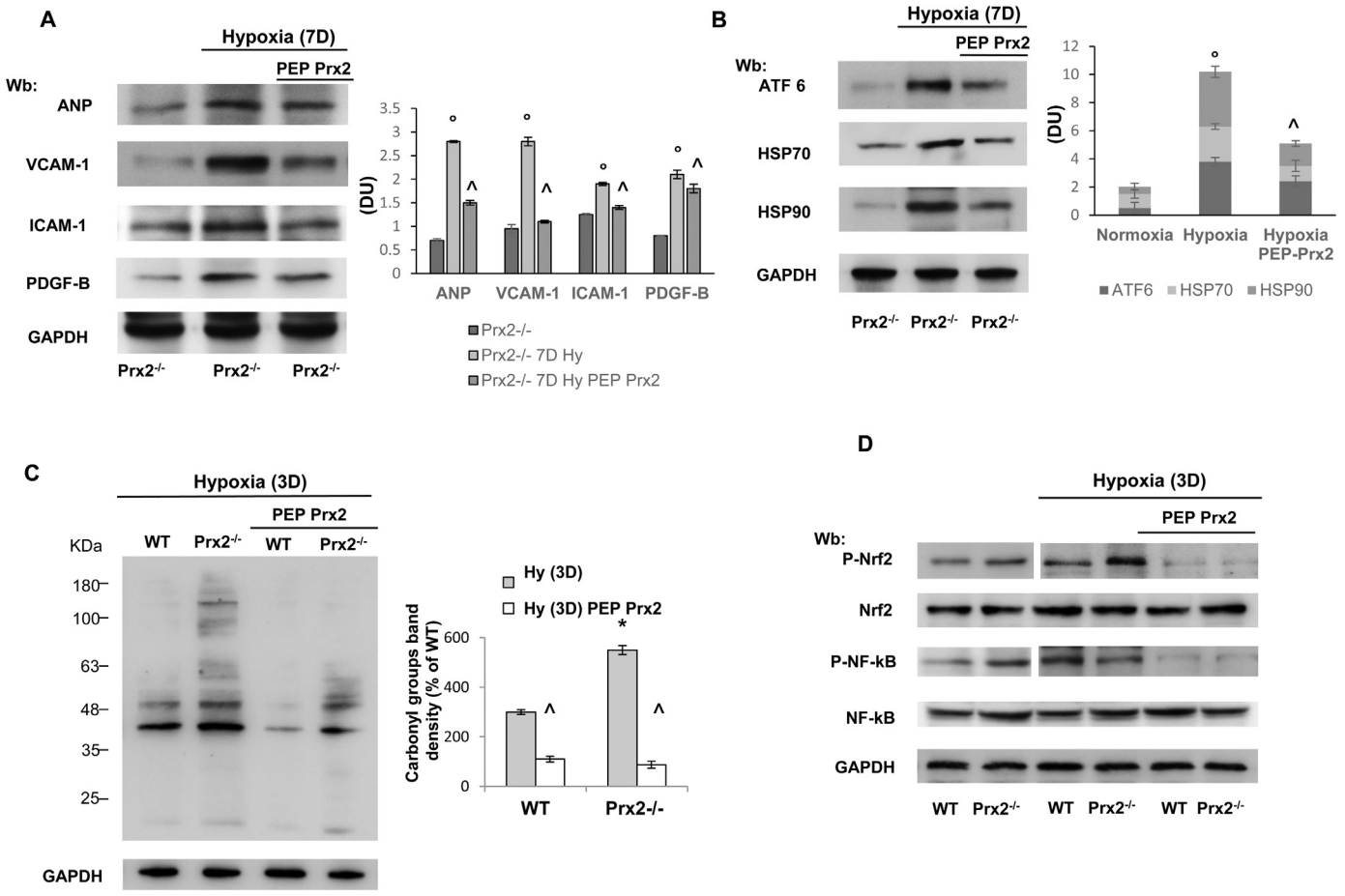

Fig. 5. PEP Prx2 administration prevents lung vascular remodeling and alleviates ER stress induced by prolonged hypoxia. A. Immunoblot analysis with specific antibodies against atrial natriuretic peptide (ANP), vascular adhesion molecule -1 (VCAM-1), intracellular adhesion-molecule- 1 (ICAM-1) and PDGF-B of lung from Prx2$^{-/-}$ mice under normoxia (lane 1) and exposed to 7 days (7D) hypoxia treated with either vehicle or PEP Prx2. One representative gel from six with similar results is presented; GAPDH was used as protein loading control. **Right panel.** Relative quantification of immunoreactivity (DU: Density Units) of ANP, VCAM-1, ICAM-1 and PDGF-B in lung from Prx2$^{-/-}$ mice under normoxia (lane 1) and exposed to 7 days (7D) hypoxia treated with either vehicle or PEP Prx2. Data are shown as means ± SD (n = 6); ^ $p < 0.05$ compared to Prx2$^{-/-}$ normoxic mice; ° $p < 0.05$ compared to Prx2$^{-/-}$ treated with vehicle. **B.** Immunoblot analysis with specific antibodies against activating transcriptional factor-6 (ATF6), heat shock protein 70 (HSP70) and heat shock protein 90 (HSP90) of lung from Prx2$^{-/-}$ mice under normoxia (lane 1) and exposed to 7 days (7D) hypoxia treated with either vehicle or PEP Prx2. One representative gel from six with similar results is presented; GAPDH was used as protein loading control. **Right panel.** Relative quantification of immunoreactivity (DU: Density Units) of ATF6, HSP70 and HSP90. Data are shown as means ± SD (n = 6); ^ $p < 0.05$ compared to Prx2$^{-/-}$ normoxic mice; ° $p < 0.05$ compared to Prx2$^{-/-}$ treated with vehicle. **C.** The carbonylated proteins (1 μg) were detected by treating with DNPH and blotted with anti-DNP antibody. **Right panel.** Quantification of band area was performed by densitometry and expressed as % of WT. The data are presented as means ± SD of at least three independent experiments *$p < 0.05$ compared to WT; ° $p < 0.05$ compared to vehicle treated mice (n = 3). **D.** Immunoblot analysis with specific antibodies against phospho-NF-kB (P-NF-kB), NF-kB, phospho-Nrf2 (P-Nrf2) and Nrf2 of lung from wildtype (WT) and Prx2$^{-/-}$ mice under normoxic condition treated with either vehicle or penetrating peptide fusion protein peroxiredoxin-2 (PEP Prx2). One representative gel from six with similar results is presented. Densitometric analysis of immunoblots is shown in Fig. 5SA.

Prx2$^{-/-}$ mice exposed to prolonged hypoxia developed signs of PAH, combined with inflammatory vasculopathy, sustained by high ET-1 expression and increased PDGF-B levels, as marker of extracellular matrix remodeling. Both molecules have been reported to accelerate the development of hypoxia induce PAH [30,39]. The increase ANP lung and heart expression indicates an attempt of endogenous system to induce pulmonary vaso-relaxation and to modulate lung and heart vascular remodeling in response to hypoxia [56,57]. This was coordinated by hypoxia induced activation of acute phase related transcriptional factors: Nrf2 and NF-kB in both mouse strains. The early and higher activation of Nrf2 in Prx2$^{-/-}$ mice compared to wildtype animals, supports the role of Nrf2 as back-up mechanism against severe oxidation in mice genetically lacking Prx2 [19]. Whereas, NF-kB seemed to be more important in prolonged hypoxia for wildtype mice compared to Prx2$^{-/-}$ animals. The rescue experiments with PEP Prx2 corroborate the importance of Prx2 in the functional cascade activated in response to hypoxia.

In this scenario, the absence of Prx2 favors ER stress with the activation of autophagy, as important mechanisms to deal with the accumulation of cytotoxic damaged proteins triggered by hypoxia and oxidation [10,44]. ER stress activates the UPR system, which is divided into three branches: ATF6, PERK and IRE1 [10,13]. In Prx2$^{-/-}$ mice, ATF6 was up-regulated in lung from animals under normoxia and after prolonged hypoxia. Whereas, GADD34, part of PERK branch, was early up-regulated at 3 days hypoxia in Prx2$^{-/-}$ mice. This indicate that the absence of Prx2 favors ER stress most likely due to a reduction of endogenous chaperone power beside the increased expression of classic heat shock proteins such as HSP70 and 90 in response to hypoxia. PEP Prx2 alleviated ER stress and prevented the hypoxia induced up-regulation of UPR system, in agreement with previous report on exogenous chemical chaperones, reducing ER stress and preventing the development of PAH [12,13]. It is of interest to note that previous reports have shown that PDGF-B and/or ET- activates UPR [13,43]. In our model, the absence of Prx2 resulted in high levels of PDGF-B and ET1 that potentiate the hypoxia induced activation of UPR system. The rescue experiments with PEP Prx2 corroborate the pivotal role of Prx2 in lung homeostasis.

The behavior of defensive autophagy in Prx2$^{-/-}$ mice exposed to

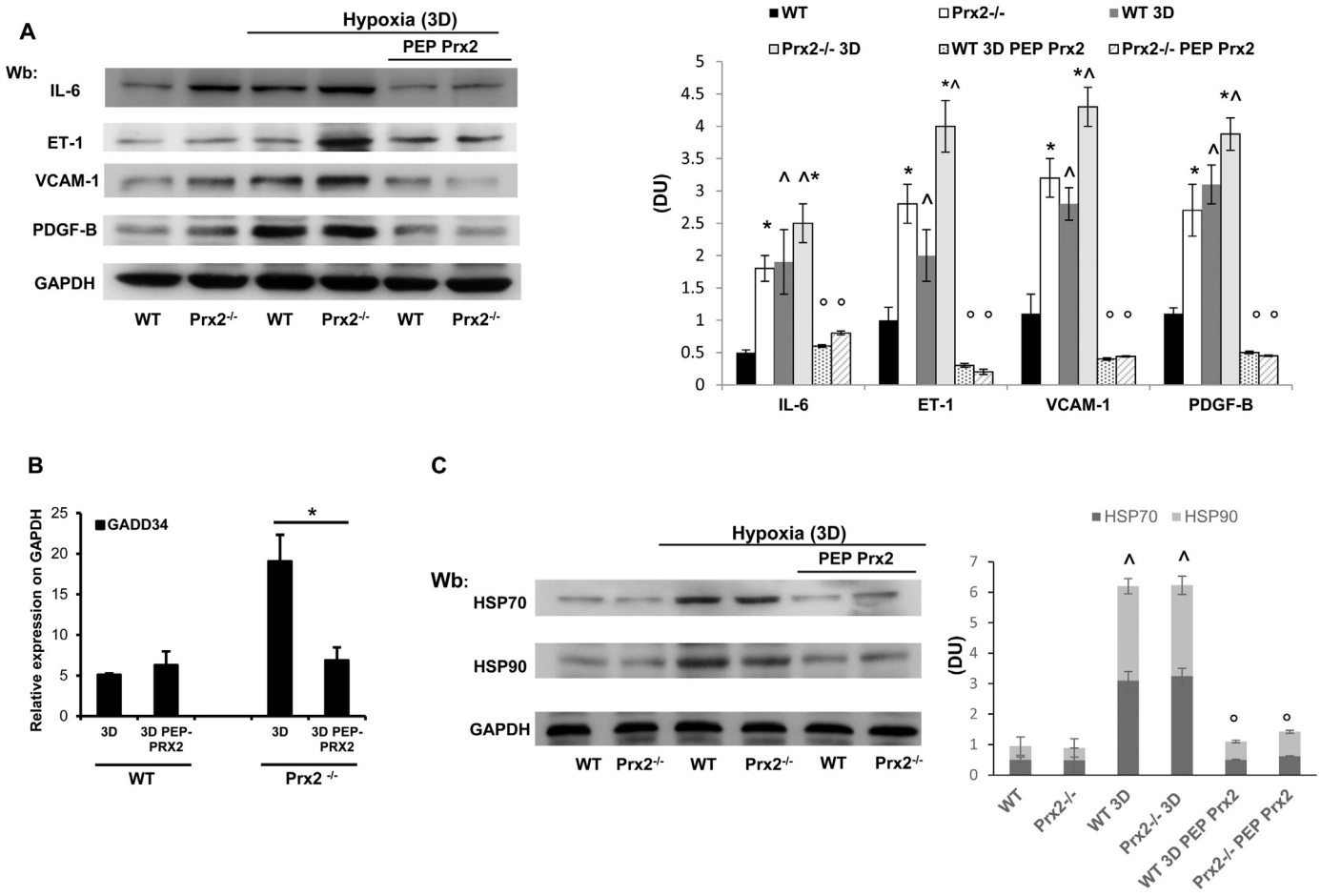

Fig. 6. PEP Prx2 administration reduces ER stress and prevents chaperone expression in the early phase of hypoxia. A. Immunoblot analysis with specific antibodies against IL-6, endothelin-1 (ET-1), vascular cell adhesion molecule-1 (VCAM-1), platelet derived growth factor-B (PDGF-B) of lung from wildtype (WT) and Prx2$^{-/-}$ mice under normoxic condition treated (lane 1–2) or exposed to hypoxia (3D) and treated with either vehicle or penetrating peptide fusion protein peroxiredoxin-2 (PEP Prx2). One representative gel from six with similar results is presented. GAPDH was used as loading control. **Right panel.** Relative quantification of immunoreactivity (DU: Density Units) of IL-6, ET-1, VCAM-1 and PDGF-B. Data are shown as means ± SD (n = 6). *p < 0.05 compared to wildtype; ^p < 0.05 compared to normoxic mice; °p < 005 compared to vehicle treated mice**. B.** GADD34 levels in lung tissues (normalized to GADPH) wildtype (WT) and Prx2$^{-/-}$ mice treated with either vehicle or penetrating peptide fusion protein peroxiredoxin-2 (PEP Prx2) exposed to hypoxia for 3D *p < 0.05 compared to wildtype. Each sample is a pool from 5 mice. Representative of three independent experiments. **C.** Immunoblot analysis with specific antibodies against heat shock protein-70 (HSP70) and -90 (HSP90) of lung from wildtype (WT) and Prx2$^{-/-}$ mice under normoxic condition treated (lane 1–2) or exposed to hypoxia (3D) and treated with either vehicle or penetrating peptide fusion protein peroxiredoxin-2 (PEP Prx2). One representative gel from six with similar results is presented. GAPDH was used as loading control. Right panel. **C.** Relative quantification of immunoreactivity (DU: Density Units) of HSP70 and HSP 90. Data are shown as means ± SD (n = 6); ^p < 0.05 compared to normoxic mice; °p < 005 compared to vehicle treated mice.

hypoxia is strongly linked to ER stress in the absence of Prx2. Treatment with PEP Prx2 reduced ER stress and switched-off autophagy as supported by the reduction in LC3II and accumulation of p62 (Fig. 6A). This was parallel by a decrease of hypoxia induced HSP70 and 90 expression and down-regulation of GADD34 and ATF6 levels in PEP Prx2 treated Prx2$^{-/-}$ mice exposed respectively to 3 and 7 days hypoxia.

Collectively, our data indicate that PEP Prx2 has a multimodal action targeting: (i) the inflammatory response; (ii) vascular and extracellular matrix remodeling, (iii) ER stress and autophagy (Fig. 7B). The correction of the imbalance between oxidation and anti-oxidant systems combined with a chaperone like function exerted by Prx2 might interrupt the vicious circle, established between oxidation-chronic inflammation with ER stress and activation of autophagy towards the generation of PAH (Fig. 7B).

In conclusion, we have firstly highlighted the novel pivotal role of Prx2 in preventing PAH induced by hypoxia. The high bio-complexity of PAH requires multimodal therapeutic approaches, which simultaneously act on different targets involved in its pathogenesis. Our data collectively support a rationale for considering Prx2 as novel therapeutic option in treatment of the early phase of PAH.

Authorship and contributions

EF, AM, LDF, IA, DM designed the experiments, analyzed data and wrote the paper; AJ, CL carried out the histologic analysis; AM, AS, LDF carried out the experiments; IA performed the molecular experiments and analyzed the data; CSY and KDW generated the PEP Prx2; SL carried out MDA measurements and analyzed data.

Conflict of interest and disclosure

The authors have nothing to disclose.

Acknowledgments

This work was supported by PRIN (LDF and AI: 201228PNX83) and FUR_UNIVR (LDF) 2016_2017.

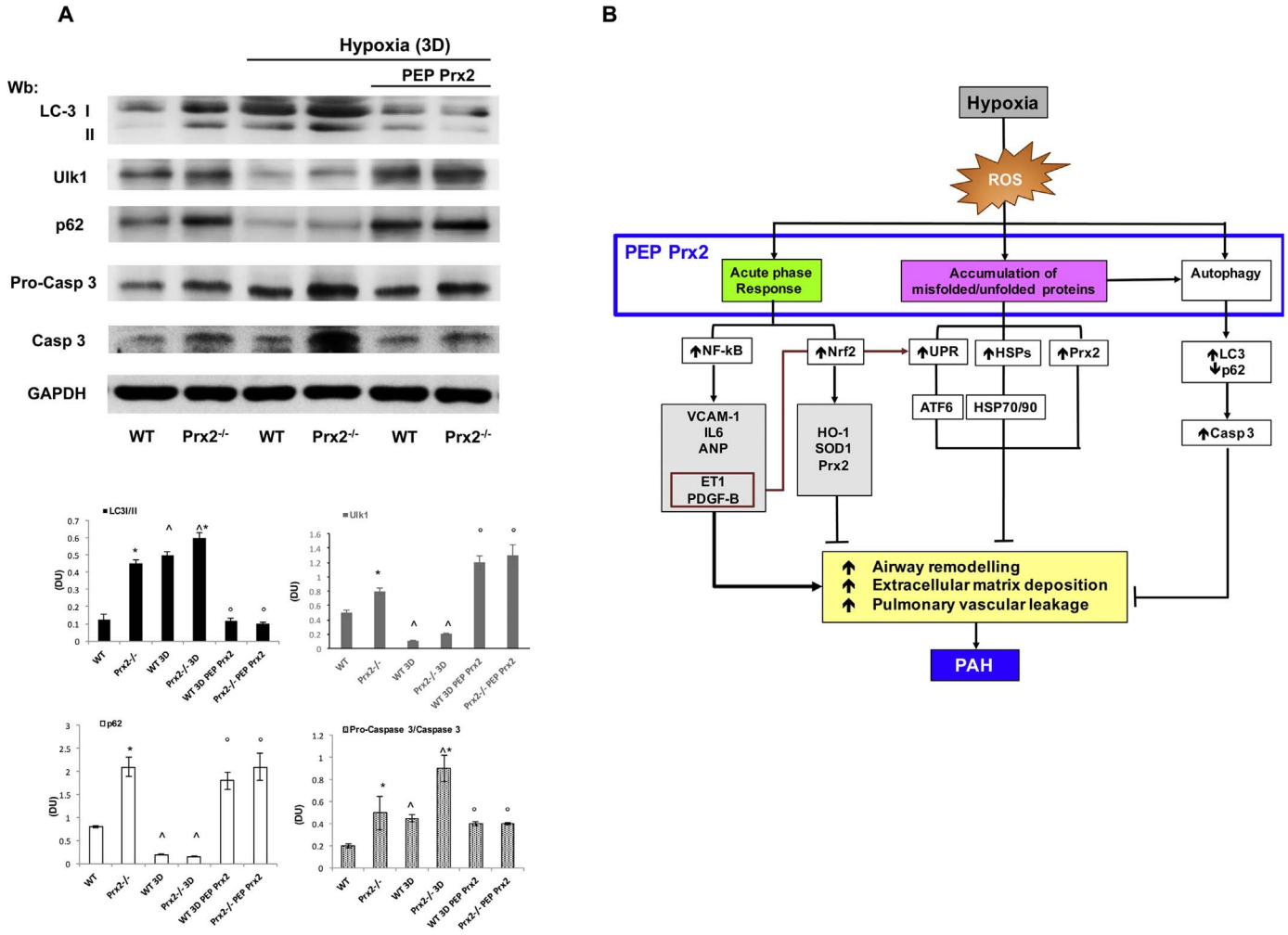

Fig. 7. A. Immunoblot analysis with specific antibodies against LC3I/II, Ulk1, p62, pro-caspase-caspase 3 of lung from wildtype (WT) and Prx2$^{-/-}$ mice under normoxic condition or exposed to 3 days (3D) hypoxia/reoxygenation stress (H/R) treated with either vehicle or penetrating peptide fusion protein peroxiredoxin-2 (PEP Prx2). One representative gel from six with similar results is presented. **Lower panel.** Relative quantification of immunoreactivity (DU: Density Units) of LC3I/II, Ulk1, p62, pro-caspase-caspase 3. Data are shown as means ± SD (n = 6). *p < 0.05 compared to wildtype; ° p < 0.05 compared to vehicle treated mice; ^ p < 0.05 compared to normoxic mice. **B.** Diagram of the novel role of Prx2 in pathogenesis of PAH induced by hypoxia and the novel multimodal action of Prx2 against hypoxia induce cytotoxic effects. Hypoxia promotes oxidation and induces acute phase inflammatory response, which is related to the activation of Nrf2, NF-kB. In the meantime, the accumulation of damage of cellular organelles and proteins results in activation of UPR system to limit endoplasmic reticulum (ER) stress, associated with increased expression of classical chaperones such as heat shock protein 70 and 90, and Prx2. ER stress leads to activation of autophagy as secondary mechanism to degraded damage proteins and reduce ER stress. This is supported by (i) conversion of LC3I to LC3II; and (ii) clearance of p62 positive lysosomes combined with the activation of caspase 3 pathway. PEP Prx2 treatment (i) prevents the hypoxia induced acute phase response activation of transcriptional factors NF-kB and Nrf2, (ii) alleviates ER stress related to hypoxia with reduction of ATF6 levels and (iii) blocks hypoxia induced autophagy. This results in reduction in markers of vascular remodeling, of extracellular matrix deposition and the abnormalities in pulmonary vascular leakage. ET1: endothelin 1; HO-1: heme-oxygenase-1; SOD1:superoxide dismutase; NF-kB: nuclear factor kappa-light-chain-enhancer of activated B cells; Nrf2: nuclear erythroid factor 2; P: phosphorylate form of indicated transcriptional factor; VCAM-1: vascular cell adhesion molecule -1; IL6:interleukin 6; PDGF-B: platelet derived growth factor-B; Casp 3: caspase 3; ANP: atrial natriuretic peptide; PEP Prx2: recombinant fusion penetrating protein Prx2; Prx2: peroxiredoxin-2; UPR: unfolded protein response; ATF6: activating transcriptional factor 6, HSPs: heat shock proteins, HSP70: heat shock protein-70, HSP90: heat shock protein-90; VCAM-1: vascular cell adhesion molecule 1; LC3 I/II: microtubule-associated protein 1A/1B-light chain 3.

Appendix A. Supporting information

Supplementary data associated with this article can be found in the online version at http://dx.doi.org/10.1016/j.freeradbiomed.2017.08.004.

References

[1] D.K. Rawat, A. Alzoubi, R. Gupte, S. Chettimada, M. Watanabe, A.G. Kahn, T. Okada, I.F. McMurtry, S.A. Gupte, Increased reactive oxygen species, metabolic maladaptation, and autophagy contribute to pulmonary arterial hypertension-induced ventricular hypertrophy and diastolic heart failure, Hypertension 64 (2014) 1266–1274.

[2] I.N. Zelko, R.J. Folz, Regulation of oxidative stress in pulmonary artery endothelium. modulation of extracellular superoxide dismutase and NOX4 expression using histone deacetylase class I inhibitors, Am. J. Respir. Cell Mol. Biol. 53 (2015) 513–524.

[3] S. Aggarwal, C.M. Gross, S. Sharma, J.R. Fineman, S.M. Black, Reactive oxygen species in pulmonary vascular remodeling, Compr. Physiol. 3 (2013) 1011–1034.

[4] D. Morales-Cano, C. Menendez, E. Moreno, J. Moral-Sanz, B. Barreira, P. Galindo, R. Pandolfi, R. Jimenez, L. Moreno, A. Cogolludo, J. Duarte, F. Perez-Vizcaino, The flavonoid quercetin reverses pulmonary hypertension in rats, PLoS One 9 (2014) e114492.

[5] B. Van Houten, Pulmonary arterial hypertension is associated with oxidative stress-induced genome instability, Am. J. Respir. Crit. Care Med. 192 (2015) 129–130.

[6] M.C. Chaumais, B. Ranchoux, D. Montani, P. Dorfmuller, L. Tu, F. Lecerf, N. Raymond, C. Guignabert, L. Price, G. Simonneau, S. Cohen-Kaminsky, M. Humbert, F. Perros, N-acetylcysteine improves established monocrotaline-induced pulmonary hypertension in rats, Respir. Res. 15 (2014) 65.

[7] H.H. Schmidt, R. Stocker, C. Vollbracht, G. Paulsen, D. Riley, A. Daiber, A. Cuadrado, Antioxidants in translational medicine, Antioxid. Redox Signal. 23 (2015) 1130–1143.

[8] R. Scherz-Shouval, Z. Elazar, Regulation of autophagy by ROS: physiology and pathology, Trends Biochem. Sci. 36 (2011) 30–38.

[9] S. Kongara, V. Karantza, The interplay between autophagy and ROS in tumorigenesis, Front. Oncol. 2 (2012) 171.

[10] R. Sano, J.C. Reed, ER stress-induced cell death mechanisms, Biochim. Biophys. Acta 1833 (2013) 3460–3470.

[11] G. Wang, S. Liu, L. Wang, L. Meng, C. Cui, H. Zhang, S. Hu, N. Ma, Y. Wei, Lipocalin-2 promotes endoplasmic reticulum stress and proliferation by augmenting intracellular iron in human pulmonary arterial smooth muscle cells, Int. J. Biol. Sci. 13 (2017) 135–144.

[12] P. Dromparis, R. Paulin, T.H. Stenson, A. Haromy, G. Sutendra, E.D. Michelakis, Attenuating endoplasmic reticulum stress as a novel therapeutic strategy in pulmonary hypertension, Circulation 127 (2013) 115–125.

[13] M. Koyama, M. Furuhashi, S. Ishimura, T. Mita, T. Fuseya, Y. Okazaki, H. Yoshida, K. Tsuchihashi, T. Miura, Reduction of endoplasmic reticulum stress by 4-phenylbutyric acid prevents the development of hypoxia-induced pulmonary arterial hypertension, Am. J. Physiol. Heart Circ. Physiol. 306 (2014) H1314–H1323.

[14] G.K. Wang, S.H. Li, Z.M. Zhao, S.X. Liu, G.X. Zhang, F. Yang, Y. Wang, F. Wu, X.X. Zhao, Z.Y. Xu, Inhibition of heat shock protein 90 improves pulmonary arteriole remodeling in pulmonary arterial hypertension, Oncotarget 7 (2016) 54263–54273.

[15] F.M. Low, M.B. Hampton, A.V. Peskin, C.C. Winterbourn, Peroxiredoxin 2 functions as a noncatalytic scavenger of low-level hydrogen peroxide in the erythrocyte, Blood 109 (2007) 2611–2617.

[16] S.G. Rhee, H.A. Woo, Multiple functions of peroxiredoxins: peroxidases, sensors and regulators of the intracellular messenger H(2)O(2), and protein chaperones, Antioxid. Redox Signal. 15 (2011) 781–794.

[17] A. Matte, A. Pantaleo, E. Ferru, F. Turrini, M. Bertoldi, F. Lupo, A. Siciliano, C. Ho Zoon, L. De Franceschi, The novel role of peroxiredoxin-2 in red cell membrane protein homeostasis and senescence, Free Radic. Biol. Med. 76C (2014) 80–88.

[18] F.M. Low, M.B. Hampton, C.C. Winterbourn, Peroxiredoxin 2 and peroxide metabolism in the erythrocyte, Antioxid. Redox Signal. 10 (2008) 1621–1630.

[19] A. Matte, L. De Falco, A. Iolascon, N. Mohandas, X. An, A. Siciliano, C. Leboeuf, A. Janin, M. Bruno, S.Y. Choi, D.W. Kim, L. De Franceschi, The interplay between peroxiredoxin-2 and nuclear factor-erythroid 2 is important in limiting oxidative mediated dysfunction in beta-thalassemic erythropoiesis, Antioxid. Redox Signal. 23 (2015) 1284–1297.

[20] S.S. Franco, L. De Falco, S. Ghaffari, C. Brugnara, D.A. Sinclair, A. Matte, A. Iolascon, N. Mohandas, M. Bertoldi, X. An, A. Siciliano, P. Rimmele, M.D. Cappellini, S. Michan, E. Zoratti, J. Anne, L. De Franceschi, Resveratrol accelerates erythroid maturation by activation of FoxO3 and ameliorates anemia in beta-thalassemic mice, Haematologica 99 (2014) 267–275.

[21] A. Matte, P.S. Low, F. Turrini, M. Bertoldi, M.E. Campanella, D. Spano, A. Pantaleo, A. Siciliano, L. De Franceschi, Peroxiredoxin-2 expression is increased in beta-thalassemic mouse red cells but is displaced from the membrane as a marker of oxidative stress, Free Radic. Biol. Med. 49 (2010) 457–466.

[22] D. Yang, Y. Song, X. Wang, J. Sun, Y. Ben, X. An, L. Tong, J. Bi, X. Wang, C. Bai, Deletion of peroxiredoxin 6 potentiates lipopolysaccharide-induced acute lung injury in mice, Crit. Care Med. 39 (2011) 756–764.

[23] C.S. Yang, D.S. Lee, C.H. Song, S.J. An, S. Li, J.M. Kim, C.S. Kim, D.G. Yoo, B.H. Jeon, H.Y. Yang, T.H. Lee, Z.W. Lee, J. El-Benna, D.Y. Yu, E.K. Jo, Roles of peroxiredoxin II in the regulation of proinflammatory responses to LPS and protection against endotoxin-induced lethal shock, J. Exp. Med. 204 (2007) 583–594.

[24] Y. Gan, X. Ji, X. Hu, Y. Luo, L. Zhang, P. Li, X. Liu, F. Yan, P. Vosler, Y. Gao, R.A. Stetler, J. Chen, Transgenic overexpression of peroxiredoxin-2 attenuates ischemic neuronal injury via suppression of a redox-sensitive pro-death signaling pathway, Antioxid. Redox Signal. 17 (2012) 719–732.

[25] S. Boulos, B.P. Meloni, P.G. Arthur, C. Bojarski, N.W. Knuckey, Peroxiredoxin 2 overexpression protects cortical neuronal cultures from ischemic and oxidative injury but not glutamate excitotoxicity, whereas Cu/Zn superoxide dismutase 1 overexpression protects only against oxidative injury, J. Neurosci. Res. 85 (2007) 3089–3097.

[26] L. de Franceschi, F. Turrini, M. Honczarenko, K. Ayi, A. Rivera, M.D. Fleming, T. Law, F. Mannu, F.A. Kuypers, A. Bast, W.J. van der Vijgh, C. Brugnara, In vivo reduction of erythrocyte oxidant stress in a murine model of beta-thalassemia, Haematologica 89 (2004) 1287–1298.

[27] B.T. Kalish, A. Matte, I. Andolfo, A. Iolascon, O. Weinberg, A. Ghigo, J. Cimino, A. Siciliano, E. Hirsch, E. Federti, M. Puder, C. Brugnara, L. De Franceschi, Dietary omega-3 fatty acids protect against vasculopathy in a transgenic mouse model of sickle cell disease, Haematologica 100 (2015) 870–880.

[28] L. De Franceschi, C. Brugnara, P. Rouyer-Fessard, H. Jouault, Y. Beuzard, Formation of dense erythrocytes in SAD mice exposed to chronic hypoxia: evaluation of different therapeutic regimens and of a combination of oral clotrimazole and magnesium therapies, Blood 94 (1999) 4307–4313.

[29] L. Dalle Carbonare, A. Matte, M.T. Valenti, A. Siciliano, A. Mori, V. Schweiger, G. Zampieri, L. Perbellini, L. De Franceschi, Hypoxia-reperfusion affects osteogenic lineage and promotes sickle cell bone disease, Blood 126 (2015) 2320–2328.

[30] N. Sabaa, L. de Franceschi, P. Bonnin, Y. Castier, G. Malpeli, H. Debbabi, A. Galaup, M. Maier-Redelsperger, S. Vandermeersch, A. Scarpa, A. Janin, B. Levy, R. Girot, Y. Beuzard, C. Leboeuf, A. Henri, S. Germain, J.C. Dussaule, P.L. Tharaux, Endothelin receptor antagonism prevents hypoxia-induced mortality and morbidity in a mouse model of sickle-cell disease, J. Clin. Investig. 118 (2008) 1924–1933.

[31] A. Matte, M. Bertoldi, N. Mohandas, X. An, A. Bugatti, A.M. Brunati, M. Rusnati, E. Tibaldi, A. Siciliano, F. Turrini, S. Perrotta, L. De Franceschi, Membrane association of peroxiredoxin-2 in red cells is mediated by the N-terminal cytoplasmic domain of band 3, Free Radic. Biol. Med. 55 (2013) 27–35.

[32] R. Bellelli, G. Federico, A. Matte, D. Colecchia, A. Iolascon, M. Chiariello, M. Santoro, L. De Franceschi, F. Carlomagno, NCOA4 deficiency impairs systemic iron homeostasis, Cell Rep. 14 (2016) 411–421.

[33] L. De Franceschi, F. Turrini, E.M. del Giudice, S. Perrotta, O. Olivieri, R. Corrocher, F. Mannu, A. Iolascon, Decreased band 3 anion transport activity and band 3 clusterization in congenital dyserythropoietic anemia type II, Exp. Hematol. 26 (1998) 869–873.

[34] V. Kumar, N. Kitaeff, M.B. Hampton, M.B. Cannell, C.C. Winterbourn, Reversible oxidation of mitochondrial peroxiredoxin 3 in mouse heart subjected to ischemia and reperfusion, FEBS Lett. 583 (2009) 997–1000.

[35] A. Cozzi, B. Corsi, S. Levi, P. Santambrogio, A. Albertini, P. Arosio, Overexpression of wild type and mutated human ferritin H-chain in HeLa cells: in vivo role of ferritin ferroxidase activity, J. Biol. Chem. 275 (2000) 25122–25129.

[36] L. De Franceschi, O.S. Platt, G. Malpeli, A. Janin, A. Scarpa, C. Leboeuf, Y. Beuzard, E. Payen, C. Brugnara, Protective effects of phosphodiesterase-4 (PDE-4) inhibition in the early phase of pulmonary arterial hypertension in transgenic sickle cell mice, FASEB J. 22 (2008) 1849–1860.

[37] G. Ingoglia, C.M. Sag, N. Rex, L. De Franceschi, F. Vinchi, J. Cimino, S. Petrillo, S. Wagner, K. Kreitmeier, L. Silengo, F. Altruda, L.S. Maier, E. Hirsch, A. Ghigo, E. Tolosano, Hemopexin counteracts systolic dysfunction induced by heme-driven oxidative stress, Free Radic. Biol. Med. 108 (2017) 452–464.

[38] S.K. Niture, R. Khatri, A.K. Jaiswal, Regulation of Nrf2-an update, Free Radic. Biol. Med. 66 (2014) 36–44.

[39] R.T. Schermuly, E. Dony, H.A. Ghofrani, S. Pullamsetti, R. Savai, M. Roth, A. Sydykov, Y.J. Lai, N. Weissmann, W. Seeger, F. Grimminger, Reversal of experimental pulmonary hypertension by PDGF inhibition, J. Clin. Investig. 115 (2005) 2811–2821.

[40] M. Thamsen, C. Kumsta, F. Li, U. Jakob, Is overoxidation of peroxiredoxin physiologically significant? Antioxid. Redox Signal. 14 (2011) 725–730.

[41] A. Adegunsoye, J. Balachandran, Inflammatory response mechanisms exacerbating hypoxemia in coexistent pulmonary fibrosis and sleep apnea, Mediat. Inflamm. 2015 (2015) 510105.

[42] M. Fartoukh, D. Emilie, C. Le Gall, G. Monti, G. Simonneau, M. Humbert, Chemokine macrophage inflammatory protein-1alpha mRNA expression in lung biopsy specimens of primary pulmonary hypertension, Chest 114 (1998) 50S–51S.

[43] M.E. Yeager, D.D. Belchenko, C.M. Nguyen, K.L. Colvin, D.D. Ivy, K.R. Stenmark, Endothelin-1, the unfolded protein response, and persistent inflammation: role of pulmonary artery smooth muscle cells, Am. J. Respir. Cell Mol. Biol. 46 (2012) 14–22.

[44] S. Bernales, K.L. McDonald, P. Walter, Autophagy counterbalances endoplasmic reticulum expansion during the unfolded protein response, PLoS Biol. 4 (2006) e423.

[45] G. Sutendra, P. Dromparis, P. Wright, S. Bonnet, A. Haromy, Z. Hao, M.S. McMurtry, M. Michalak, J.E. Vance, W.C. Sessa, E.D. Michelakis, The role of Nogo and the mitochondria-endoplasmic reticulum unit in pulmonary hypertension, Sci. Transl. Med. 3 (2011) 88ra55.

[46] J.C. Moon, Y.S. Hah, W.Y. Kim, B.G. Jung, H.H. Jang, J.R. Lee, S.Y. Kim, Y.M. Lee, M.G. Jeon, C.W. Kim, M.J. Cho, S.Y. Lee, Oxidative stress-dependent structural and functional switching of a human 2-Cys peroxiredoxin isotype II that enhances HeLa cell resistance to H2O2-induced cell death, J. Biol. Chem. 280 (2005) 28775–28784.

[47] A.V. Peskin, N. Dickerhof, R.A. Poynton, L.N. Paton, P.E. Pace, M.B. Hampton, C.C. Winterbourn, Hyperoxidation of peroxiredoxins 2 and 3: rate constants for the reactions of the sulfenic acid of the peroxidatic cysteine, J. Biol. Chem. 288 (2013) 14170–14177.

[48] Q. Li, Y. Qiu, M. Mao, J. Lv, L. Zhang, S. Li, X. Li, X. Zheng, Antioxidant mechanism of Rutin on hypoxia-induced pulmonary arterial cell proliferation, Molecules 19 (2014) 19036–19049.

[49] M.C. Sobotta, A.G. Barata, U. Schmidt, S. Mueller, G. Millonig, T.P. Dick, Exposing cells to H2O2: a quantitative comparison between continuous low-dose and one-time high-dose treatments, Free Radic. Biol. Med. 60 (2013) 325–335.

[50] G. Marino, M. Niso-Santano, E.H. Baehrecke, G. Kroemer, Self-consumption: the interplay of autophagy and apoptosis, Nat. Rev. Mol. Cell Biol. 15 (2014) 81–94.

[51] J. Xiong, Atg7 in development and disease: panacea or Pandora's Box? Protein Cell 6 (2015) 722–734.

[52] F. Lupo, E. Tibaldi, A. Matte, A.K. Sharma, A.M. Brunati, S.L. Alper, C. Zancanaro, D. Benati, A. Siciliano, M. Bertoldi, F. Zonta, A. Storch, R.H. Walker, A. Danek, B. Bader, A. Hermann, L. De Franceschi, A new molecular link between defective autophagy and erythroid abnormalities in chorea-acanthocytosis, Blood 128 (2016) 2976–2987.

[53] C. Delaney, R.H. Wright, J.R. Tang, C. Woods, L. Villegas, L. Sherlock, R.C. Savani, S.H. Abman, E. Nozik-Grayck, Lack of EC-SOD worsens alveolar and vascular development in a neonatal mouse model of bleomycin-induced bronchopulmonary dysplasia and pulmonary hypertension, Pediatr. Res. 78 (2015) 634–640.

[54] T. Zhuang, M. Zhang, H. Zhang, P.A. Dennery, Q.S. Lin, Disrupted postnatal lung development in heme oxygenase-1 deficient mice, Respir. Res. 11 (2010) 142.

[55] O.D. Liang, S.A. Mitsialis, M.S. Chang, E. Vergadi, C. Lee, M. Aslam, A. Fernandez-Gonzalez, X. Liu, R. Baveja, S. Kourembanas, Mesenchymal stromal cells expressing heme oxygenase-1 reverse pulmonary hypertension, Stem Cells 29 (2011) 99–107.

[56] D. Wang, I.P. Gladysheva, T.H. Fan, R. Sullivan, A.K. Houng, G.L. Reed, Atrial natriuretic peptide affects cardiac remodeling, function, heart failure, and survival in a mouse model of dilated cardiomyopathy, Hypertension 63 (2014) 514–519.

[57] F. Werner, B. Kojonazarov, B. Gassner, M. Abesser, K. Schuh, K. Volker, H.A. Baba, B.K. Dahal, R.T. Schermuly, M. Kuhn, Endothelial actions of atrial natriuretic peptide prevent pulmonary hypertension in mice, Basic Res. Cardiol. 111 (2016) 22.

Data in Brief 15 (2017) 376–381

Contents lists available at ScienceDirect

Data in Brief

journal homepage: www.elsevier.com/locate/dib

Data Article

Data demonstrating the role of peroxiredoxin 2 as important anti-oxidant system in lung homeostasis

Enrica Federti [a], Alessandro Matte [a], Alessandra Ghigo [b], Immacolata Andolfo [c], Cimino James [b], Angela Siciliano [a], Christophe Leboeuf [d], Anne Janin [d,e,f], Francesco Manna [c], Soo Young Choi [g], Achille Iolascon [c], Elisabetta Beneduce [a], Davide Melisi [a], Dae Won Kim [g], Sonia Levi [h,i], Lucia De Franceschi [a,*]

[a] Dept. of Medicine, University of Verona-AOUI Verona, Verona, Italy
[b] Molecular Biotechnology Center and Department of Molecular Biotechnology and Health Science, University of Torino, Torino, Italy
[c] CEINGE and Dept. of Biochemistry, University of Naples, Naples, Italy
[d] Inserm, U1165, Paris F-75010, France
[e] Université Paris 7- Denis Diderot, Paris, France
[f] AP-HP, Hôpital Saint-Louis, F-75010 Paris, France
[g] Institute of Bioscience and Biotechnology, Hallym University, Gangowo-do, Republic of Korea
[h] Division of Neuroscience, San Raffaele Scientific Institute, Milano, Italy
[i] Vita-Salute San Raffaele University, Milano, Italy

ARTICLE INFO

Article history:
Received 22 August 2017
Received in revised form
19 September 2017
Accepted 26 September 2017
Available online 30 September 2017

ABSTRACT

The data presented in this article are related to the research paper entitled "peroxiredoxin-2 plays a pivotal role as multimodal cytoprotector in the early phase of pulmonary hypertension" (Federti et al., 2017) [1]. Data show that the absence of peroxiredoxin-2 (Prx2) is associated with increased lung oxidation and pulmonary vascular endothelial dysfunction. Prx2$^{-/-}$ mice displayed activation of the redox-sensitive transcriptional factors, NF-kB and Nrf2, and increased expression of cytoprotective system such as heme-oxygenase-1 (HO-1). We also noted increased expression of both markers of vascular activation and extracellular matrix remodeling. The administration of the recombinant fusion

DOI of original article: http://dx.doi.org/10.1016/j.freeradbiomed.2017.08.004
* Corresponding author.
E-mail address: lucia.defranceschi@univr.it (L. De Franceschi).

http://dx.doi.org/10.1016/j.dib.2017.09.062

protein PEP Prx2 reduced the activation of NF-kB and Nrf2 and was paralleled by a decrease in HO-1 and in vascular endothelial abnormal activation. Prolonged hypoxia was used to trigger pulmonary artery hypertension (PAH). Prx2$^{-/-}$ precociously developed PAH compared to wildtype animals.

Specifications Table

Subject area	*Health Sciences*
More specific subject area	*Oxidation, peroxiredoxin-2 and pulmonary artery hypertension*
Type of data	*Text file, Figures*
How data was acquired	Image Quant Las Mini 4000 Digital Imaging System (GE Healthcare Life Sciences). Densitometric analyses were performed using the ImageQuant TL software (GE Healthcare Life Sciences).
Data format	*Raw analyzed*
Experimental factors	*C57B6/2J as wildtype mice and Prx2$^{-/-}$ mice*
Experimental features	*Protein expression was analyzed by Western-blotting.* Oxidized proteins were revealed by the Oxyblot Protein Oxidation Detection Kit (EMD Millipore); MDA pulmonary levels were evaluated by Oxiselect MDA Immunoblot kit (GE Healthcare).
Data source location	*Dept. of Medicine, LURM, Policlinico GB Rossi, University of Verona and AOUI Verona; Verona; Italy*
Data accessibility	*Data are available with this article*

Value of the data

- Our data show that the absence of Prx2 is associated with increased lung oxidation and abnormal pulmonary vascular leakage.
- Treatment with fusion protein PEP Prx2 prevents the activation of redox related transcriptional factors and modulates anti-oxidant systems in both wildtype and Prx2$^{-/-}$ mice.
- PEP Prx2 significantly reduces protein oxidation in lung from exposed to prolonged hypoxia used to trigger pulmonary artery hypertension.

1. Data

Data show increased lung oxidation (Fig. 1A) and abnormal pulmonary vascular leakage in the absence of Prx2 (Fig. 1B). This was paralleled by the activation of redox-sensitive transcriptional factors NF-kB and Nrf2 in lung from Prx2$^{-/-}$ compared to wildtype animals (Fig. 2A). Indeed, in Prx2$^{-/-}$ we observed (i) increased expression of heme-oxygenase 1 (HO-1), a Nrf2 related cytoprotective system; (ii) markers of vascular endothelial activation such as endothelin-1 (ET-1) and vascular cell adhesion molecule -1 (VCAM-1) and (iii) marker of extracellular matrix remodeling as the platelet growth factor- B (PDGF-B) that has been recently function linked to the development of pulmonary artery hypertension (Fig. 2B). To verify the role of Prx2 as important anti-oxidant system in pulmonary homeostasis, we administrated the recombinant fusion protein PEP Prx2 at the dosage of 3 mg/Kg/d ip or vehicle for 4 weeks [1–3]. As shown in Fig. 2, PEP Prx2 significantly reduced both

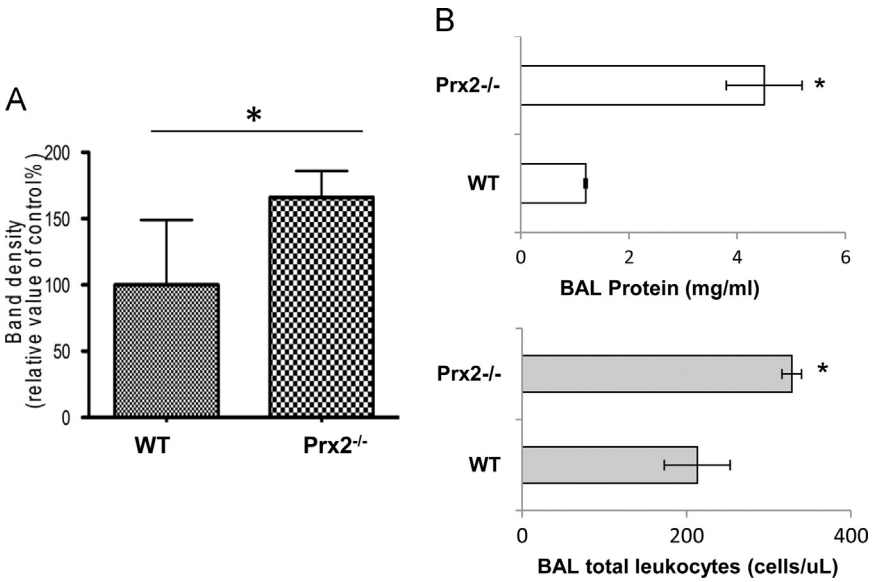

Fig. 1. A. 10 μg of soluble proteins of lung homogenate were tested for MDA-protein adducts. Quantification of band area was performed by densitometry and expressed as % of WT. The data are presented as means ± SD of at least three independent experiments; statistically significant differences were determined by Student's t-test. $^{*}p < 0.05$. **B. Upper panel.** BAL protein content from wildtype (WT) and Prx2$^{-/-}$ mice under normoxic condition. Data are presented as means ± SD ($n = 6$; $^{*}p < 0.05$ compared to WT mice). **Lower panel.** BAL leukocyte content from wildtype (WT) and Prx2$^{-/-}$ mice under normoxic condition. Data are presented as means ± SD ($n = 6$; $^{*}p < 0.05$ compared to WT mice).

NF-kB and Nrf2 activation in lung from Prx2$^{-/-}$ and decreased the expression of both HO-1 and markers of vascular endothelial activation or extracellular matrix remodeling.

Using prolonged hypoxia to trigger pulmonary artery hypertension, we observed severe lung pathologic damage and the precocious development of pulmonary artery hypertension in Prx2$^{-/-}$ mice compared to wildtype animals [4–6]. This was associated with (i) marked activation of redox-related transcriptional factors; (ii) severe endoplasmic-reticulum stress with activation of the unfolded protein response (UPR) system; and (iii) activation of autophagy [1].

PEP Prx2 treatment prevented the hypoxia induced protein oxidation in mice exposed to prolonged hypoxia (7 days; Fig. 3A) and reduced the hypoxia induced increased expression of HO-1 in both mouse strains exposed to 3 days hypoxia (Fig. 3B). Collectively, these data indicate the important role of Prx2 in lung homeostasis against hypoxia, a known trigger of lung injury.

2. Experimental design, materials and methods

2.1. MDA assay

MDA was determined as previously reported [7,8].

2.2. Measurement of BAL protein content

2.2.1. Bronchoalveolar lavage assay

Bronchoalveolar lavage (BAL) fluids were collected and cellular contents were recovered by centrifugation and counted by microcytometry as previously reported [6,9].

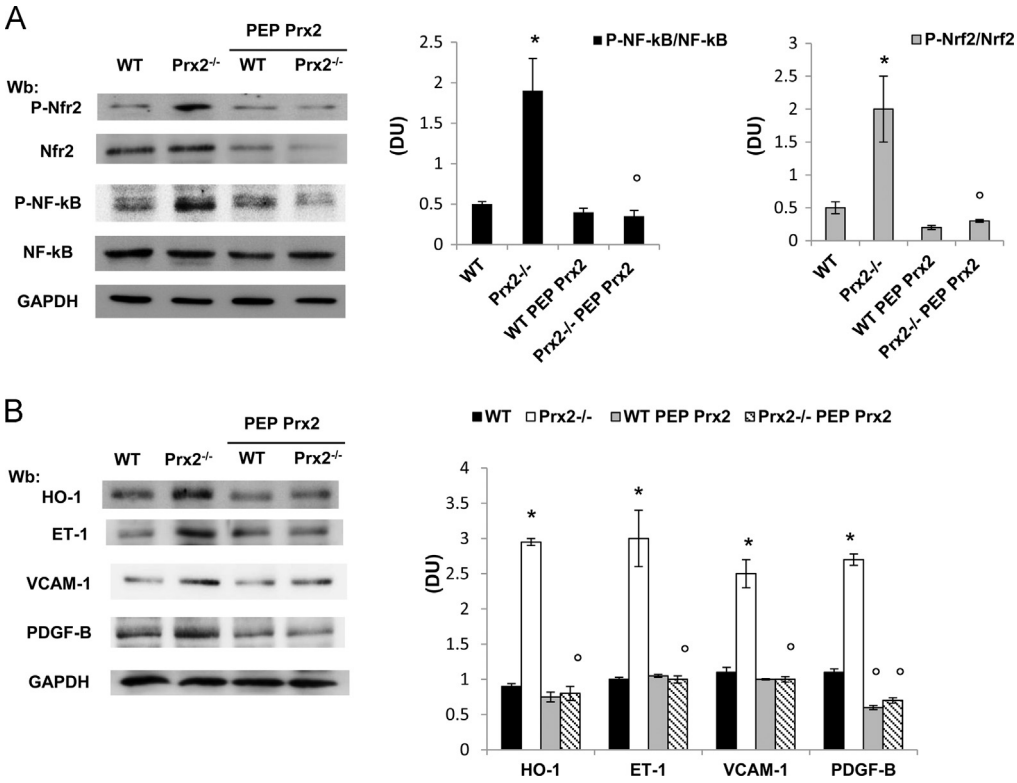

Fig. 2. A. Immunoblot analysis with specific antibodies against phospho-Nrf2 (P-Nrf2), Nrf2 phospho-NF-kB (P-NF-kB) and NF-kB of lung from wildtype (WT) and Prx2$^{-/-}$ mice under normoxic condition. One representative gel from six with similar results is presented. **Right panel.** Relative quantification of immunoreactivity (DU: Density Units) of phospho-NF-kB (P-NF-kB), NF-k, phospho-Nrf2 (P-Nrf2) and Nrf2 of lung from wildtype (WT) and Prx2$^{-/-}$ mice under normoxic condition treated with either vehicle or penetrating peptide fusion protein peroxiredoxin-2 (PEP Prx2). Data are shown as means ± SD ($n = 6$). $^{*}p < 0.05$ compared to wildtype; $^{\circ}p < 005$ compared to vehicle treated mice. **B.** Immunoblot analysis with specific antibodies against heme-oxygenase 1 (HO-1), endothelin-1 (ET-1), vascular cell adhesion molecule-1 (VCAM-1), under normoxic condition treated with either vehicle or penetrating peptide fusion protein peroxiredoxin-2 (PEP Prx2). One representative gel from six with similar results is presented. **Right panel.** Relative quantification of immunoreactivity (DU: Density Units) of heme-oxygenase 1 (HO-1), endothelin-1 (ET-1), vascular cell adhesion molecule-1 (VCAM-1), platelet derived growth factor-B (PDGF-B) of lung from wildtype (WT) and Prx2$^{-/-}$ mice under normoxic condition treated with either vehicle or penetrating peptide fusion protein peroxiredoxin-2 (PEP Prx2). Data are shown as means ± SD ($n = 6$). $^{*}p < 0.05$ compared to wildtype; $^{\circ}p < 0.05$ compared to vehicle treated mice.

2.2.2. *Immunoblot analysis*

Frozen lung from each studied group were homogenized and lysed with iced lyses buffer as previously described [3,10,11]. Gels were transferred to nitrocellulose membranes for immuno-blot analysis with specific antibody: anti-NFkB-phospho-S536 (93H1) (Cell Signaling Technology, Leiden, NL); anti-NFkB p65 (C22B4) (Cell Signaling Technology, Leiden, NL); anti-Nrf2-phospho-S40 (Clone EP1809Y, AbCam, Cambridge, UK); anti-Nrf2 (AbCam, Cambridge, UK); anti-Heme Oxygenase-1 (HO-1) (Santa Cruz Biotechnology, Heidelberg, Germany), anti-Endothelin-1 (ET-1) (Santa Cruz Biotechnology, Heidelberg, Germany); anti-VCAM-1 (R and D Systems, Minneapolis, MN, USA); anti-PDGF-B (AbCam, Cambridge, UK); anti-GAPDH (Sigma Aldrich, Saint Louis, MO, USA) was used as loading control. Images were acquired using Image Quant Las Mini 4000 Digital Imaging System (GE Healthcare Life Sciences). Densitometric analyses were performed using the ImageQuant TL software (GE Healthcare Life Sciences) [11].

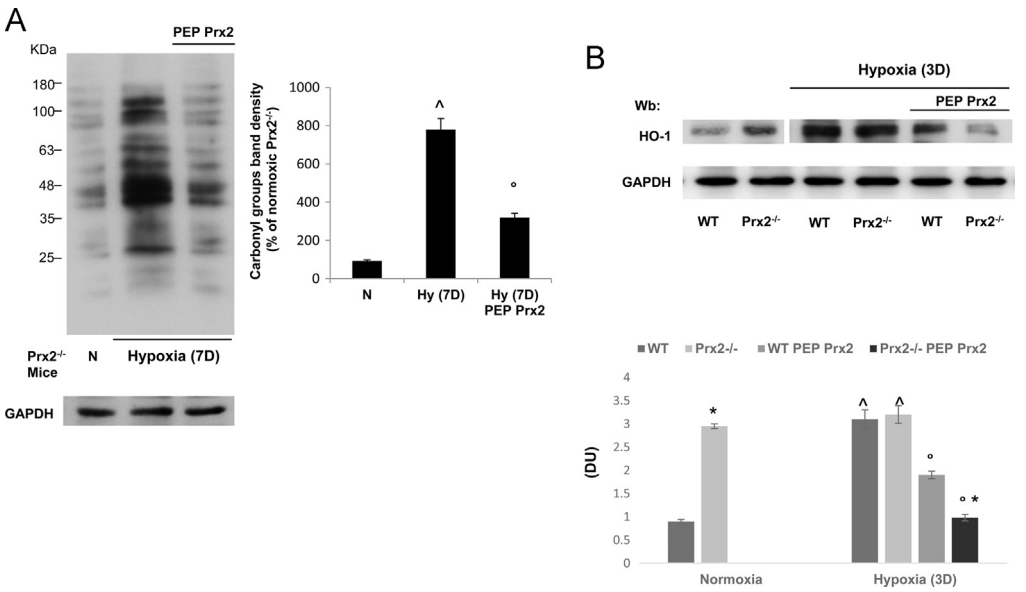

Fig. 3. A. The carbonylated proteins (1 ug) from lung of Prx2$^{-/-}$ mice under normoxic condition or exposed to 7 days (7D) hypoxia/reoxygenation stress (H/R) treated with either vehicle or penetrating peptide fusion protein peroxiredoxin-2 (PEP Prx2) at the dosage of 3 mg/Kg/d ip or vehicle for 4 weeks before and during hypoxia (8% oxygen for 7 days). **Right panel.** Quantification of band area was performed by densitometry and expressed as % of Prx2 under normoxia. The data are presented as means $\pm$ SD of at least three independent experiments; ^$p < 0.05$ compared to Prx2$^{-/-}$ normoxic mice; °$p <$ 005 compared to vehicle treated mice. ($n = 3$). **B.** Immunoblot analysis with specific antibodies against heme-oxygenase-1 (HO-1) of lung from wildtype (WT) and Prx2$^{-/-}$ mice under normoxic condition or exposed to 3 days (3D) hypoxia/reoxygenation stress (H/R) treated with either vehicle or penetrating peptide fusion protein peroxiredoxin-2 (PEP Prx2) at the dosage of 3 mg/Kg/d ip or vehicle for 4 weeks before and during hypoxia (8% oxygen for 3 days). One representative gel from five with similar results is presented. **Lower panel.** Relative quantification of immunoreactivity (DU: Density Units) of heme-oxygenase 1 of lung from wildtype (WT) and Prx2$^{-/-}$ mice under normoxic condition or exposed to 3 days (3D) hypoxia/reoxygenation stress (H/R) treated with either vehicle or PEP Prx2. Data are presented as means $\pm$ SD of at least five independent experiments; *$p < 0.05$ compared to wildtype; ^$p < 0.05$ compared to Prx2$^{-/-}$ normoxic mice; °$p <$ 005 compared to vehicle treated mice. ($n = 5$).

2.2.3. *Measurement of lung protein oxidation*

Oxidized proteins were revealed by the Oxyblot Protein Oxidation Detection Kit (EMD Millipore). In brief, the soluble protein extracts were derivatized to 2,4-dinitrophenylhydrazone (DNP) and 1 μg was loaded on 12% SDS-PAGE, blotted and incubated with an anti-DNP antibody, followed by an HRP conjugated secondary antibody. The bound activity was revealed by ECL (GE Healthcare). Oxidized proteins were revealed by the Oxyblot Protein Oxidation Detection Kit (EMD Millipore). In brief, the soluble protein extracts were derivatized to 2,4-dinitrophenylhydrazone (DNP) and 1 ug was loaded on 12% SDS-PAGE, blotted and incubated with an anti-DNP antibody, followed by an HRP conjugated secondary antibody. The bound activity was revealed by ECL (GE Healthcare) [12–14].

2.2.4. *Generation of recombinant-PEP Prx2 fusion protein (PEP Prx2)*

The fusion protein PEP Prx2 was generated as previously reported [2,3].

Acknowledgements

This work was supported by PRIN (LDF and AI: 201228PNX83) and FUR_UNIVR (2016_2017_LDF).

Transparency document. Supplementary material

Transparency data associated with this article can be found in the online version at http://dx.doi.org/10.1016/j.dib.2017.09.062.

References

[1] E. Federti, A. Matte, A. Ghigo, I. Andolfo, C. James, A. Siciliano, C. Leboeuf, A. Janin, F. Manna, S.Y. Choi, A. Iolascon, E. Beneduce, D. Melisi, D.W. Kim, S. Levi, L. De Franceschi, Peroxiredoxin-2 plays a pivotal role as multimodal cytoprotector in the early phase of pulmonary hypertension, Free Radic. Biol. Med. (2017).

[2] A. Matte, L. De Falco, A. Iolascon, N. Mohandas, X. An, A. Siciliano, C. Leboeuf, A. Janin, M. Bruno, S.Y. Choi, D.W. Kim, L. De Franceschi, The interplay between peroxiredoxin-2 and nuclear factor-erythroid 2 is important in limiting oxidative mediated dysfunction in beta-thalassemic erythropoiesis, Antioxid. Redox Signal. 23 (2015) 1284–1297.

[3] A. Matte, L. De Falco, E. Federti, A. Cozzi, A. Iolascon, S. Levi, N. Mohandas, A. Zamo, M. Bruno, C. Leboeuf, A. Janin, A. Siciliano, T. Ganz, G. Federico, F. Carlomagno, S. Mueller, I. Silva, C. Carbone, D. Melisi, D.W. Kim, S.Y. Choi, L, D. E. F, Peroxiredoxin-2: a novel regulator of iron homeostasis in ineffective erythropoiesis, Antioxid. Redox Signal. (2017).

[4] L. de Franceschi, A. Baron, A. Scarpa, C. Adrie, A. Janin, S. Barbi, J. Kister, P. Rouyer-Fessard, R. Corrocher, P. Leboulch, Y. Beuzard, Inhaled nitric oxide protects transgenic SAD mice from sickle cell disease-specific lung injury induced by hypoxia/reoxygenation, Blood 102 (2003) 1087–1096.

[5] L. De Franceschi, O.S. Platt, G. Malpeli, A. Janin, A. Scarpa, C. Leboeuf, Y. Beuzard, E. Payen, C. Brugnara, Protective effects of phosphodiesterase-4 (PDE-4) inhibition in the early phase of pulmonary arterial hypertension in transgenic sickle cell mice, FASEB J. 22 (2008) 1849–1860.

[6] B.T. Kalish, A. Matte, I. Andolfo, A. Iolascon, O. Weinberg, A. Ghigo, J. Cimino, A. Siciliano, E. Hirsch, E. Federti, M. Puder, C. Brugnara, L. De Franceschi, Dietary omega-3 fatty acids protect against vasculopathy in a transgenic mouse model of sickle cell disease, Haematologica 100 (2015) 870–880.

[7] F. Maccarinelli, A. Pagani, A. Cozzi, F. Codazzi, G. Di Giacomo, S. Capoccia, S. Rapino, D. Finazzi, L.S. Politi, F. Cirulli, M. Giorgio, O. Cremona, F. Grohovaz, S. Levi, A novel neuroferritinopathy mouse model (FTL 498InsTC) shows progressive brain iron dysregulation, morphological signs of early neurodegeneration and motor coordination deficits, Neurobiol. Dis. 81 (2015) 119–133.

[8] A. Matte, P.S. Low, F. Turrini, M. Bertoldi, M.E. Campanella, D. Spano, A. Pantaleo, A. Siciliano, L. De Franceschi, Peroxiredoxin-2 expression is increased in beta-thalassemic mouse red cells but is displaced from the membrane as a marker of oxidative stress, Free Radic. Biol. Med. 49 (2010) 457–466.

[9] L. de Franceschi, G. Malpeli, A. Scarpa, A. Janin, E.M. Muchitsch, P. Roncada, C. Leboeuf, R. Corrocher, Y. Beuzard, C. Brugnara, Protective effects of S-nitrosoalbumin on lung injury induced by hypoxia-reoxygenation in mouse model of sickle cell disease, Am. J. Physiol. Lung Cell Mol. Physiol. 291 (2006) L457–L465.

[10] R. Bellelli, G. Federico, A. Matte, D. Colecchia, A. Iolascon, M. Chiariello, M. Santoro, L. De Franceschi, F. Carlomagno, NCOA4 deficiency impairs systemic iron homeostasis, Cell Rep. 14 (2016) 411–421.

[11] F. Lupo, E. Tibaldi, A. Matte, A.K. Sharma, A.M. Brunati, S.L. Alper, C. Zancanaro, D. Benati, A. Siciliano, M. Bertoldi, F. Zonta, A. Storch, R.H. Walker, A. Danek, B. Bader, A. Hermann, L. De Franceschi, A new molecular link between defective autophagy and erythroid abnormalities in chorea-acanthocytosis, Blood 128 (2016) 2976–2987.

[12] S.S. Franco, L. De Falco, S. Ghaffari, C. Brugnara, D.A. Sinclair, A. Matte, A. Iolascon, N. Mohandas, M. Bertoldi, X. An, A. Siciliano, P. Rimmele, M.D. Cappellini, S. Michan, E. Zoratti, J. Anne, L. De Franceschi, Resveratrol accelerates erythroid maturation by activation of FoxO3 and ameliorates anemia in beta-thalassemic mice, Haematologica 99 (2014) 267–275.

[13] F. Lupo, R. Russo, A. Iolascon, D. Ieluzzi, A. Siciliano, P. Toniutto, A. Matte, S. Piovesan, E. Raffetti, F. Turrini, D. Dissegna, F. Donato, A. Alberti, V. Zuliani, G. Fattovich, L. De Franceschi, Protease inhibitors-based therapy induces acquired spherocytic-like anaemia and ineffective erythropoiesis in chronic hepatitis C virus patients, Liver Int. 36 (2016) 49–58.

[14] L. de Franceschi, F. Turrini, M. Honczarenko, K. Ayi, A. Rivera, M.D. Fleming, T. Law, F. Mannu, F.A. Kuypers, A. Bast, W.J. van der Vijgh, C. Brugnara, in vivo reduction of erythrocyte oxidant stress in a murine model of beta-thalassemia, Haematologica 89 (2004) 1287–1298.

59th Congress of the American Society of Hematology, December 2017, Atlanta, Georgia

FYN KINASE IS INVOLVED IN EPO RECEPTOR SIGNALING AND IS REQUIRED TO HARMONIZE THE RESPONSE TO OXIDATION

Elisabetta Beneduce, Alessandro Matte, Luigia De Falco, Serge Cedrick Mbiandijeu Toya, Emanuela Tolosano, Deborah Chiabrando, Angela Siciliano, Achille Iolascon, Mohandas Narla, Lucia De Franceschi

CEINGE and Dept. of Biochemistry, Federico II University, Naples; Italy
New York Blood Center, NY, USA
Dept. Molecular Biotechnology and Health Sciences, University of Torino, Torino, Italy

Erythropoiesis is a complex multistep process during which committed erythroid progenitors undergo terminal differentiation to produce circulating mature red cells. Erythroid differentiation is characterized by the production of reactive oxygen species (ROS) both in response to erythropoietin (EPO) and to the large amount of iron imported into the cells for heme biosynthesis. During erythropoiesis, ROS might function as second messenger by modulating intracellular signaling pathways. Fyn, an Src kinase, has been previously reported to participate in signaling pathways in response to ROS in various cell types. Here, we explore the potential contribution of Fyn to normal and stress erythropoiesis by studying 2-4 months-old Fyn knockout mouse strain ($Fyn^{-/-}$) and C57B6/2J as wild-type controls. $Fyn^{-/-}$ mice showed a mild compensated microcytic anemia associated with signs of dyserythropoiesis. Increased ROS levels and Annexin-V+ cells were presented in all $Fyn^{-/-}$ erythroblast subpopulations compared to wild-type, suggesting a possible reduction in the efficiency of erythropoietin (EPO) signaling pathway in the absence of Fyn. Indeed, in $Fyn^{-/-}$ erythroblasts we observed a reduction in Tyr-phosphorylation state of EPO-R associated with a compensatory activation of Jak2 without major change in Lyn activity. A reduction in STAT5 activation resulting in down-regulation of *Cish,* a known direct STAT5 target gene, was noted in $Fyn^{-/-}$ erythroblasts. This was paralleled by a reduction in GATA1 and increased HSP70 nuclear translocation compared to wild type, supporting a higher cellular pro-oxidant environment in the absence of Fyn. Using the vitro cell forming colony unit assay, we found a lower in

CFU-E and BFU-E cells production, which once again was associated with decreased activation of EPO mediated cascade in the absence of Fyn. To explore the possible role of Fyn in stress erythropoiesis, mice were treated with either phenylhydrazine (PHZ) or doxorubicin (Doxo). $Fyn^{-/-}$ mice showed prolonged anemia after either PHZ or Doxo treatment with a delayed hematologic recovery compared to wild-type animals. When we analyzed the expression of a battery of ARE-genes related to oxidative response such as catalase, Gpx, heme-oxygenase 1 and peroxiredoxin-2, we noted up-regulated expression of these genes in sorted $Fyn^{-/-}$ erythroblasts compared to wild-type cells. In agreement, we observed increased activation of the redox-sensitive transcriptional factor Nrf2 targeting ARE-genes, whose regulation has been previously linked to Fyn. In fact, Nrf2 is switched-off by Fyn, ubiquitylated and delivered to the autophagosome by the p62 cargo protein. In $Fyn^{-/-}$ sorted erythroblasts, we observed (i) accumulation of p62 in large clusters; and (ii) reduction of Nrf2-p62 complex compared to wild-type cells. To address the question whether the perturbation of Nrf2-p62 system results in impairment of autophagy in the absence of Fyn, we used Lysotrack to explore late phases of autophagy. Lysosomal progression was defective in $Fyn^{-/-}$ reticulocytes and it was associated with accumulation of p62 during in vitro reticulocyte maturation. These data indicate that the absence of Fyn blocks the Nrf2 post-induction response to oxidation, resulting in impaired autophagy. To validate our working hypothesis, we treated $Fyn^{-/-}$ mice with Rapamycin, an inducer of autophagy. In $Fyn^{-/-}$ mice, Rapamycin treatment resulted in decrease dyserythropoiesis, ROS levels and Annexin V+ cells, associated with reduction in accumulation of p62 in $Fyn^{-/-}$ erythroblasts. As a proof of concept, we treated both mouse strains with PHZ with or without Rapamycin. This latter worsened PHZ induced acute anemia in wild-type mice but not in $Fyn^{-/-}$ animals. Collectively, our data enabled us to document a novel role for Fyn in erythropoiesis, contributing to EPO-R activation and harmonizing the Nrf2-p62 adaptive cellular response against oxidation during normal and more importantly in stress erythropoiesis.

59th Congress of the American Society of Hematology, December 2017, Atlanta, Georgia

REPROGRAMMING CELL-SIGNALING BY DELIVERING THE CATALYTIC DOMAIN OF PTPRG AMELIORATES ANEMIA OF β-THALASSEMIA

Matte Alessandro, Elisabetta Beneduce,* Michela Mirenda,* Roberta Russo,* Achille Iolascon, Antonella Pantaleo, Franco Turrini, Angela Siciliano, Enrica Federti, Serge Cedrick MbiandijeuToya, Janin Anne, Lebouef Christophe, Carlo Laudanna, Lucia De Franceschi

*These authors have equally contributed

β-thalassemia (β-thal) is one of the most common monogenetic disorders worldwide, characterized by ineffective erythropoiesis leading to a chronic, debilitating anemia associated with high morbidity and mortality. Erythroid maturation is a dynamic process tightly regulated by complex signaling mechanisms, only partially described either in normal and diseased erythropoiesis. To investigate this issue, we carried out a high throughput kinome analysis by taking advantage of Kinexus array technology (http://www.kinexus.ca), in sorted erythroid precursors from mouse model of ($Hbb^{3th/+}$) compared to wildtype animals. In β-thal mice, we found differential modulation of many protein kinases. Network computational analysis unveiled common as well as erythroid precursor-specific signaling mechanisms of altered erythrocyte differentiation in beta thalassemia, suggesting a selective perturbation in protein kinase/phosphatase balance in β-thal erythropoiesis.

We reasoned that balancing kinome anomalies, by increasing phosphatome activity, could normalize kinome signaling pathways, thus ameliorating erythropoiesis. We explore the expression and function of different protein phosphatase and we found reduced expression and function of protein Tyr-phosphatase receptor type, gamma (PTPRG). To investigate PTPRG role in erythropoiesis, we exploited a novel Trojan-fusion protein (TAT-ICD) we recently patented that delivers intracellularly the catalytic domain of PTPRG and up-modulates its signaling cascade, as both a research tool to map dysfunctional pathways and as a potential therapeutic agent. In β-thal mice, TAT-ICD acted on multiple abnormally activated targets identified by computational analysis. TAT-ICD significantly reduced the activation of (i) Jak2-STAT5 pathway; (ii) Bruton tyrosine kinase (BTK) that has been reported to be part

of the erythropoietin cascade; (iii) Akt that is involved in TGF-b-smad signaling pathway. This was associated with down-regulation of *Erfe* and *Gdf11* gene expression in sorted erythroblasts from TAT-ICD treated β-thal mice. Collectively, TAT-ICD treatment resulted in amelioration of β-thal ineffective erythropoiesis, evaluated by multiple approaches, including the profile of erythroid maturation and the amount of Annexin-V^+erythroid cells, reticulocyte count, circulating erythroblasts and hemolytic indices (*U.S. Patent #62/109,555).* The improvement of anemia was also associated with reduction in alpha aggregates and membrane bound hemichromes in circulating erythrocytes. We also found a reduction of liver and spleen iron accumulation in agreement with the beneficial effects on the hematologic phenotype. It is of note that TAT-ICD treatment did not affect either peripheral leukocyte counts or spleen lymphocyte pattern.

Our data unveil abnormalities in signal transduction pathways as new mechanism involved in β-thal erythropoiesis, and validate a novel, breakthrough, therapeutic approach to reset back to homeostatic equilibrium altered kinome in diseased erythropoiesis.

58th Congress of the American Society of Hematology, December 2016, San Diego, California

A Selective ORAL GLYT1 Inhibitor, Improves Anemia and RED CELL Survival in a MOUSE MODEL of Beta-Thalassemia

Carlo Brugnara, MD[1], Anja Harmeier[2*], **Lucia De Franceschi, MD**[3], Alessandro Matte[4*], Michael Winter[2*], Annette Koerner[2*], Omar Khwaja[2*], Thomas Singer[5*], Elisabetta Beneduce[6*], Enrica Federti[7*] and Angela Siciliano[7*]

[1]Laboratory Medicine, Boston Children's Hospital, Boston, MA
[2]F. Hoffmann-La Roche Ltd, Basel, Switzerland, Basel, Switzerland
[3]University of Verona, Verona, Italy
[4]University of Verona-AOUI Verona, Verona, Italy
[5]F. Hoffmann-La Roche Ltd, Basel, Switzerland, basel, Switzerland
[6]University of Verona-AOUI Verona, Policlinico GB Rossi, Verona, Italy
[7]Department of Medicine, University of Verona and AOUI-Verona, Verona, Italy

The unbalanced hemoglobin chain synthesis in beta-thalassemias leads to hemichrome-induced damage that contributes to ineffective erythropoiesis, hemolysis and reduced red cell survival. Iron overload related to ineffective erythropoiesis and abnormally low Hepcidin (Hamp), combined with the cytotoxic effects of free heme with free-alpha-chains play a key role in the increased generation of reactive oxygen species (ROS) in beta thalassemias.[2][HA{3] Here we used a specific and selective inhibitor of the plasma membrane expressed glycine transporter GlyT1 (Ro4917838). Use of Ro4917838 has been associated with a dose-dependent decrease in MCH, Hb, soluble transferrin receptor, and increase in absolute reticulocytes and RBC counts in several animal species, attributed to reduce glycine bioavailability in erythroblasts and decreased heme synthesis. In rats, Ro4917838 reduces heme synthesis, and down-regulates erythroid transferrin receptor, but does not interfere with hepcidin regulation and systemic iron homeostasis (Winter et al. Exp Hematol, DOI: 10.1016/j.exphem.2016.07.003). We aimed to determine if reduced cellular availability of glycine in erythroblasts may reduce heme synthesis, and impact pathologic erythropoiesis in a mouse model for b-thalassemia. Wild-type control (WT) C57B6/2J, and beta-thalassemia Hbbth3/+ mice were treated with either vehicle or Ro4917838 at dosages of 3, 10, 30 mg/kg/d administered over 4 weeks once daily by gavage. [6]RO4917838 administration was associated with significant improvements of central hallmarks of the b-thalassemia pathology. Reduced erythrocyte destruction was seen bydemonstrated by [8][WM{9]as significant improvements in erythrocyte morphology and amelioration of hemoglobin reduction in reticulocytes. We also observed an impressively quick reduction of the circulating erythroblast count within 1 week of initiating treatment. This was also associated with decreased hemolysis biomarkers. Ro4917838 induced a significant reduction in extramedullary erythropoiesis and reduction in orthochromatic erythroblasts as well as insoluble alpha chain aggregates in circulating red cells. Red cell survival of b-thal mice treated with 30 mg/kg/day Ro4917838 significantly increased by more than 50%. CD71+ erythroid precursors significantly decreased in WT mice treated with Ro4917838 at 30 mg/kg and in b-thal mice at the dosage of 30 mg/kg/ d. [10]These data suggest that Ro4917838 ameliorates anemia in a b-thalassemia mouse model and positively affects ineffective erythropoiesis and red cell survival in peripheral circulation. Ro4917838 may represent a novel therapeutic approach for the treatment of anemia in b-thalassemia patients. [1] I do see the point for beta-thalassemia, but this does not apply for all thalassemias, I mean the free alpha chains. The ROS yes, they have in common. In this sentence it seems to be that the alpha chains are culprit for ROS in all thalassemias. [HA{3]I do see the point for beta-

thalassemia, but this does not apply for all thalassemias, I mean the free alpha chains. The ROS yes, they have in common. In this sentence it seems to be that the alpha chains are culprit for ROS in all thalassemias. ROS was not measured, therefore I would refrain mentioning it. No data is shown. [HA{5]ROS was not measured, therefore I would refrain mentioning it. No data is shown. I propose deletion of the PK info. Although the information is correct I don't think this is the level of detail needed for the abstract. It may even be confusing as it is not the focus of the abstract to do a cross species comparison. [AK7]I propose deletion of the PK info. Although the information is correct I don't think this is the level of detail needed for the abstract. It may even be confusing as it is not the focus of the abstract to do a cross species comparison. Dosing and dosing frequency is already described above, we do not need to repeat this here. [WM{9]Dosing and dosing frequency is already described above, we do not need to repeat this here. Was the liver expression determined or the serum Hepcidin levels measured? I would rephrase it if latter is the case. [HA{11]Was the liver expression determined or the serum Hepcidin levels measured? I would rephrase it if latter is the case.

Abstract Submission

25. Red blood cells and iron - Biology
EHA-3228

THE PYRUVATE KINASE ACTIVATOR AG-348 IMPROVES MURINE B-THALASSEMIC ANEMIA AND CORRECTS INEFFECTIVE ERYTHROPOIESIS

alessandro matte[1], elisabetta beneduce[1], angela siciliano[1], penelope kosinski[2], anne janin[3], christophe lebouef[3], achille iolascon[4], luigia de falco[4], lenny dang[2], charles kung[2], Lucia De Franceschi[* 1]

[1]medicine, University of Verona, verona, Italy, [2]development, agios, Cambridge, United States, [3]pathology, universite, Paris, France, [4]ceinge, University, naples, Italy

Background: β-thalassemias (β-thal) are worldwide distributed red cell disorders, characterized by ineffective erythropoiesis and reduced red blood cell (RBC) lifespan. Increased levels of reactive oxygen species (ROS) have been reported to play a key role in anemia of β thal, targeting both erythropoiesis and circulating RBCs. Pyruvate kinase (PK) is an important enzyme in the glycolytic pathway, responsible for conversion of phosphoenolpyruvate to pyruvate, with concomitant formation of the energy carrier adenosine triphosphate (ATP). As mature erythrocytes lack mitochondria, they rely almost exclusively on glycolysis to generate ATP, as well as the interlinked pentose phosphate pathway shunt to generate the reducing agent NADPH. The possible impact of PK activity on erythropoiesis is supported by evidence of ineffective erythropoiesis in human subjects with PK deficiency as well as mouse models of PK deficiency. The PK activator AG-348 has been evaluated in Phase I trials in healthy human subjects (NCT02149966) and is currently in Phase II studies in PK deficiency patients (NCT02476916). In the Phase I studies, AG-348 was shown to decrease levels of an upstream metabolite 2,3-diphosphoglycerate (2,3-DPG) and increased levels of ATP in whole blood, consistent with *in vivo* activation of PK.
Aims: To evaluate the impact of AG-348 on anemia and ineffective erythropoiesis in a mouse model of β thal intermedia.
Methods: Mouse strains C57B6/2J, as wildtype (WT) controls, and $Hbb^{th3/+}$, as a mouse model of β-thal intermedia, were used. Female mice aged between 2-3 months were treated with either vehicle or AG-348 at 50 mg/kg bid by oral gavage. Hematologic parameters, RBC indices, morphology, and reticulocyte count were evaluated at baseline, 7, 14, 21 days of treatment. Mouse erythropoiesis was studied using the CD44/TER119 gating strategy by FACS. ROS levels and the amount of Annexin-V+ cells were evaluated in erythroblast populations. Liver iron accumulation was evaluated by Pearl's staining and expression of liver hepcidin was measured by RT-PCR.
Results: In $Hbb^{3th/+}$ mice, 21 days of AG-348 treatment was associated with (i) a marked amelioration of anisopoykylocytosis; (ii) significantly increased Hb levels, MCV and MCH; (iii) a significant reduction in circulating erythroblasts (Es) and reticulocyte count; and (iv) reduction of ROS levels in circulating RBCs. In addition, AG-348 significantly decreased the amount of membrane precipitated α-globin chains and increased the amount of soluble Hb compared to the vehicle treated $Hbb^{3th/+}$ group. Consistent with these findings, we observed (i) a reduction of extramedullar erythropoiesis as indicated by both a decrease in spleen weight/mouse weight ratio and total Es (CD44TER119 Fsc high cells); (ii) a significant increase in pro-Es and basophilic Es, associated with reduction in orthochromatic Es; (iii) a reduction in ROS levels of $Hbb^{3th/+}$ Es and the amount of apoptotic orthochromatic Es compared to vehicle treated $Hbb^{3th/+}$ mice, suggesting an amelioration of β thal ineffective erythropoiesis.. The amelioration of ineffective erythropoiesis was paralleled by a reduction in liver iron overload and up-regulation of hepcidin mRNA in liver from AG-348 treated $Hbb^{3th/+}$ mice.

Summary/Conclusion: Our data show that the PK activator AG-348 beneficially affects ineffective erythropoiesis in a mouse model of β thal and might represent a novel therapeutic tool in clinical management of anemia in β thalassemic syndromes.

Keywords: Red blood cell, Thalassemia

Fyn plays a novel key role in erythropoiesis as oxidative sensor

Beneduce E[1], Matte A[1], De Falco L[2], Cedrick Mbiandjeu Toya S[1], Iolascon A[2], Siciliano A[1], Valenti MT[1], Tolosano E[3], Chiabrando D[3], De Franceschi L[1]

[1]Dept. of Medicine, University of Verona and AOUI-Verona, Italy;[2]CEINGE, Advanced Biotechnologies, Naples, Italy;[3]Dept of Molecular Biotechnology and Health Sciences and Molecular Biotechnology Center, University of Turin, Italy.

Background

Fyn is a member of the Src family of tyrosine kinases (SFKs) and shares high homology with Lyn that has been previously involved in erythropoiesis. Previous reports have shown that Lyn targets EPO-R/Jak2/STAT5 signaling pathway. Although progresses have been done in the knowledge of molecular mechanisms involved in normal and diseased erythropoiesis, much still remains to be investigated on signal transduction pathway during erythroid differentiation and maturation.

Aims

Functional characterization of erythropoiesis in $Fyn^{-/-}$ mice.

Methods

Female aged between 2-4 months from C57BL/6J, as wild-type (WT) controls, and $Fyn^{-/-}$ mouse strains were used. Phenylhydrazine (PHZ) at 40 mg/kg or Doxorubicin at 0,25mg/kg by intraperitoneal injection were used to explore stress erythropoiesis. Hematologic parameters, red indices and reticulocyte count were evaluated as previously reported (Matte A, et al. ARS, 2015). Mouse erythropoiesis was studied using the CD44/Ter119 gating strategy by FACS. ROS levels and the amount of Annexin V^+ cells were also evaluated in erythroblast subpopulations. In vitro colony-forming unit assay was performed to obtain CFU-Es and BFU-Es. Immunoblot analysis was carried out to study early and late erythropoiesis.

Results

$Fyn^{-/-}$ mice showed signs of dyserythropoiesis associated with increased total erythroblasts ($CD44^+TER119^+FSC^{high}$), without extramedullar erythropoiesis. $Fyn^{-/-}$ erythroblasts showed higher ROS levels and increased amount of Annexin V^+ cells, compared to WT, indicating increase oxidative stress and cell aptoptosis. High ROS levels in erythroblasts have been described in β-thalassemic mouse erythroid cells as model of stress erythropoiesis. This has been linked with instability of GATA-1, which nuclear translocation is prevented and requires the stabilization of heat shock protein (HSP70-90). In $Fyn^{-/-}$ mice, we explored GATA-1/HSP70 distribution in subcellular fractions. $Fyn^{-/-}$ erythroblasts showed reduction in GATA-1 nuclear translocation, compared to WT. In agreement with reduced GATA-1 nuclear translocation, a marked decrease in β–globin chain synthesis, resulting in an imbalance in α/β globin chain levels, was observed in $Fyn^{-/-}$ mice.

To further characterize the impact of the absence of Fyn on erythropoiesis, we set up a colony-forming unit assay for CFU-E and BFU-E. The lack of Fyn resulted in a significant decrease in CFU-E and BFU-E colonies, suggesting an impairment of early erythropoiesis. Erythroid commitment and differentiation is strictly dependent on EPO-R/Jak2/STAT5 signaling pathway. The absence of Fyn resulted in a marked decrease in STAT5 activation, supported by a significant down-regulation of *Cish*, that is strictly regulated by STAT5 function.

Using Doxorubicin and PHZ, we found a delay in increased reticulocyte count related to either Doxorubicin or PHZ treatment, shedding new light on the role of Fyn in stress erythropoiesis.

In addition, we found chronic activation of Nrf2 related to lack of its physiologic inhibitor, Fyn. Indeed, we found increased ARE-related genes such as heme oxygenase-1 (HO-1), which expression seems to became independent from heme concentration in the absence of Fyn. In fact, bilverdin reductase (BVR) that is functionally link to Nrf2 but it depends from another transcriptional factor was similar to that observed in WT mice.

Conclusions

Our preliminary data support a novel role of Fyn as both oxidative sensor and new modulator of the EPO/STAT5 pathway.